FUNCTIONAL DYNAMICS OF REPLICATION PROTEIN A IN INITIATION OF SV40 DNA REPLICATION

By

Xiaohua Jiang

Dissertation

Submitted to the Faculty of the

Graduate School of Vanderbilt University

in partial fulfillment of the requirements

for the degree of

DOCTOR OF PHILOSOPHY

in

Biological Sciences

May, 2008

Nashville, Tennessee

Approved:

Professor Ellen Fanning

Professor James G. Patton

Professor Katherine Friedman

Professor Walter Chazin

Professor Mark Denison

ACKNOWLEDGMENTS

I am in deeply debt to my mentor Dr. Ellen Fanning. She is a real scientist with great passion. Her devotion to science influences me greatly and provokes my interest in the DNA replication field. She helped me in every step of my growth in science. I would like to thank my other committee members, Dr. James G. Patton, Dr. Walter Chazin, Dr. Katherine Friedman, Dr. Mark Denison. Their help has greatly strengthened the quality of this project.

I would like to thank all my co-workers in this project, Dr. Robert Ott, Dr. Vitaly Klimovich, Erik Hysinger, Dr. Yingda Wang. Dr. Ott introduced me to the basic experimental methods of the replication field. Dr. Ott also started the project I worked on. Dr. Klimovich worked with me on the same project. I am very lucky to have a talented undergraduate student, Erik Hysinger, to work with me.

I would like to thank our collaborators Dr. Walter Chazin, Dr. Alphonse Arunkumar and Brian Weiner in the Chazin lab for their contributions to this project. This project is a successful collaboration work. We combine the biochemical methods from the Fanning lab with the structural methods from the Chazin lab to study the mechanisms of DNA replication.

I also want to thank both the past and present members of the lab, Dr. Haijiang Zhang, Dr. Xiaorong Zhao, Dr. Kun Zhao, Dr. Hanjian Liu, Dr. Jinming Gu, Dr. Steven Gray, Hao Huang, Gulfem Guler, Dr. Peijun Yan, Dr. Jeannine Gerhardt, and Isi Tolliver. They really make the lab a fun environment in which to work.

I owe my thanks to many friends, especially my best friends Xingkui Guo and Dr. Hong Ji. The moral support from Xingkui helped me through the toughest time of my Ph.D life. My progress as a graduate would not haven been possible without the support from Xingkui. Hong and I have been classmates and friends for more than ten years. We shared our memories as high school students, college students and graduate students. I'd like to thank my parents for supporting me. Without their love and support, I would not present this work to you.

I would like to thank the financial support of National Institute of Health, Howard Hughes Medical Institute and Vanderbilt University.

TABLE OF CONTENTS

Page

ACKNOWLEDGMENTS ii

LIST OF FIGURES vi

LIST OF TABLES ix

LIST OF ABBREVIATIONS x

Chapter

I. INTRODUCTION 1

Simian Virus 40 4
T antigen 11
Replication Protein A structure and function 23
DNA polymerase α-primase structure and function 29
Hand off model 31
Initiation of SV40 DNA replication 33

II. INSIGNTS INTO HRPA32 C-TERMINAL DOMAIN-MEDIATED ASSEMBLY OF THE SIMIAN VIRUS 40 REPLISOME 37

Introduction 37
Materials and methods 39
Protein preparation 39
NMR spectroscopy 40
Structure calculations 41
SV40 DNA replication (monopolymerase) assay 42
T antigen-dependent primer synthesis and extension assays on ssDNA 43
Results 43
An RPA32C antibody inhibits initiation of SV40 replication 43
RPA32C interacts specifically with the Tag-OBD 46
Structural model of the complex 48
Tag and DNA repair factors bind to the same site on RPA32C 52
RPA32C binds to the same site on Tag-OBD as origin DNA 54
Binding site mutations inhibit interaction 56
RPA32C is required for initiation of SV40 DNA replication 62
RPA32C interaction with Tag promotes primer synthesis 66
Discussion 69
Mechanism of Tag stimulation of primer synthesis? 71
Acknowledgments 74

III. STRUCTRAL MECHANISM OF RPA LOADING ON DNA DURING ACTIVATION OF A SIMPLE PRE-REPLICATION COMPLEX 75

Introduction 75
Materials and methods 79
Protein and DNA 79
NMR spectroscopy 79
Limited proteolysis 80
Tag-RPA pull-down assays 80
ssDNA filter binding assays 81
Native gel electrophoresis 81
Initiation of SV40 DNA replication 82
Results 82
Selective loading of human RPA during unwinding of the SV40 replication origin 83
Domain mapping of interactions between Tag and RPA 85
RP70AB binds ssDNA and Tag-OBD at distinct sites 89
Tag-OBD associates with RPA70AB through electrostatic interactions 93
Physical interaction with Tag-OBD stimulates ssDNA binding of RPA 96
Discussion 103
The ternary complex: A coupling device for protein-mediated RPA loading during DNA unwinding 103
Acknowledgments 108

IV. CONCLUSION AND DISCUSSION 109

Summary of RPA dynamics during DNA replication initiation 109
How does RPA associate with newly exposed ssDNA? 111
Significance and future direction 112
The significance of studying RPA dynamics 112
Future directions 116
RPA dynamics in eukaryotic DNA replication initiation 117

APPENDIX 120

Introduction 120
Material and Methods 126
Protein purification 126
Co-immunoprecipitation Assays 126
Results 127
T antigen binds to the C-terminal region of TopBP1 127
TopBP1 interacts with pol-prim 132
Discussion 132

REFERENCES 136

LIST OF FIGURES

Figure Page

1. Eukaryotic DNA replication fork. 3
2. Model of the initiation process of DNA replication. 5
3. SV40 genomic map. 6
4. Diagram of the polyomavirus life cycle in a permissive host cell. 8
5. Core origin of SV40 DNA replication. 10
6. Digital image processing of the T antigen double hexamer at the SV40 origin of replication. 13
7. Cartoon representation of the known T antigen domain structures. 14
8. Overall structure of the DnaJ domain of SV40 large T antigen (aa 7-117). 15
9. DNA binding surface of T antigen-OBD. 18
10. Side (a) and top (b) views of the T antigen residues 251–627 hexameric structure. 20
11. A looping model showing the coupling of the β hairpin movement to the dsDNA translocation into the T antigen double hexamer for unwinding. 21
12. Schematic showing the RPA domain structure. 24
13. Structural models of several domains of RPA 25
14. RPA binds ssDNA with different binding modes. 28
15. Key concepts in DNA processing. 32
16. Monoclonal antibody 34A recognizes hRPA32C and inhibits SV40 replication. 45
17. The interaction of RPA32C with Tag-OBD. 47
18. Mapping the Tag-OBD binding site of RPA32C. 49
19. Mapping the RPA32C binding site of Tag-OBD. 50

20. Analysis of Tag-OBD and RPA32C complex..... 53

21. Side chains at the intermolecular interface. 55

22. Effects of DNA binding and mutations on the interaction between RPA32C and Tag-OBD. 57

23. Electrostatic surfaces of the two molecules in the Tag-OBD/RPA32C complex. 58

24. NMR chemical shift analysis of the interaction of wild type and mutant Tag-OBD with RPA32C. 60

25. Comparative analysis of human and yeast RPA32C. 61

26. Mutations in hRPA32C that weaken interaction with Tag are defective in initiation of SV40 DNA replication..... 63

27. Characterization of the hRPA32C and hRPAy32C mutant proteins. 64

28. Quantitative comparison of wild type and mutant RPA in replication assays. 65

29. Mutations in hRPA32C that weaken interaction with Tag are defective in priming. . 67

30. hRPA32C is needed for primosome activity, but not for primer extension..... 68

31. Model for SV40 primosome activity on RPA-coated ssDNA. 73

32. Domain organization of RPA with Tag binding regions shaded. 76

33. Tag interaction with RPA70AB actively loads human RPA onto ssDNA during initiation of SV40 DNA replication..... 84

34. Tag-OBD binds to two regions of RPA. 87

35. Tag-OBD protects RPA70AB from proteolytic digestion. 88

36. Structural mapping of RPA70AB binding site for Tag-OBD. 91

37. Structural mapping of Tag-OBD binding site for RPA70AB. 94

38. Similarity of NMR chemical shifts reveals that the R154E mutation in Tag-OBD does not significantly affect protein structure. 97

39. Transient Tag binding to RPA facilitates ssDNA binding of RPA. 98

40. Migration of RPA- and Tag-ssDNA complexes in native gel electrophoresis. 101

41. Proposed mechanism for coupling activation of the SV40 pre-replication complex with RPA loading on ssDNA. 105

42. The structure of T antigen origin binding domain..... 113

43. Schematic drawing of human TopBP1 and its homology in other species..... 122

44. T antigen interacts with TopBP1..... 128

45. T antigen interacts with TopBP1(aa 541-1522) fragment. 130

46. T antigen interacts with TopBP1(aa 978-1522) fragment. 131

47. Pol-prim interacts with TopBP1..... 133

LIST OF TABLES

Table Page

1. Ten cellular proteins and viral T antigen are required for viral DNA replication in vitro.....2

2. Structural Statistics of the 20 best RPA32C/Tag-OBD model structures 51

LIST OF ABBREVIATIONS

^{0}C	Degree Celsius
aa	Amino acid
AAA+	ATPase associated with various cellular activities
ATM	Ataxia telangiectasia mutated
ATP	Adenosine 5’ triphosphate
ATR	ATM and Rad3-related
ATRIP	ATR-interacting protein
BRCA1	breast-ovarian cancer susceptibility 1
BRCT	BRCA1 carboxyl terminus
BSA	Bovine serum albumin
Ci	Curie
Co-IP	Co-immunoprecipitation
cpm	Counts per minute
CTD	Carboxyl- terminal domain
CTP	Cytidine 5’triphosphate
Da	Dalton
dATP	Deoxyadenosine 5’-triphosphate
DBD	DNA binding domain
dCTP	Deoxycytidine 5’-triphosphate
dGTP	Deoxyguanosine 5’-triphosphate
DNA	Deoxynucleic Acid

dNTPs	Deoxynucleoside triphosphate
DSB	double stranded DNA break
dsDNA	double stranded DNA
DTT	Dithiothreitol
dTTP	Deoxythymidine 5'-triphosphate
dT_{30}	oligodeoxythymidylate
E.coli	Escherichia coli
EDTA	(Ethylenedinitrilo)tetraacetic acid
EGTA	Ethylene glycol-bis-(β-aminoethylether)-N,N'-teraacetid acid
EMSA	Electrophoretic Mobility Shift Assay
EP	early panlindrome
g	Gram
GST	Glutathione S-tranferase
h	Hour
HCl	Hydrochloric acid
HEPES	N-[2-hydroxyethyl] piperazine-N'-[2ethansulfonic acid]
His	Histidine tagged
HPV	human papillomavirus
hRPA	human RPA
HSQC	heteronuclear single quantum correlation
IgG	Immunoglobulin G
IPTG	Isopropyl β-D-thiogalactopyranoside
IR	ionizing radiation

kb	kilobase
Kd	dissociation constant
kDa	kilodalton
Kpi	Potassium phosphate monobasic
KOH	Potassium Hydroxide
l	Liter
LB	Luria broth
M	Molar (m/l)
mg	Milligram
$MgCl_2$	Magnesium Chloride
min	Minute
ml	Milliliter
mM	Millimolar
MRN	Mre11-Rad50-Nbs1
μCi	Microcurie
μg	Microgram
μl	Microliter
μM	Micromalor
NaCl	Sodium Chloride
Ni-NTA	Nickel-nitrilotracetic acid agarose
ng	Nanogram
NLS	Nuclear Localization Signal
nm	Nanometer

nmol	Nanomol
NP-40	Nonidet-P40
nt	nucleotide
OB	oligonucleotide/oligosaccharide-binding
OBD	Origin binding domain
P-loop	Phosphate-binding loop
PAGE	polyacrylamide gel electrophoresis
PBS	Phosphate buffered saline
PCNA	Proliferating cell nuclear antigen
PIPES	Piperazine-N,N'-bis-2-ethansulfonyl acid
PML	promyelocytic leukarmia
Pmol	Picomol
PMSF	Phenylmethylsulfonyl fluoride
Pol-prim	DNA Polymerase α-primase
Pol δ	DNA Polymerase δ
Pol ε	DNA Polymerase ε
pol-prim	DNA polymerase α-primase
RFC	Replication factor C
RNA	Ribonucleic acid
RPA	Replication protein A
RPA70AB	the DNA binding domains A and B of RPA
RPA70N	the N-terminus of the RPA70 subunit
RPA32C	the C-terminus of the RPA32 subunit

rpm	revolutions pre minute
RT	room temperature
RMSD	root-mean-square deviation
Sc	Saccharomyces cerevisiae
SDS	Sodium Dodecyl sulfate
Sec	Second
SSB	Single stranded DNA binding protein
ssDNA	Single stranded DNA
SV40	Simian Virus 40
T antigen/Tag	large Tumor antigen
TBE	Tris borate EDTA buffer
TBS	Tris buffered saline
TBST	Tris buffered saline tween-20
TCA	trichloroacetic acid
TopBP1	Topoisomerase IIβ binding protein 1
Tris	Tris- (Hydroxymethyl-)aminomethane
V	Volt
WT	Wild type
yRPA	yeast RPA

CHAPTER I

INTRODUCTION

DNA is the genetic material passed from generation to generation in most of the organisms. DNA replication is an essential process for cell proliferation. Since DNA integrity is crucial for cell viability, replication machinery needs to copy the genomic information completely and accurately.

Establishing the fundamental features of the initiation process of DNA replication in human cells is difficult since basic components of the initiation process such as replication origins have yet to be isolated and characterized (Bullock, 1997). Moreover, there are unidentified proteins in human DNA replication. Here we use simian virus 40 (SV40) as a model system to study the initiation of DNA replication. SV40 has a well-defined origin of replication and requires only one viral protein, large Tumor antigen (T antigen/Tag) for initiation of viral DNA replication (Bullock, 1997). All the other proteins required for viral DNA replication are supplied by host cells and have been identified. In addition, viral DNA replication can be reconstituted *in vitro* with T antigen and nine host proteins (Table 1), which makes it a good model system to study the interaction of human replication proteins. Although key differences have emerged (see Appendix), there are many similarities between viral and host replication pathways. The replication fork of SV40 is the minimal set of the replication fork for eukaryotes as shown in Figure 1. T antigen replaces MCM proteins to function as a helicase. SV40 has served as a model system to identify host replication proteins and their functions. These

Table 1: Ten cellular proteins and viral T antigen are required for viral DNA replication in vitro

Protein	Subunit Composition	Replication Activity
SV40 T antigen	90	Origin binding/unwinding, helicase
Replication Protein A (RPA)	70, 32, 14	Single stranded DNA binding
DNA polymerase alpha	180, 68, 58, 48	DNA polymerase, primase
DNA polymerase delta	125, 66, 55, 12	DNA polymerase, 3' to 5'exonuclease
Proliferating Cell Nuclear Antigen (PCNA)	29	Serves as sliding clamp- increases pol δ processivity
Replication Factor C (RFC)	140, 40, 38, 37, 36	Loads PCNA, increases processivity of pol δ
Topoisomerase I	100	Relieves torsional stress in DNA
Topoisomerase II	140	Relieves torsional stress in DNA, Unlinks daughter duplexes
RNase H1	68-90	Endonuclease specific for hybrid RNA/DNA primers
MF1/FEN-1	44	5' to 3' exonuclease
DNA ligase I	85-125	Joins Okazaki Fragments

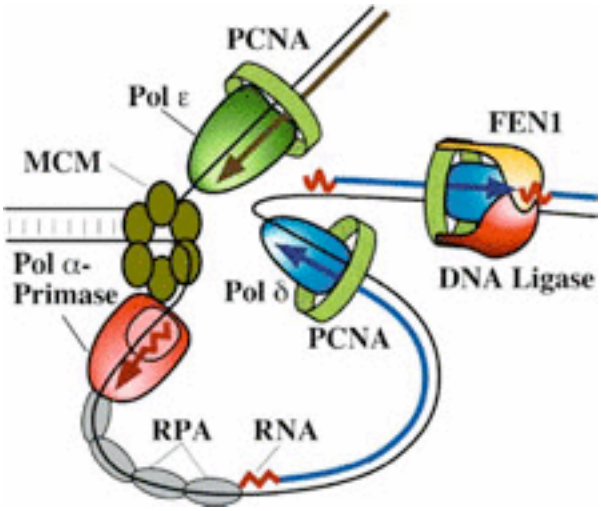

Figure 1: Eukaryotic DNA replication fork. The minimal set of proteins for fork propagation are indicated (Garg & Burgers, 2005).

studies infer their roles that these proteins may play in the more complex network of host DNA replication.

The initiation of DNA replication can be dissected into four basic steps (Figure 2). First, the initiator recognizes the replicator on DNA, called recognition step. Second, initiator melts the origin, named melting step. Third, the helicase unwinds dsDNA, which is called unwinding step. Fourth, all replication initiation factors are recruited to the replication site and primer synthesis starts. This step is called priming step or primer synthesis step (Stenlund, 2003).

During initiation of viral DNA replication, RPA first binds to parental ssDNA during unwinding and then dissociates from ssDNA for daughter DNA synthesis during primer synthesis. I am especially interested in the mechanism of RPA dynamics in these processes. Our lab collaborates with Dr. Chazin's lab to combine biochemical and structural methods to reveal the details of RPA interaction with T antigen, and elucidate the functional importance of this interaction.

Simian Virus 40

Simian virus 40 (SV40), family *polyomaviridae*, is a non-enveloped virus that is comprised of a 5.2 kb genome, a major capsid protein VP1, two minor capsid proteins VP2 and VP3, and a later protein VP4 (Ahuja et al., 2005; Daniels et al., 2007). The viral genome (Figure 3) is double stranded circular DNA and assembles as a mini-chromosome with 24-25 host nucleosomes (Fiers et al., 1978; Reddy et al., 1978; Fanning et al., 2008). SV40 infects a variety of cultured mammalian cells, but initiates a

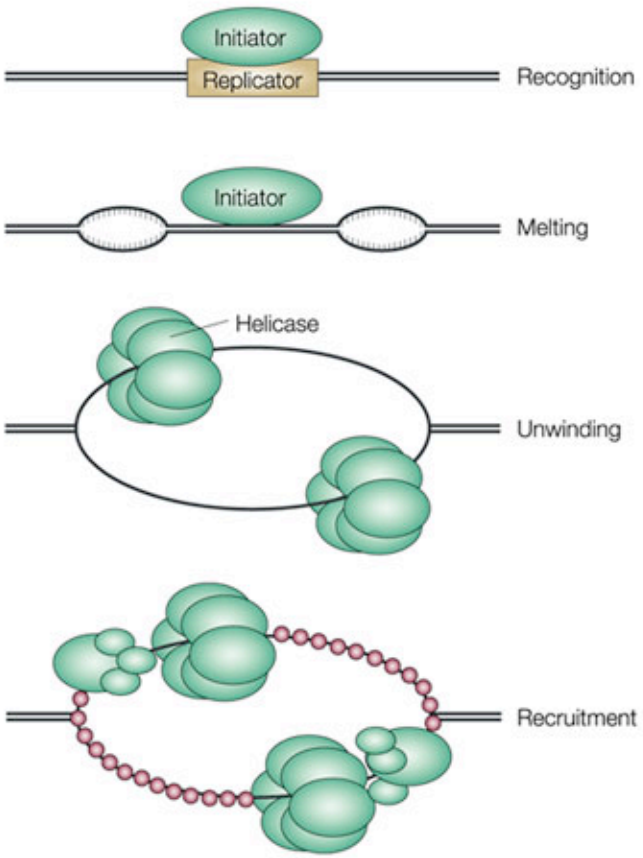

Figure 2: Model of the initiation process of DNA replication. The initiation process can generally be considered to involve four steps: recognition (binding of the initiator to the replicator), melting, unwinding (which requires helicase activity) and recruitment of replication factors, such as DNA polymerases and single-stranded DNA-binding proteins (SSBs). The cellular initiator proteins from both eukaryotes and prokaryotes carry out a subset of these functions. Some viral initiators, such as E1 and T antigen, carry out all of these functions (Stenlund, 2003).

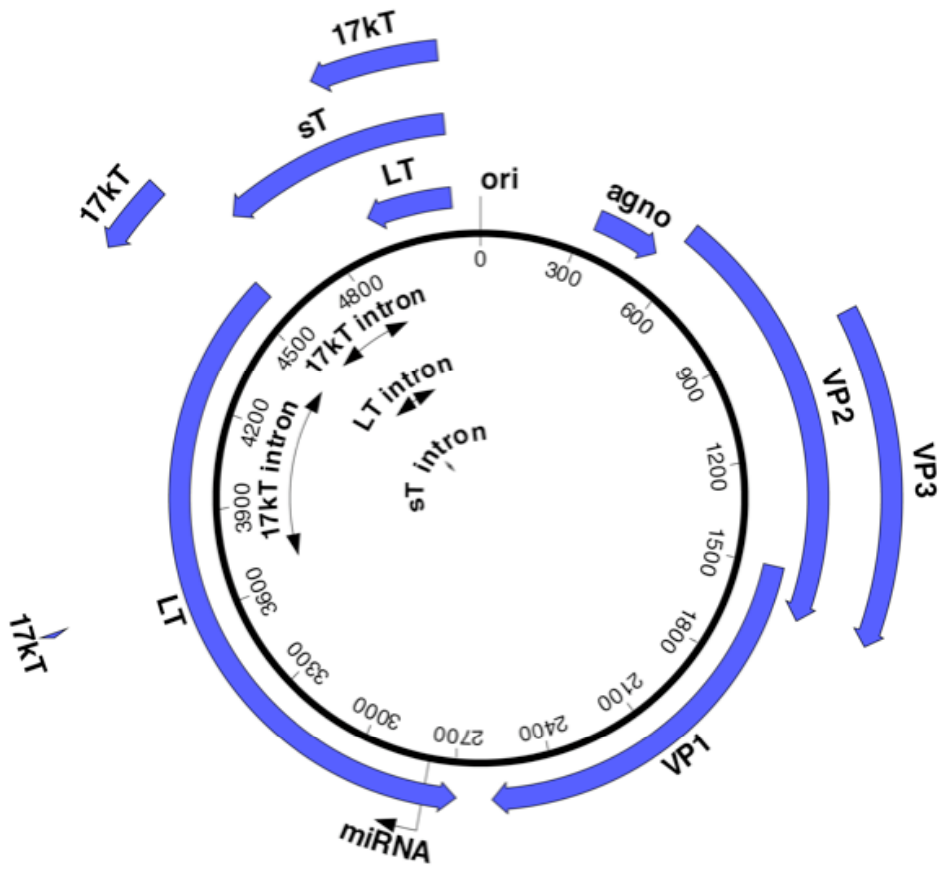

Figure 3: SV40 genomic map. The SV40 DNA contains a control region (top) composed of the origin of DNA replication (ori), the early and late promoters, enhancer, and packaging signal. The early transcription unit (left) encodes T antigens, and the late genes (right) encode capsid proteins, and agno protein, in alternatively spliced mRNAs as indicated. A pre-micro RNA expressed (miRNA) late in infection limits immune recognition by reducing early gene expression (Sullivan et al., 2005). Nucleotide numbers are diagrammed clockwise around the genome beginning in the origin.

productive infection cycle only in monkey cells and in cells of other primate species (Fanning & Knippers, 1992).

The capsid of SV40 is icosahedral, composed of 72 VP1 pentamers, which are linked together by interchain Cys9-Cys9 and Cys104-Cys104 disulfide bonds (Jao et al., 1999; Burckhardt & Greber, 2008). Each VP1 pentamer is associated with one minor capsid protein, either VP2 or VP3 (Liddington et al., 1991; Chen et al., 1998). The genome of SV40 includes three parts: a regulatory region containing the replication origin, an early gene region coding for T antigen, small t antigen, 17 kDa T antigen, and a late gene region coding for the viral structural proteins VP1, VP2, VP3 and the nonstructural agno protein as shown in Figure 3.

SV40 enters cells through atypical endocytosis (Figure 4). VP1 binds to the ganglioside GM1 and class I major histocompatibility proteins to attach the virus to the cell membrane (Fanning et al., 2008). The virus enters host cells through plasma membrane structures called caveolae, not the typical clathrin-coated pits (Norkin et al., 2002). SV40 internalized in pH neutral caveosome is transported directly to the smooth endoplasmic reticulum (ER) through a microtubule-dependent pathway, bypassing endosomes and the Golgi. The viral disassembly takes advantages of the protein folding and quality control machinery in the ER (Norkin et al., 2002; Schelhaas et al., 2007). ERp57, a disulfide isomerase and PDI, a disulfide reductase in the ER isomerize specific interchain disulfides connecting the major capsid protein VP1 (Schelhaas et al., 2007; Burckhardt & Greber, 2008). SV40 uses ER-associated degradation to escape from the ER lumen to the cytosol (Schelhaas et al., 2007). The mini-chromosome is imported into the nucleus through a nuclear localization signal in VP3 that is exposed after viral

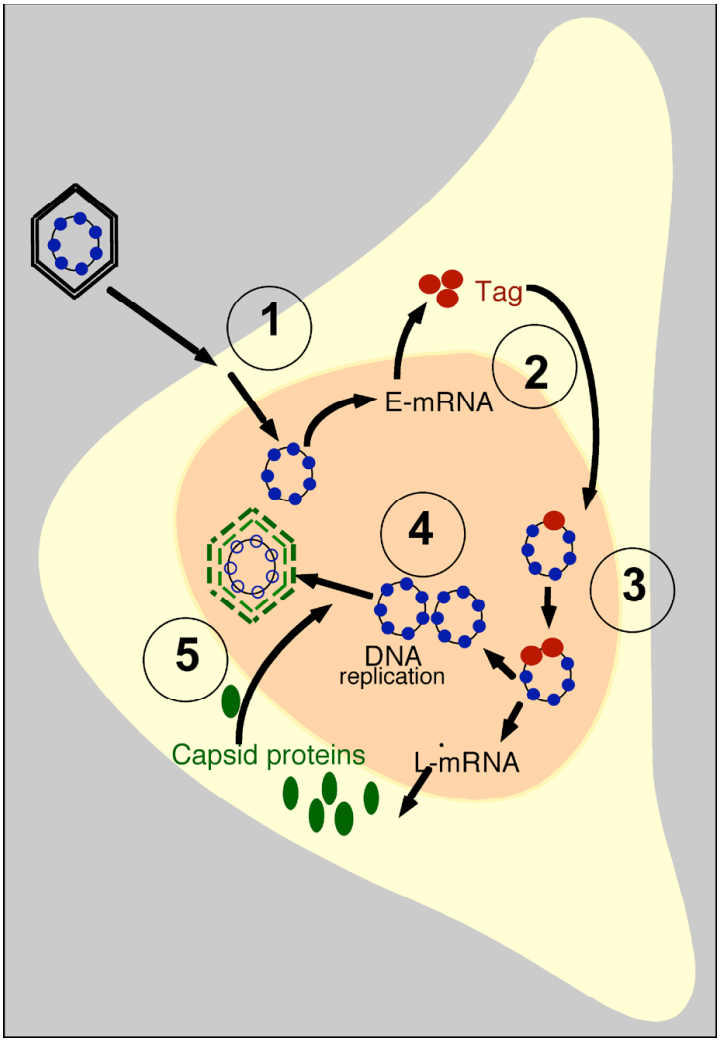

Figure 4: Diagram of the polyomavirus life cycle in a permissive host cell. E-mRNA, early gene mRNA; L-mRNA, late gene mRNA. (1) Virus attachment, entry, and intracellular trafficking. (2) T antigen expression, structure and function. (3) T antigen-directed re-programming of the cellular milieu. (4) Viral DNA replication. (5) Late gene expression, virion assembly and release (Fanning et al., 2008).

disassembly and interacts with importin (Nakanishi et al., 1996; Nakanishi et al., 2002; Nakanishi et al., 2006; Nakanishi et al., 2007).

When the viral chromosome enters the nucleus, the early gene region of SV40 genome encoding T antigen, small t antigen, 17 kDa T antigen is transcribed, processed, and then translated in the cytoplasm (Fanning et al., 2008). T antigen is present primarily in the nucleus (Dickmanns et al., 1994). SV40 is well adapted to its host and replies on its multifunctional regulatory protein, T antigen, to carry out sophisticated re-programming of the host cell milieu for virus reproduction. T antigen is essential to drive quiescent infected cells into S phase, to initiate and complete viral DNA replication, to activate the late viral promoter and to promote virion assembly (Pipas, 1992; Sullivan & Pipas, 2002; Ahuja et al., 2005).

As a model system for DNA replication, SV40 has a well-defined origin from nucleotide 5211 through 31 as shown in Figures 3 and 5 (Deb et al., 1986a). This 64 bp region is both necessary and sufficient for initiation of SV40 replication in vivo and in vitro (Myers & Tjian, 1980; Deb et al., 1986a; Deb et al., 1986b; DeLucia et al., 1986; Li et al., 1986; Dean et al., 1987; Deb et al., 1987). The origin contains three functional regions: an early palindrome (EP) region, a palindrome region (also called binding site II) with four GAGGC pentanucleotide repeats, and a 17-bp adenosine-thyminidine (AT) rich domain. The four GAGGC repeats in the palindrome region are arranged as two pairs in inverted direction to each other. The palindrome region serves as a T antigen-binding site. All four pentanucletotides are required for initiation of viral replication and in addition, spacing between GAGGC repeat is critical (DeLucia et al., 1986; Bullock, 1997). The EP from 5213 to 5227 nt contains two parts, an 8-bp region (5210 to 5217 nt)

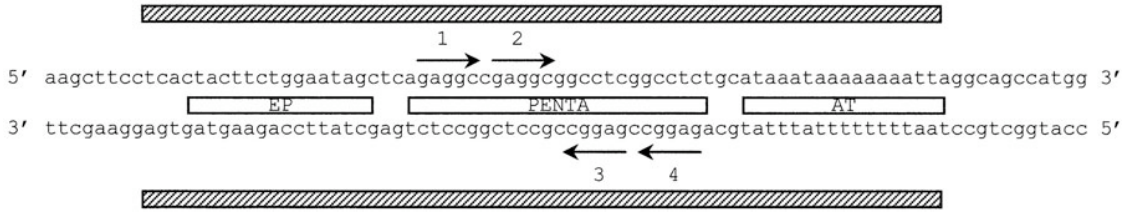

Figure 5: Core origin of SV40 DNA replication. The GAGGC pentameric sequences are labeled 1 to 4 as indicated. The arrangement of the pentamers positions the major grooves of 1 and 3 on approximately the same face of the DNA. The same is true for 2 and 4. In addition, 1 and 2 (like 3 and 4) are on opposite faces of the DNA. The AT-rich, EP region and panlindrome region sequences are indicated as AT, EP, PENTA.

and a region close to the palindrome. The 8-bp region in EP is highly conserved among papovaviruses of primates and mutations in this region cause a significant loss of function (Bullock, 1997). The region in EP close to the palindrome functions as a spacer with only small defect in replication when mutated (Deb et al., 1986a). AT base pairs are a common feature among origins in prokaryotes and eukaryotes. The relatively weak base pairing facilitates strand separation, an early but indispensable step for DNA replication initiation (Figure 2). The AT region directs DNA bending and coordinately regulates DNA replication (Deb et al., 1986b). In summary, the precise structure of the origin is critical for efficient viral replication.

T antigen

T antigen was identified as a viral protein of 86 kDa by immunoprecipitation using anti-SV40 serum (Kress et al., 1978). Subsequent studies in many laboratories revealed that T antigen is a multifunctional protein, involved in all aspects of viral replication, transcription, virus-host interaction (Fanning & Knippers, 1992). In viral DNA replication, T antigen is both an initiator protein and a DNA helicase that couples the energy of nucleoside triphosphate hydrolysis to nucleic acid unwinding and movement. As a motor protein family, helicases are very abundant and are involved in almost every aspect of nucleic acid metabolism including DNA replication, repair, recombination and transcription. T antigen is a member of the SF3 viral helicase of AAA+ (ATPase associated with various cellular activities) family. Helicase activity is an intrinsic function of T antigen independent of its origin recognition activity (Stahl et al., 1986). Most helicases require at least one ssDNA tail to begin unwinding DNA, but T antigen

can initiate unwinding of duplex DNA when provided with the viral origin of replication (Dean et al., 1987; Deb & Tegtmeyer, 1987; Borowiec & Hurwitz, 1988). T antigen unwinds DNA in a 3′ to 5′ direction coupled with ATP hydrolysis in the presence of magnesium (Stahl et al., 1986; Goetz et al., 1988; Wiekowski et al., 1988).

T antigen can exist as a monomer or hexamer in solution and hexamer formation is stimulated by ATP (Gai et al., 2004a). T antigen assembles around origin as a double hexamer in the presence of ATP and Mg++ (Figure 6), which is the active form of T antigen in initiation and elongation (Valle et al., 2000; Alexandrov et al., 2002).

T antigen contains 708 amino acids with a calculated molecular weight of 82.5 kDa (Fanning & Knippers, 1992). It has four functional domains: an N-terminal J domain (aa 1-102), an origin binding domain (aa 131-250) (OBD), a helicase domain (aa 251-627) and a C-terminal host-range domain (aa 683-708), as stated in Figure 7.

The N-terminus of T antigen is essential to drive cells into S phase and therefore is required for viral replication *in vivo*. However it is not required for viral replication *in vitro* (Bullock, 1997; Sullivan & Pipas, 2002). The N-terminus has sequence similarity with the J domain of the molecular chaperones, DnaJ (Kelley & Landry, 1994; Ahuja et al., 2005). Like DnaJ molecules, the N-terminus of T antigen interacts with hsc70, the major DnaK homologue in mammalian cells (Sawai & Butel, 1989; Sullivan et al., 2001). The structure of the N-terminus of T antigen has been solved as shown in Figure 8. Residues in helix 2 and the loop connecting helices 2 and 3 bind to a cleft in the hsc70 ATPase domain (Greene et al., 1998; Suh et al., 1998; Kim et al., 2001). Hsc70 has two domains: the ATPase domain and the substrate-binding domain. As a chaperone protein, T antigen interacts with the hsc70 ATPase domain to stimulate ATPase activity and

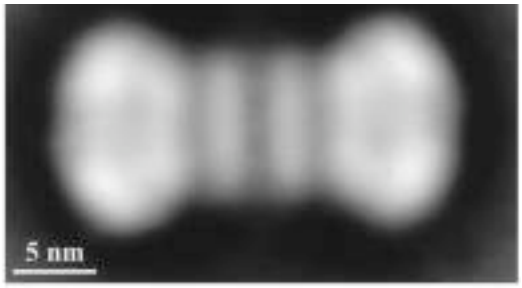

Figure 6: Digital image processing of the T antigen double hexamer at the SV40 origin of replication. Refined average image from a total of 1,010 particles. The image was filtered to the calculated resolution of 2.8 nm (Valle et al., 2000).

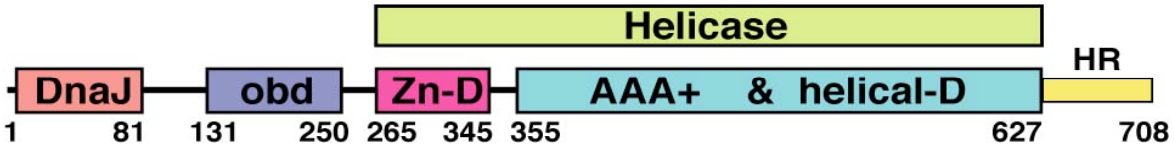

Figure 7: Cartoon representation of the known T antigen domain structures. Amino acid numbers are indicated at the bottom. The functional domains are represented by open boxes and are labeled accordingly. The linkers between domains are represented by thin lines. The C-terminal domain from residue 628 to 708, which contains the host-range fragment (aa 682-708), is labeled HR (in yellow). The HR domain is thought to be unstructured (Gai et al., 2004a).

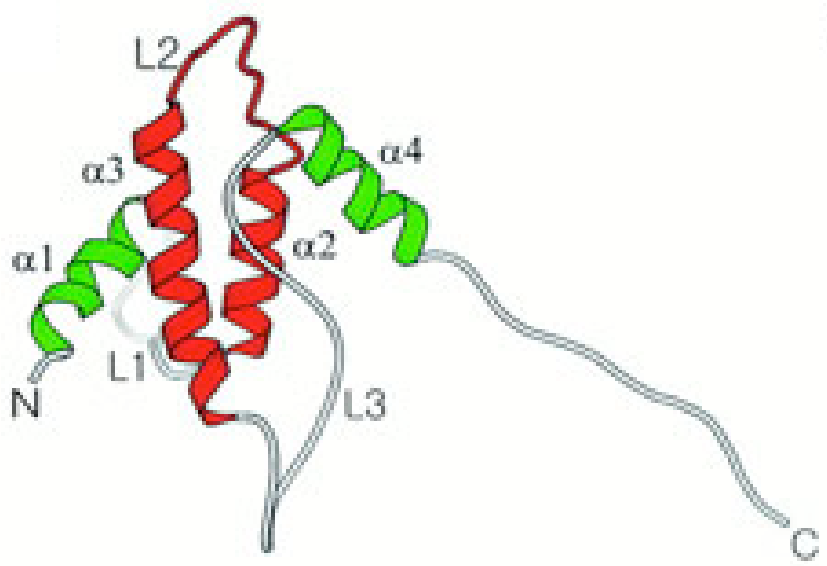

Figure 8: Overall structure of the DnaJ domain of SV40 large T antigen (aa 7-117). The two central helices and connecting loop are colored red, surrounding helices are in green and the other loops are colored gray (Kim et al., 2001).

release of the substrate peptides from the substrate-binding domain of hsc70 (Srinivasan et al., 1997).

T antigen interacts with the Retinoblastoma (Rb) tumor suppressor protein to induce the cell from quiescence to S phase (Chen & Paucha, 1990; Christensen & Imperiale, 1995; Zalvide & DeCaprio, 1995; Srinivasan et al., 1997). Like many other Rb-binding proteins, T antigen interacts with Rb through a loop with the LXCXE motif of T antigen. In addition, helices 2 and 4 (Figure 8) are also involved (Kim et al., 2001). The interaction between T antigen and Rb disrupts the activity of Rb to regulate the E2F transcription factor (Bullock, 1997; Ahuja et al., 2005). The E2F family has eight members, all of which contain a DNA binding domain to regulate the expression of E2F-regulated genes (Sullivan & Pipas, 2002; Ahuja et al., 2005). In quiescent cells, E2F-regulated genes, many of which encode proteins required for replication, are not expressed because Rb forms a complex with E2F to prevent transcription activation. Inactivation of Rb by phosphorylation, catalyzed by a cyclin-dependent kinase, releases E2F and leads to the gene transcription. T antigen disrupts the interaction between Rb and E2F through two different mechanisms. One mechanism involves the chaperone activity of T antigen. The J domain of T antigen recruits hsc70 and the substrate-binding domain of hsc70 in turn binds the Rb-E2F complex (Sullivan & Pipas, 2002). T antigen stimulates the ATPase activity of hsc70 to free E2F from the complex (Sullivan & Pipas, 2002). The other mechanism is independent of the chaperone activity of T antigen, but it is less efficient than chaperone-mediated release of Rb (Sullivan & Pipas, 2002).

Origin recognition is the first step of DNA replication as shown in Figure 2 (Stenlund, 2003).The T antigen-OBD from amino acids 131 to 259 is responsible for

recognizing the viral DNA origin (Arthur et al., 1988; Joo et al., 1997). This domain is sufficient for sequence-specific binding to the SV40 origin (Arthur et al., 1988; Bullock, 1997). The T antigen-OBD also plays a role in oligomerization, DNA structural distortions including melting and untwisting the SV40 origin, non-specific dsDNA and ssDNA binding, DNA unwinding, helicase activity and RPA binding (Dornreiter et al., 1992; Melendy & Stillman, 1993; Luo et al., 1996; Bullock, 1997; Joo et al., 1997; Weisshart et al., 1998; Meinke et al., 2006).

The NMR structure of the T antigen-OBD (Figure 9) shows that it consists of a central five-stranded antiparallel β-sheet flanked by two α-helices on one side and one α-helix and one 3_{10}-helix (right-handed helical structure) on the other (Luo et al., 1996). Elements 147-159 (A1) and 203-207 (B2), two closely juxtaposed loops, are involved in direct contact with the GAGGC pentanucleotide sequences in the binding sites (Simmons et al., 1990a; Luo et al., 1996). The most important residues for origin-specific binding are Asn153, Thr155 and Arg204 (Luo et al., 1996). Ser147, Ser152, Val205 and Ala207 also participate in sequence specific binding at origin (Simmons et al., 1990a). The surface of the DNA binding site is very hydrophobic with regions of positive potential near Arg154 and Arg204 (Figure 9). Furthermore, Ala149, Phe159 and His203 in elements A1 and B2 are involved in nonspecific double stranded and single stranded DNA binding (Simmons et al., 1990b). These residues that are involved in non-specific contacts with DNA are essential for helicase activity, while the residues required for origin-specific binding are not needed for helicase activity (Simmons et al., 1990b).

The helicase domain contains a zinc-finger subdomain and an AAA+ ATPase subdomain. The zinc finger region is essential for the assembly of stable T-antigen

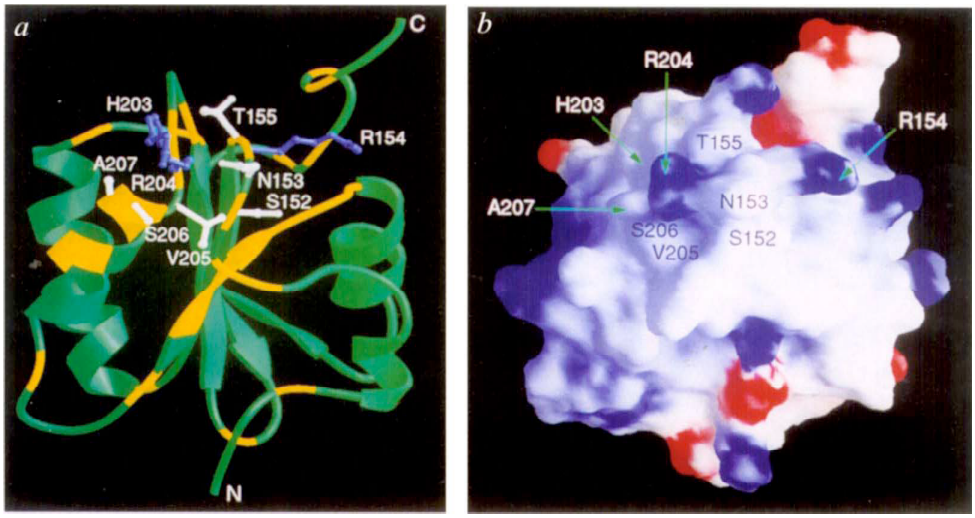

Figure 9: DNA binding surface of T antigen-OBD. (a) Ribbon diagram of T antigen-OBD with perturbed regions in the GAGGC (part of the sequence in the panlindrome region of SV40 DNA origin) titration colored in yellow. All the resonances with significant perturbations are shown. The side chains of residues in elements A1(aa 147-159) and B2 (aa 203-207) are drawn. (b) Molecular surface of T antigen-OBD shown in the same orientation as (a). T antigen-OBD was colored by local electrostatic potential. Blue and red represent positive and negative charges respectively (Luo et al., 1996).

hexamers at the origin of DNA replication (Loeber et al., 1991). AAA+ domains are found in many proteins involved in remodeling protein–DNA complexes. The helicase domain (aa 251-627) can form a hexamer by itself that has functional helicase activity (Li et al., 2003; Gai et al., 2004b). The structure of the helicase domain in hexamer formation has been solved (Figure 10). The hexamer of the helicase domain contains a long positively charged channel with an unusually large central chamber that binds both ssDNA and dsDNA (Li et al., 2003). On the hexameric channel surface are six β hairpin structures and loops, emanating from each of the six subunits (Shen et al., 2005). At the tips of the β hairpins and the loop structures are two ring-shaped residues, His513 and Phe459, respectively (Shen et al., 2005). Additionally, two positively charged residues, Lys512 and Lys516, are near the tip of the β- hairpin (Shen et al., 2005). These four residues form DNA contacts that are critical for T antigen helicase function (Shen et al., 2005). T antigen has an all-or-none nucleotide-binding mode unlike the sequential binding of nucleotide model of other known hexameric molecular machines (Gai et al., 2004b). Conformational changes between all-or-none nucleotide-binding states are thought to link to the mechanism of T antigen unwinding function (Gai et al., 2004b). With the structural data available, a model is proposed as shown in Figure 11. In the nucleotide free state, the β hairpins are in a relaxed state (Gai et al., 2004b). When T antigen binds ATP, the β hairpins move toward the center of the double hexamer by about 17Å, which is proposed to push/pull dsDNA into the double hexamer by about 5-6 bp, promoting strand separation and propelling ssDNA extrusion from the side channel. ATP hydrolysis and ADP release cause the hairpins to move towards their nucleotide free

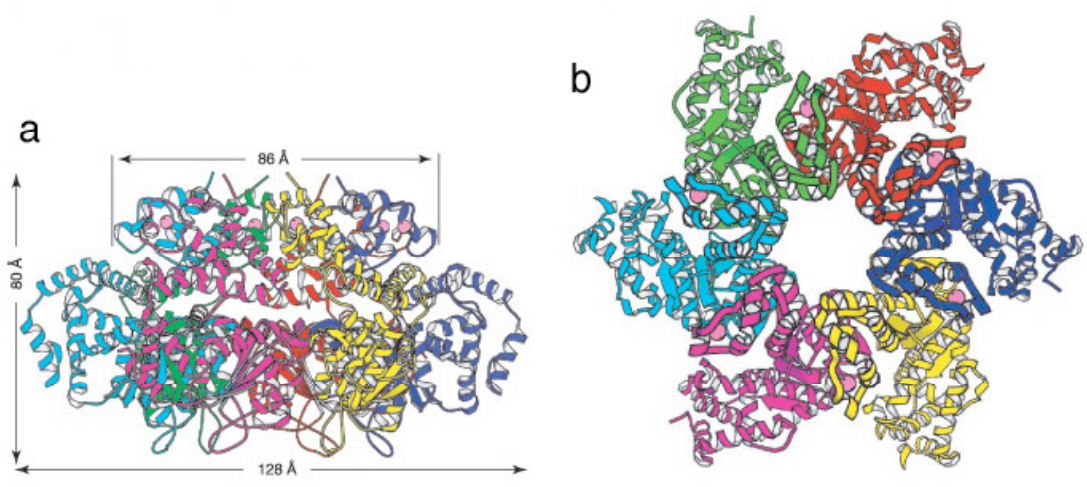

Figure 10: Side (a) and top (b) views of the T antigen residues 251–627 hexameric structure. The pink balls represent zinc atoms. Each monomer is depicted with a distinct color (Li et al., 2003).

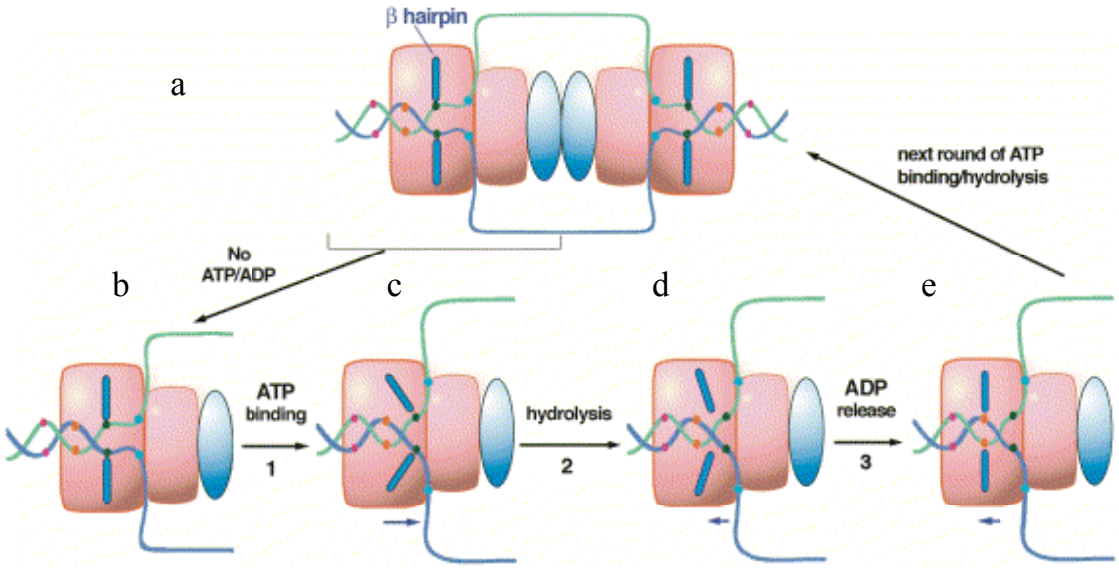

Figure 11: A looping model showing the coupling of the β hairpin movement to the dsDNA translocation into the T antigen double hexamer for unwinding. The β hairpins move along the central channel in response to ATP binding (step 1), hydrolysis (step 2), and ADP release (step 3). (a) T antigen double hexamer with two ssDNA loops coming out from the side channels. Each hexamer contains a helicase domain (represented by two rectangles in pink) and an OBD (oval in light blue). The β hairpin structure is represented by two bars (in blue) within the helicase domain. The colored dots on the DNA (red, orange, black, and blue) are position markers for translocation. (b) A T antigen hexamer corresponding to the left half of the double hexamer in (a) in the nucleotide-free state. (c) The movement of β hairpins upon ATP binding, which serves to pull dsDNA into the helicase for unwinding. The unwound ssDNA extrudes from the side channels. For clarity, only one hexamer is shown. (d) The β hairpins move back about halfway toward the nucleotide-free position after ATP hydrolysis. (e) The ADP is released from the T antigen hexamer, and the β hairpins return to the original Nucleotide-free position (Gai et al., 2004b).

status, ready for the next cycle of ATP binding and hydrolysis during DNA unwinding (Gai et al., 2004b).

The helicase domain of T antigen interacts with a tumor suppressor p53 to block the growth-suppressive functions of p53. T antigen down regulates p53 by several mechanisms (Sullivan & Pipas, 2002). First, T antigen blocks p53 function through direct interaction. T antigen binding induces dramatic conformational changes in the DNA-binding region of p53 (Lilyestrom et al., 2006). When complexed with T antigen, T antigen occupies the whole p53 DNA-binding surface and likely interferes with formation of a functional p53 tetramer (Lilyestrom et al., 2006). Second, T antigen can also block p53 transcriptional activation and growth arrest in a manner independent of p53 binding (Quartin et al., 1994; Rushton et al., 1997). That inhibition requires the N-terminus of T antigen including the J domain and the LXCXE motif.

T antigen is a multiple functional protein with multiple posttranslation modifications. T antigen has two clusters of phosphorylated serines and theronines, one at the N-terminus and the other at the C-terminus (Fanning & Knippers, 1992). Most of the phosphorylation directly affects the binding to origin DNA or origin unwinding but has no effect on the ATPase or helicase activity of T antigen (Fanning & Knippers, 1992) . T antigen is hypophosphorylated when translated in the cytoplasm; but because most kinases phosphorylate T antigen in the nucleus, hyperphosphorylaeted T antigen accumulates in the nucleus. This hyperphosphorylated form of T antigen cannot support SV40 DNA replication either *in vivo* or *in vitro*. Dephosphorylation of T antigen by PP2A (protein phosphotase 2A) prepares it for viral replication (Fanning & Knippers, 1992). However, purified T antigen expressed in *E. coli* doesn't support SV40 DNA

replication, suggesting unphosphorylated T antigen doesn't support replication. Studies found that Thr124 phosphorylation is required for viral replication both *in vivo* and *in vitro* (Fanning & Knippers, 1992).

Replication Protein A structure and function

Human single-stranded DNA binding protein, Replication Protein A (RPA), was first identified as a cellular protein essential for SV40 DNA replication *in vitro* (Wobbe et al., 1987; Fairman & Stillman, 1988; Wold & Kelly, 1988). The primary function of RPA is to protect ssDNA from nucleases and to inhibit hairpin formation. In addition, RPA aids the sequential assembly and disassembly of many proteins involved in DNA metabolism. Thus RPA is crucial for cell proliferation and cell survival.

RPA has three subunits: RPA70, RPA32, and RPA14 (named after their molecular weights in kDa as shown in Figure 12). It is a modular protein with multiple domains connected by flexible linkers. There are four DNA binding domains (DBDs) in RPA. DBDs A, B, C are located in RPA70 and DBD D in the RPA32 subunit.

RPA70 is composed of several functional domains: an N-terminal domain (aa 1-110, termed RPA70N), DBD A (aa 181-290), DBD B (aa 301-422) and DBD C (aa 436-616) (Bochkareva et al., 2002). RPA70N has an oligonucleotide/oligosaccharide-binding (OB) fold (Figure 13)(Daughdrill et al., 2001); but binds only weakly to ssDNA because two conserved aromatic amino acids essential for DNA binding are missing (Bochkarev & Bochkareva, 2004). RPA70N interacts with many proteins in DNA metabolism such as p53 and other transcription factors (Fanning et al., 2006). Therefore, it plays an important role in the threshold response to DNA damage in DNA damage signaling pathways. The

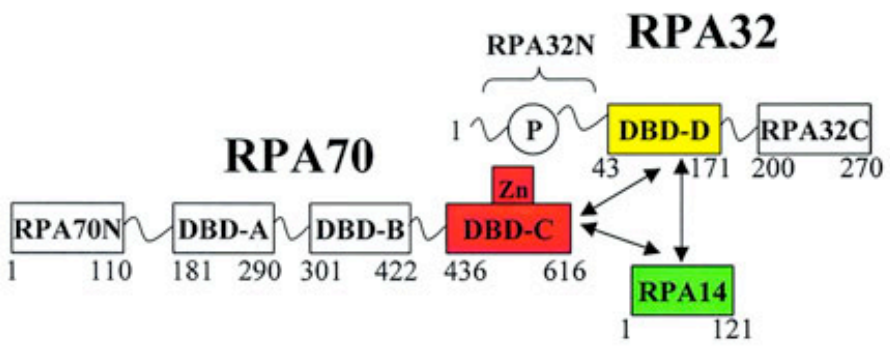

Figure 12: Schematic showing the RPA domain structure. Domains are presented as boxes, amino acid positions of their borders are as indicated. Zn, zinc ribbon; P, unstructured, phosphorylated N-terminus of subunit RPA32. Domains comprising the trimerization core are colored in red, yellow and green (for DBD-C, DBD-D and RPA14, respectively). The regions of subunit interaction are indicated by arrows (Bochkareva et al., 2002).

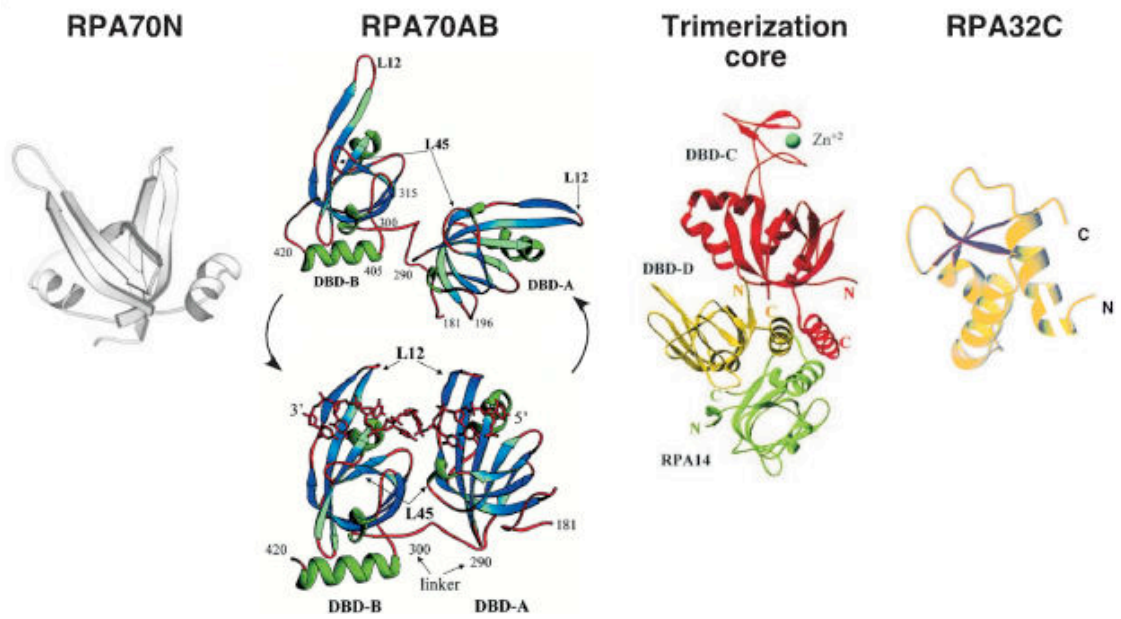

Figure 13: Structural models of several domains of RPA (Jacobs et al., 1999; Mer et al., 2000; Bochkareva et al., 2001; Bochkareva et al., 2002).

structures of RPA70AB with or without DNA (Figure 13) were determined by X-ray crystallography (Bochkarev et al., 1997; Bochkareva et al., 2001). RPA70A and 70B, two OB folds, are connected by a short flexible linker, which is unstructured without DNA (Bochkareva et al., 2001). NMR data also confirmed that the linker is flexible enough to allow the two domains to move independently of each other (Arunkumar et al., 2003). In the presence of ssDNA, RPA70AB aligns in a fixed position with the linker parallel to the bound oligonucleotide, but on the opposite side of the protein as shown in Figure 13 (Bochkarev et al., 1997). DBD C is distinct from other OB folds since it has two structural insertions: a zinc ribbon between the first and second β strands and a three-helix bundle between the third and fourth β strands as indicated in Figure 13 (Bochkarev & Bochkareva, 2004). Zinc (II) is essential to stabilize the tertiary structure of DBD C and the DNA binding activity of DBD C is modulated by zinc (Bochkareva et al., 2000). RPA mutant with a point mutation in DBD C, which retains unwinding activity and the activity to stimulate pol-prim and polymerase δ, nevertheless abolishes SV40 DNA replication completely (Lin et al., 1998). The three-helix bundle in DBD C interacts with RPA32 and RPA14 to form a heterotrimer.

RPA32 has three functional regions: N-terminus (aa 1-40, RPA32N) (Gomes et al., 1996), central DBD D (aa 43-171) (Bochkarev et al., 1999) and C-terminus (aa 200–270) (Mer et al., 2000). Ser23 and Ser29 are phosphorylated in a cell-cycle dependent manner (Dutta & Stillman, 1992). In addition, RPA32N is hyperphosphorylated *in vivo* in response to various genotoxic agents (Liu & Weaver, 1993; Gately et al., 1998). Phosphorylation regulates DNA replication and repair since RPA32N hyperphosphorylation prevents RPA from associating with chromosomal replication

centers in human cells (Vassin et al., 2004). Phosphorylated RPA32N interacts with RPA70N, which suggests that phosphorylation might cause conformational changes in the RPA complex to regulate RPA function (Binz et al., 2003; Bochkareva et al., 2005). RPA32C adopts a winged helix-loop-helix structure (Figure 13). The structure includes a three-helix bundle and three-stranded β sheet that interacts with multiple proteins (Mer et al., 2000). RPA32C is important for different DNA repair processes by interacting with DNA repair proteins such as UNG2, XPA and Rad52 (Mer et al., 2000).

RPA14 contains a single OB fold, but like RPA70N, it lacks two conserved aromatics. Thus it has little or no affinity for ssDNA. The main function of RPA14 is to stabilize the RPA trimer complex (Wold, 1997).

RPA binds ssDNA with specific polarity, from 5' to 3' (de Laat et al., 1998; Iftode & Borowiec, 2000). The binding affinity for ssDNA decreases from DBD A to D. The multiple DNA binding domains of RPA allow it to bind ssDNA with different modes as illustrated in Figure 14. First, DBD A positions and initiates binding of RPA complex to ssDNA. Since DBDs A and B are connected by a very short linker, the local concentration of DBD B is very high once DBD A binds ssDNA (Arunkumar et al., 2003). DBD A has low affinity for ssDNA by itself, while DBD A together with DBD B direct stable, high-affinity binding to ssDNA (Arunkumar et al., 2003; Wyka et al., 2003). This binding mode, called the compact form, occupies about 8 to 10 nucleotides with an affinity of 0.18×10^9 M^{-1} (Blackwell & Borowiec, 1994; Blackwell et al., 1996). Then DBD C, together with DBDs A and B, bind in a transient form that covers about 12 to 23 nucleotides (Bastin-Shanower & Brill, 2001). Finally all four DBDs contact ssDNA in an extended form that occupies about 30 nucleotides with the highest affinity of 2.6 x

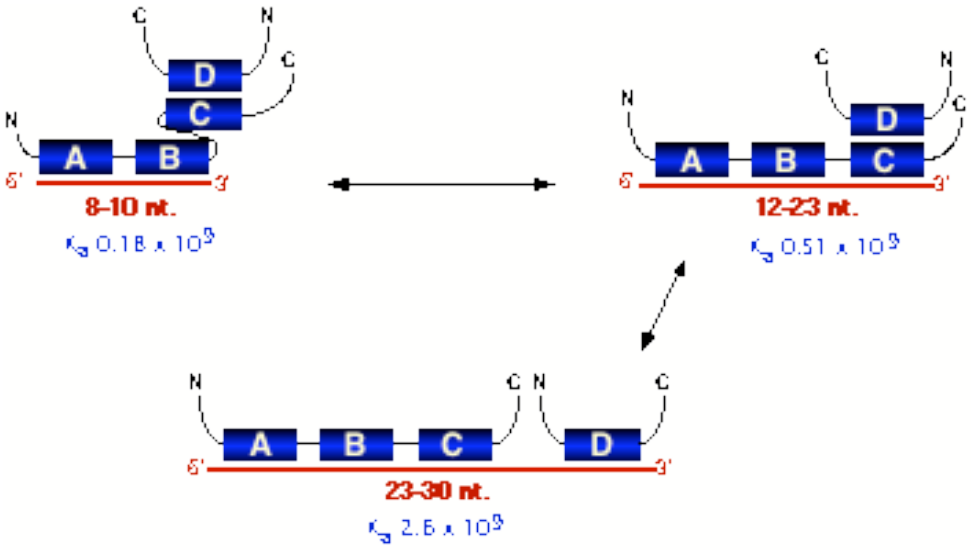

Figure 14: RPA binds ssDNA with different binding modes. The four DBDs of RPA are represented with boxes. The domains are proposed to bind ssDNA in a sequential fashion with domains A and B binding the first 8-10 nt. Subsequent binding by DBDs C and D require the indicated lengths of ssDNA (Ott, 2002).

$10^9\ M^{-1}$ (Blackwell et al., 1996; Bastin-Shanower & Brill, 2001; Kim & Park, 2002). The three different binding modes suggest that RPA adopts different structural conformations, consistent with scanning transmission electron micrographs and gel filtration (Blackwell et al., 1996). DBD D has the weakest ssDNA binding activity compared to other DBDs. Thus the exchanges between binding to and dissociation from ssDNA happen rapidly, making DBD D a natural target for unloading RPA.

RPA interacts with multiple proteins and is involved in many aspects of cellular activities. RPA70N, RPA70A, 70B and RPA32C are common interaction sites for a variety of proteins, many of which interact with two or more sites on RPA (Fanning et al., 2006). RPA70A alone has been reported to be sufficient to interact with papillomavirus E1 helicase (Loo & Melendy, 2004), SV40 T antigen (Loo & Melendy, 2004; Park et al., 2005). RPA70AB together is reported to interact with SV40 T antigen, primase subunit of pol-prim and Rec Q family Werner and Bloom Syndrome helicases (Dornreiter et al., 1992; Nasheuer et al., 1992; Braun et al., 1997; Shen et al., 2003).

DNA polymerase α-primase structure and function

Human DNA polymerase α-primase (pol-prim) is a heterotetrameric protein, consisting of p180, p68, p58 and p48 subunits (named after their molecular weights in kDa). P180 and p48 are the catalytic subunits of DNA polymerase and primase respectively (Pizzagalli et al., 1988; Wong et al., 1988; Nasheuer et al., 1991; Santocanale et al., 1993). Pol-prim initiates DNA replication by synthesizing short RNA primers *de novo* on leading and lagging strand templates. It requires divalent magnesium ions and has no associated 3' to 5' exonuclease activity (Fisher & Korn, 1981).

P180 belongs to the DNA polymerase B family whose conformation resembles a human right hand composed of three distinct domains designated as palm, thumb, and fingers (Hubscher et al., 2002). The minimum length of primer that can interact with the polymerase subunit effectively is eight nucleotides. P180 is divided into three domains: an N-terminal protein interaction domain (aa 1-329), a core polymerase domain (aa 330–1279), and a C-terminal domain (aa 1235–1465) (Mizuno et al., 1999; Hubscher et al., 2002). The N-terminus of p180 interacts with the helicase domain of T antigen (Dornreiter et al., 1990; Weisshart et al., 1996). The core domain contains all the conserved regions responsible for DNA binding, dNTP binding, and phosphoryl transfer (Mizuno et al., 1999; Hubscher et al., 2002). The C-terminal domain is dispensable for catalysis but necessary for the interaction with p68 and p58 (Mizuno et al., 1999).

P68 interacts with p180 and facilitates both the expression and the nuclear import of p180 (Mizuno et al., 1996; Mizuno et al., 1998). P68 is required for priming in the presence of RPA and T antigen, during initiation at replication origins and lagging strand replication (Foiani et al., 1994; Ott et al., 2002).

The heterodimeric DNA primase (p48 and p58) is associated with p180 and p68 (Arezi & Kuchta, 2000). P58 contains a nuclear localization signal that can direct both p58 and the p58/48 complex to the nucleus (Arezi & Kuchta, 2000). The function of p58 is to stabilize p48, increase primase efficiency, and regulate the length of primers synthesized by primase (Arezi & Kuchta, 2000). Structural studies of the p48 subunit reveal that the active sites of the enzyme contains three aspartic acids that interact with NTP (Ito et al., 2003). P48 interacts with p180 through the p58 subunit and p48 also interacts with RPA (Dornreiter et al., 1992; Nasheuer et al., 1992; Copeland & Wang,

1993; Braun et al., 1997). RPA enhances both the processivity and fidelity of primer extension by pol-prim and other SSBs cannot replace RPA for these function (Braun et al., 1997; Maga et al., 2001), suggesting the interaction of primase dimer with RPA is essential for primer synthesis.

Hand off model

DNA replication is a highly coordinated process that involves many proteins that work cooperatively to ensure the accurate and efficient replication of DNA (Waga & Stillman, 1998). These proteins assemble and disassemble when needed and do not exist as a pre-assembled, ready for action machinery (Kowalczykowski, 2000; Mer et al., 2000). The dynamic nature of this process is thought to allow different levels of regulation and also recycling of the commonly used proteins such as RPA and PCNA (Kowalczykowski, 2000; Stauffer & Chazin, 2004b).

Cells adopt several mechanisms to assemble and disassemble protein complexes. One widely used mechanism is a "hand-off" model, the successive exchange of proteins on DNA, a term coined by Dr. John Tainer in 2000 (Mol et al., 2000; Tainer & Friedberg, 2000). Proteins are described as "trading places" from the aspect of DNA (Yuzhakov et al., 1999a; Yuzhakov et al., 1999b; Stauffer & Chazin, 2004b). As shown schematically in Figure 15 (Stauffer & Chazin, 2004b), two proteins interact via two weak binding sites. The assembly of the protein complex might involve both of the binding sites or either of the binding sites. A third protein only needs to bind one of the binding sites to disrupt the interaction in the complex and another protein may come in to form a new complex.

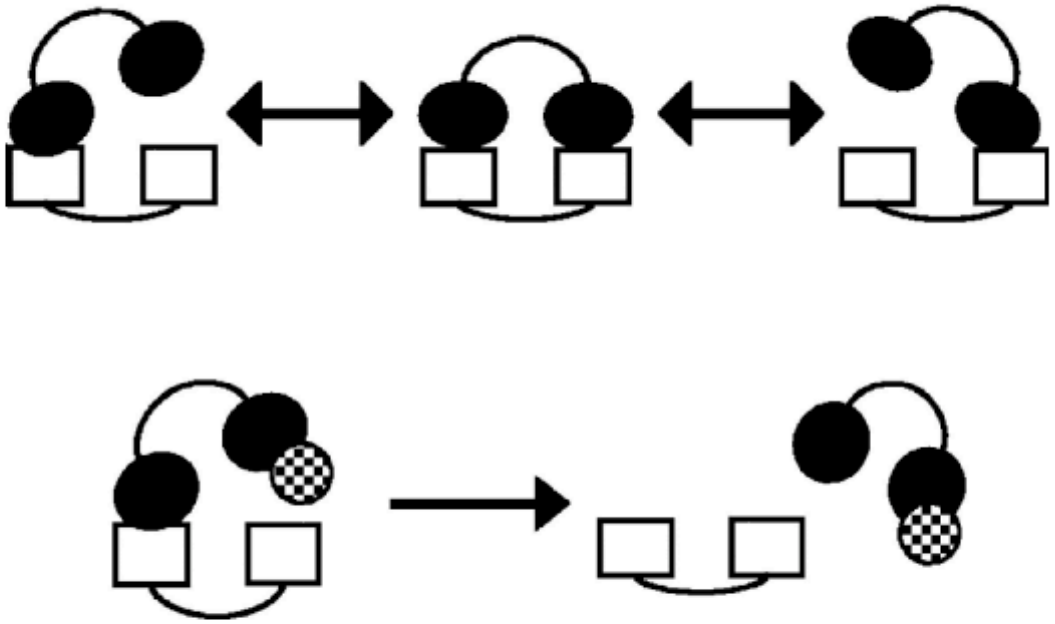

Figure 15: Key concepts in DNA processing. The upper panel symbolizes the interaction between two multidomain proteins (A, two open rectangles; B, two filled ovals) that have two contact points. The overall affinity between the two proteins results from two modest affinity interactions, each of which has an appreciable off rate. This corresponds to one representation of the linkage effect. The lower panel represents the facilitation of hand-off in this system. A third protein (checked circle) needs to bind to only one of the two domains of protein B to drastically reduce the overall binding affinity and promote release of B from A (Stauffer & Chazin, 2004b).

RPA is required for protecting ssDNA during DNA metabolism but it needs to be removed from ssDNA for other proteins to function later. The hand off mechanism is proposed to be commonly used in removing RPA (Mer et al., 2000; Fanning et al., 2006). For example, during eukaryotic homologous recombination, RPA binds ssDNA to protect it and remove secondary structures. RPA is later replaced by Rad51 to form the Rad51 filament. In yeast, Rad52 facilitates displacement of RPA from ssDNA by forming a transient complex with RPA and ssDNA while concurrently binding Rad51 (Sugiyama & Kowalczykowski, 2002). Rad52 probably remodels RPA from its extended binding mode to the compact binding mode, thus facilitating Rad51 loading (Fanning et al., 2006). These data led me to hypothesize that the same hand-off mechanism is involved in removing RPA during SV40 DNA replication or even host chromosomal DNA.

Initiation of SV40 DNA replication

T antigen is both the initiator and helicase for SV40 replication. It assembles around the origin as a double hexamer in the presence of ATP and Mg++ as shown in Figure 6 (Mastrangelo et al., 1989; Dean et al., 1992). T antigen induces melting of 8 nt within the early panlindrom region (Borowiec & Hurwitz, 1988). Once T antigen distorts the dsDNA, it shifts to a DNA helicase mode and the OBD binds ssDNA non-specifically. As a helicase, T antigen works as a double hexamer to pump in dsDNA (Moarefi et al., 1993). RPA is necessary to protect the newly exposed ssDNA during SV40 DNA unwinding process. Pol-prim is recruited to replication origins through interacting with T antigen to start primer synthesis. Primase first synthesizes about 8-10 nt and then the polymerase in the same pol-prim complex elongates the primer to 30 nt (Copeland &

Wang, 1993). Later, Pol δ, a more processive and error-free DNA polymerase, takes the place of the pol-prim to elongate the new DNA strand (Figure 1).

The initiation of SV40 DNA replication can be reconstitute *in vitro* with four purified proteins, T antigen, RPA, pol-prim, and Topoisomerase I, and a plasmid with SV40 origin (Matsumoto et al., 1990). In this assay, synthesis of radiolabeled DNA depends on T antigen assembly on the SV40 origin DNA, unwinding of the duplex, and synthesis of RNA primers that can then be extended. Radiolabeled replication products are analyzed by denaturing gel electrophoresis, followed by autoradiography. Different protein mutants have been tested in this assay in Chapters II and III. Electrophoretic Mobility Shift Assay (EMSA, also called native gel electrophoresis) is a useful tool for identifying proteins that interact with DNA. The electrophoretic mobilities of free DNA and DNA/protein complexes are different in native (non-denaturing) polyacrylamide gel. Radiolabeled DNA is used to identify the position of free DNA or DNA/protein complex. EMSA has been used to test the interactions among T antigen, RPA and DNA in Chapters II and III.

During the initiation of DNA replication, the interaction between T antigen and RPA is essential for primer synthesis (Weisshart et al., 1998). As I began my thesis work, the mechanism of this interaction remained unknown. Although T antigen-OBD interaction with RPA70AB domain had been extensively studied, the details of this interaction remained unclear. *E.coli* SSB can replace RPA in unwinding. Since *E.coli* SSB doesn't interact with T antigen, this result suggests that only ssDNA binding activity is needed. One might expect that ssDNA protection during unwinding is unrelated to protein-protein interaction. Moreover, T antigen relieves the inhibition of primer

synthesis of pol-prim on RPA-saturated ssDNA, suggesting that this may be the step at which the RPA/T antigen interaction is critical. In homologous recombination, RPA is thought to be displaced by a hand-off mechanism as discussed before (Mer et al., 2000; Sugiyama & Kowalczykowski, 2002). We hypothesized that the same mechanism of unloading RPA happens during SV40 DNA replication initiation.

At the time I began my thesis, it was not clear how many binding sites of RPA were involved in T antigen interaction. The importance of RPA32C for SV40 DNA replication remained controversial. Studies had demonstrated that an antibody that recognizes RPA32C could block DNA replication and pol-prim stimulation by RPA (Kenny et al., 1990). In addition, Lee and Kim showed that the RPA32C deletion mutant was impaired in SV40 replication assay (Lee & Kim, 1995). On the other hand, Braun et al. revealed that RPA32C deletion mutants functioned well in SV40 replication assay (Braun et al., 1997). Braun et al. argued that the defect observed by Lee's group was due to RPA conformational changes caused by deletion (Braun et al., 1997). The C-terminus of RPA might be important for DNA replication since several SSBs has a C-terminus essential for DNA replication, such as phage T4 gene 32, phage T7 gene 2.5 and *E. coli* SSB. T7 gene 2.5 acidic C-terminus interacts with gene 5 polymerase to recruit gene 5 to replication forks (Hamdan et al., 2005). The C-terminus of *E. coli* SSB interacts with χ subunit of RFC to help the clamp loading process (Kelman et al., 1998; Yuzhakov et al., 1999a; Yuzhakov et al., 1999b).

The goal of my dissertation research was to study the interaction between T antigen and RPA and if possible to develop models for the functional importance of this interaction. In the following two chapters, I focus on the detailed mapping of the

interaction between T antigen and RPA. The work in Chapters II and II were carried out in close collaboration with Dr. Chazin's lab to reveal the mechanism of the initiation of DNA replication at atomic level. We found that RPA32C interaction with T antigen-OBD is critical for primer synthesis during the initiation of SV40 DNA replication, while RPA70AB interaction with T antigen is essential for T antigen loading RPA onto ssDNA in concert with SV40 origin DNA unwinding. Taken together, our data suggest that T antigen-mediated RPA remodeling is essential for loading onto and unloading from ssDNA.

CHAPTER II

INSIGNTS INTO HRPA32 C-TERMINAL DOMAIN-MEDIATED ASSEMBLY OF THE SIMIAN VIRUS 40 REPLISOME[1]

Introduction

The fundamental biochemical steps in eukaryotic DNA replication were first elucidated in studies of a simple but powerful model system, the cell-free replication of the simian virus 40 (SV40) genome. A single viral protein, large T antigen (Tag), orchestrates the entire replication process in primate cell extracts. Tag directs the initiation of viral replication by specifically binding to the SV40 origin of DNA replication, assembling into a double hexameric helicase that unwinds the duplex DNA bidirectionally, and recruiting cellular initiation proteins (Fanning & Knippers, 1992; Bullock, 1997; Simmons, 2000; Stenlund, 2003). The progression of SV40 replication requires a ssDNA-binding protein, replication protein A (RPA), which binds to the free ssDNA generated by the Tag helicase, and together with Tag, enables primer synthesis and extension by DNA polymerase alpha-primase (pol-prim). The host replication machinery carries out all subsequent steps.

The molecular mechanism for the coordinated activities of Tag and human RPA (hRPA) in initiation of SV40 DNA replication in not known. It has become increasingly apparent that DNA processing events involve modular proteins that contain multiple

[1] Arunkumar, A. I*., Klimovich, V*., Jiang, X., Ott, R. D., Mizoue, L., Fanning, E., and Chazin, W. J. (2005). Structural and functional insights into RPA32 C-terminal domain-mediated assembly of the simian virus 40 replisome. Nat. Struc. Mol. Biol., 12(4):332-9, *These authors contributed equally to this work.

structural/functional domains and have multiple points of contact (Stauffer & Chazin, 2004b). Tag and RPA are both modular proteins (Bullock, 1997; Wold, 1997; Iftode et al., 1999; Mer et al., 2000; Bochkarev & Bochkareva, 2004; Gai et al., 2004a; Weisshart et al., 2004) and the activity of hRPA in initiation of viral DNA replication correlates well with its ability to interact physically with Tag; budding yeast RPA and bacterial single-standed DNA-binding proteins that support origin unwinding but not initiation bind poorly to Tag (Collins & Kelly, 1991; Dornreiter et al., 1992; Melendy & Stillman, 1993). These results and other genetic and biochemical data strongly suggest that direct physical interactions between Tag and RPA are crucial for initiation of SV40 replication.

To elucidate the molecular mechanism that coordinates Tag-hRPA activities in initiation of replication, the interaction site(s) between the two proteins must be mapped. The Tag origin DNA-binding domain (Tag-OBD) has been identified as an RPA interacting site (Weisshart et al., 1998), and the 70 kDa subunit of RPA was shown to be involved in Tag interactions (Braun et al., 1997). RPA32C, a winged helix-loop-helix, is a known protein interaction module (Mer et al., 2000), but its role in Tag interactions as well as in SV40 replication has been controversial (Lee & Kim, 1995; Braun et al., 1997). Here, we demonstrate that RPA32C does indeed interact with Tag and in fact, plays a critical role in stimulating the initiation of SV40 replication. These findings show that the interaction between Tag and RPA involves multiple contact points, a critical feature that we incorporate into a refined mechanistic model for primer synthesis during SV40 replication.

Materials and methods

Protein preparation

Human RPA32C was expressed and purified as described (Mer et al., 2000), except the final reversed phase high performance liquid chromatography (HPLC) step was replaced by a gel filtration column using HiLoad 16/60 Superdex 75 (Amersham Pharmacia). Yeast RPA32C domain was cloned into the same vector (pET15b), expressed in BL21 (DE3) cells, and purified in a similar manner as hRPA32C. Point mutants were generated by QuikChange (Stratagene) site-directed mutagenesis following vendor protocols, including: RPA32C E252A, E252R, Y256A, S257A, T267A, D268A and D268R; Tag R154A and R154E.

Recombinant RPA heterotrimers were expressed in *E. coli* and purified as described (Henricksen et al., 1994). Single amino acid substitutions in RPA32 of the hRPA heterotrimer were introduced by QuikChange.

SV40 Tag, topoisomerase I, and pol-prim were purified as described (Ott et al., 2002).

$Tag_{131\text{-}259}$ (Tag-OBD) was cloned into an in-house pSV278 expression vector, which contains a 6x His tag followed by an N-terminal MBP fusion and a thrombin cleavage site before the insert. The fusion protein was purified over Ni-NTA. After thrombin cleavage and another passage over Ni-NTA, the protein was further purified over MonoS 10/10 and HiLoad 16/60 Superdex 75 (Amersham Pharmacia).

Uniformly enriched ^{15}N and $^{13}C,^{15}N$ samples were prepared in minimal medium containing 1 g/L $^{15}NH_4Cl$ (CIL, Inc.) and 2 g/L unlabeled or [$^{13}C_6$] glucose (CIL, Inc.),

respectively. The DNA duplex [d(GCAGAGGCCGA).d(TCGATTCTTGC)] was purchased from Midland Certified Co. and used without further purification.

NMR spectroscopy

All NMR samples were concentrated to 100 μM in a buffer containing 2 mM DTT, 5 mM MgCl2, and 20 mM Tris-d11 at pH 7.0. NMR experiments were performed at 25 ºC using a Bruker AVANCE 600 MHz NMR spectrometer equipped with a single axis z-gradient Cryoprobe. Two-dimensional, gradient-enhanced ^{15}N-^{1}H HSQC and TROSY-HSQC spectra were recorded with 4K complex data points in the ^{1}H and 200 complex points in ^{15}N dimension. The ^{13}C-^{1}H HSQC spectra were acquired with 4096 x 600 complex data points. Attempts to obtain NOE distance constraints for the intermolecular interface by acquiring ^{13}C,^{1}H-filter, edited spectra were unsuccessful, presumably due to the intrinsically low sensitivity of the experiments and the relatively short lifetime of the complex.

To determine K_d for the interaction between RPA32C and Tag-OBD, a series of spectra were acquired after addition of unlabeled RPA32C into a 100 μM solution of ^{15}N-labeled Tag-OBD. Additions were made such that 8 to 12 HSQC spectra were recorded starting with a molar ratio of 1:0 (labeled:unlabeled) up to a ratio of 1:10. The pH of the sample after each addition was monitored and corrected if necessary. Changes in amide proton and amide nitrogen chemical shifts of Thr199 and His203 were fit to a standard single-site binding equation as described previously (Arunkumar et al., 2003).

Residual dipolar couplings (D_{NH}) were measured using the strain-induced gel alignment procedure (Jares & Blow, 2000; Tycko et al., 2000). Briefly, a 4%

polyacrylamide gel with an inner diameter of 6 mm was soaked with a solution of the complex containing ^{15}N-enriched RPA32C or Tag-OBD with unlabeled partner protein at a molar ratio of 1:3 (labeled:unlabeled). After soaking for 24 hours at 4^{o} C, the sample was stretched into the NMR tube using the funnel like device described by Bax(Bax, 2003). Residual dipolar couplings were determined from the difference between one bond ^{15}N-^{1}H splittings ($^{1}J_{NH} + {}^{1}D_{NH}$) measured in the absence and presence of alignment media. The splittings were measured using a combination of HSQC and TROSY spectra. A total of 65 useable $^{1}D_{NH}$ values were obtained, 28 from RPA32C and 37 from Tag-OBD. Back-calculation of residual dipolar couplings from the structure of the complex was carried out using the program PALES (Zweckstetter & Bax, 2000). NMR data were processed using XWINMR (Bruker) and analyzed using either FELIX2000 (Accelrys, Inc.) or Sparky (Goddard & Kneller).

Structure calculations

The structure of the complex was modeled using HADDOCK (Dominguez et al., 2003) run on a home-built Linux cluster. The chemical shift perturbation data along with the solvent accessibility of the interacting side chains (calculated using the program NACCES; http://wolf.bms.umist.ac.uk/naccess) was used to obtain a set of ambiguous interaction restraints (AIRs) as described in the HADDOCK manual. The target distance of these constraints was set to 3.0 Å and all other parameters were set to the default values. A rigid body docking procedure was used to obtain 1500 conformers of the RPA32C-Tag complex using only the AIRs, van der Waal's energy and electrostatic terms using the program CNS (Brunger et al., 1998). The 200 best conformers based on

the intermolecular energy were subsequently used for semi-flexible simulated annealing followed by refinement using explicit water. Residues 249-257, 259-262 and 266-270 of RPA32C, and 152-156, 181-182, 199-204 and 255-258 of Tag-OBD were allowed to be flexible in all stages of the docking procedure. Cluster analysis using an RMSD cut-off of 1.5 Å revealed two clusters, with 189 conformers in one and only 4 conformers in the other. The structure of the complex is represented by an ensemble of 20 conformers with lowest energy. The single representative structure (with the lowest energy) was used to back calculate $^{1}D_{NH}$ for comparison to the experimental values. Structures were visualized and figures were generated using MolMol (Koradi et al., 1996).

SV40 DNA replication (monopolymerase) assay

A published protocol (Matsumoto et al., 1990) was modified as follows: reaction mixtures (20 μl) contained 250 ng of supercoiled pUC-HS plasmid DNA (2.8 kb) containing the complete SV40 origin (Ott et al., 2002), 200 ng of RPA, 300 ng of topoisomerase I, 100 to 400 ng of pol-prim as indicated in the figure legends, and 250-750 ng of Tag in initiation buffer (30 mM Hepes-KOH (pH 7.9), 7 mM magnesium acetate, 10 μM $ZnCl_2$, 1 mM DTT, 4 mM ATP, 0.2 mM each GTP, UTP, and CTP, 0.1 mM each dGTP, dATP, and dCTP, 0.02 mM dTTP, 40 mM creatine phosphate, 40 μg/ml of creatine kinase supplemented with 3 μCi of [α-^{32}P] dTTP (3,000 Ci/mmol; Dupont NEN, Boston, MA). Reactions were carried out and results evaluated as described previously (Podust et al., 2002). Primer synthesis reactions were identical except that 20 μCi of [α-^{32}P] CTP (3,000 Ci/mmol; Dupont NEN) was the labeled nucleotide and the

dNTPs and the ATP regenerating system were omitted. Products were analyzed as described (Ott et al., 2002).

T antigen-dependent primer synthesis and extension assays on ssDNA

The reaction mixture was identical to that in the SV40 monopolymerase assay except that the template was generally 100 ng of M13mp18 ssDNA (USB Corp., Cleveland, OH) that had been pre-incubated for 20 min on ice with a saturating amount of RPA. After the pre-incubation, the remaining components were added and the assay was completed as described for the monopolymerase assay. Singly primed template ssDNA was prepared by mixing 4.2 pmol each of M13mp18 and a 17-mer sequencing primer (-40 primer, USB Corp.), heating at 60 ^{o}C for 2 min and annealing at room temperature. The product was purified by 1% agarose gel electrophoresis and extracted from the gel using a kit (Qiagen). The primer extension reaction was carried out as described above, except that the singly primed ssDNA was substituted for unprimed ssDNA in the pre-incubation with RPA, and that ribonucleotides, Tag, creatine phosphate, and creatine kinase were omitted.

Results

An RPA32C antibody inhibits initiation of SV40 replication

Our studies were initiated based on the observation that an antibody against RPA32 (Ab34A) specifically inhibited SV40 DNA replication in crude extracts in vitro (Kenny et al., 1990). Ab34A has little effect on the ssDNA binding activity of RPA, its ability to

support origin DNA unwinding, or to stimulate DNA polymerase delta activity, but it does inhibit RPA stimulation of DNA polymerase alpha activity (Kenny et al., 1990). To map the epitope recognized by Ab34A, human RPA (hRPA) and yeast RPA (yRPA), as well as hRPA carrying mutations in RPA32, were tested in western blots (Figure 16). Ab34A detected hRPA32 but not yRPA32 (Figure 16c, lanes 1 and 2). hRPA32C alone (residues 172-270) was sufficient to bind Ab34A (lane 3), but an hRPA chimera with hRPA32C substituted by the yeast domain (hRPAy32C) did not bind Ab34A (lane 4). Moreover, deletions of 33 or 48 residues from the C-terminus of hRPA32, which are predicted to destroy the globular structural domain of RPA32C, also prevented binding of Ab34A (lanes 5, 6). These data imply that the antibody recognizes an epitope in the winged helix-loop-helix domain of RPA32.

To confirm that Ab34A inhibits initiation of SV40 DNA replication, monopolymerase reaction assays (Matsumoto et al., 1990) were performed using purified proteins. In this assay, synthesis of radiolabeled DNA depends on Tag assembly on the SV40 origin DNA, unwinding of the duplex, and synthesis of RNA primers that can then be extended. Radiolabeled products were analyzed by denaturing gel electrophoresis, followed by autoradiography. Robust DNA replication occurred in a positive control reaction carried out in the absence of antibody (Figure 16d, lane 12). Negative control reactions yielded no detectable products (Figure 16d, lanes 4, 5 and 9-11). Addition of Ab34A inhibited initiation in a dose-dependent manner, but the presence of a non-immune control antibody had no effect (Figure 16d, compare lanes 1-3 with 6-8).

Previous studies with Ab34A indicated that the antibody did not interfere with origin DNA unwinding (Kenny et al., 1990), suggesting that it might inhibit the

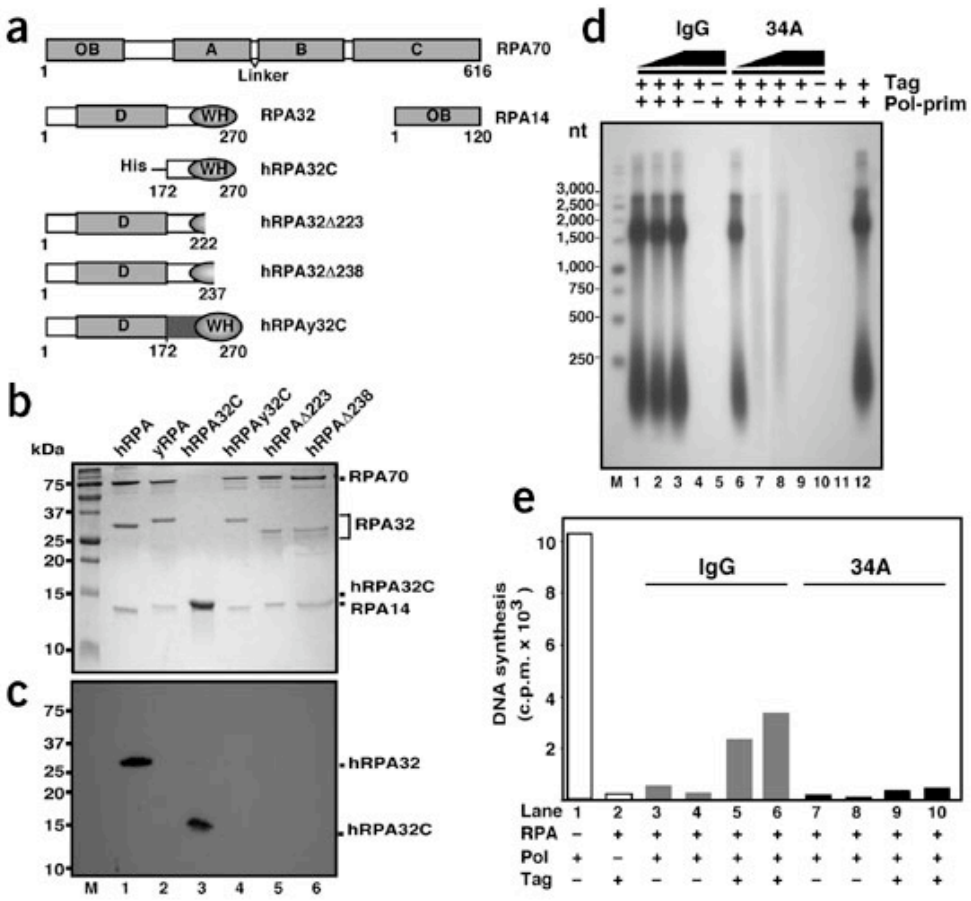

Figure 16: Monoclonal antibody 34A recognizes hRPA32C and inhibits SV40 replication. (a) hRPA subunits and mutant proteins used in this study. Residue numbers are listed below each construct. OB, oligonucleotide-oligosaccharide binding folds, including the ssDNA-binding domains A-D; WH, winged helix-loop-helix domain. (b) Purified recombinant hRPA proteins were analyzed by 15% (w/v) SDS-PAGE and Coomassie blue staining. M, protein markers of indicated mass. (c) Western blot assay of the proteins shown in b, probed with 34A monoclonal antibody and visualized by chemiluminescence. (d) Ab34A IgG or nonimmune mouse IgG was titrated into SV40 monopolymerase assays reconstituted with purified recombinant proteins. Products were resolved by alkaline agarose gel electrophoresis and visualized by autoradiography. Lanes 1-3 and 6-8, reactions containing 100, 300 or 500 ng of the indicated antibody. Control reactions carried out in the presence of 500 ng of antibody and in the absence of Tag or pol-prim are indicated (-). M, DNA size marker of the indicated length in nucleotides (nt). (e) Primer synthesis and extension on M13mp18 ssDNA (25 ng) preincubated with 500 ng (lanes 3, 5, 7 and 9) or 750 ng (lanes 2, 4, 6, 8 and 10) of hRPA was tested in the presence of 250 ng pol-prim and 500 ng of either nonimmune IgG (lanes 3-6) or Ab34A (lanes 7-10). Control reactions with pol-prim alone (lane 1) and in the absence of pol-prim (lane 2) are indicated (-).

subsequent primer synthesis and elongation steps in initiation. To determine if RPA32C is required for these processes, ssDNA saturated with hRPA was used as a template for synthesis of unlabeled primers and extension into radiolabeled DNA products by pol-prim. Priming is inhibited on ssDNA saturated with RPA, but in the presence of Tag, pol-prim assembles into a functional primosome capable of primer synthesis on the RPA-ssDNA template (Matsumoto et al., 1990; Collins & Kelly, 1991; Melendy & Stillman, 1993). As expected, robust primer synthesis and elongation was observed on naked ssDNA template (Figure 16e, lane 1), but when the ssDNA was saturated with RPA, little synthesis was detected (lanes 3, 4, 7, 8). Addition of Tag stimulated priming and elongation in the presence of the non-immune control antibody (compare lanes 5 and 6 with 3 and 4). However, in the presence of Ab34A, Tag failed to stimulate priming and elongation (compare lanes 9 and 10 with 5 and 6). Hence, Ab34A interferes with the ability of Tag to mediate priming and elongation by pol-prim. Together, these data suggest a possible physical interaction between Tag and hRPA32C that facilitates priming and extension.

RPA32C interacts specifically with the Tag-OBD

We tested for direct interaction between Tag and hRPA32C using affinity chromatography experiments. Initial experiments suggested an interaction with the Tag-OBD. To confirm this observation, the Tag-OBD was passed over columns (I, II, III) containing increasing amounts of hRPA32C attached to the stationary phase (Figure 17a). After vigorous washing, the eluted fractions were collected and separated on SDS-PAGE. Eluates from the hRPA32C column contained increasing amounts of Tag-OBD as the

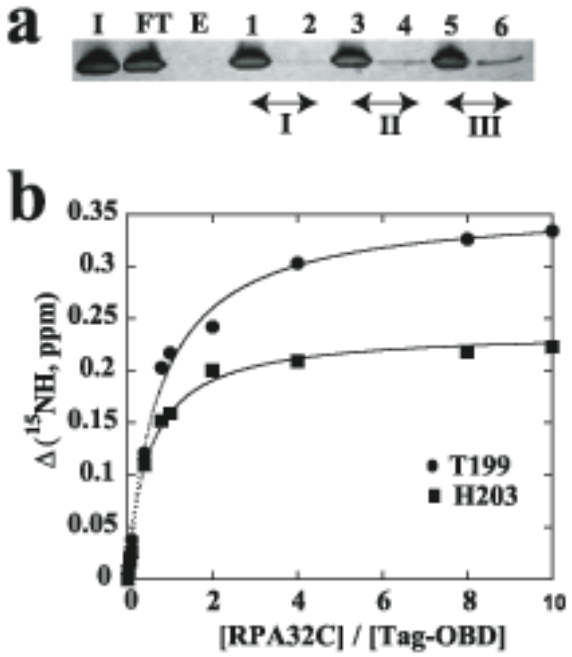

Figure 17: The interaction of RPA32C with Tag-OBD. (a) Tag-OBD affinity chromatography. Lanes, from left to right: I, column input; FT and E are the flow-through and elution fractions from the control column; 1 and 2 are flow-through and elution fractions from column I; 3 and 4 are flow-through and elution fractions from column II, 5 and 6 are flow-through and elution fractions from column III. (b) NMR ^{15}N chemical shift titration curves for the binding of RPA32C to ^{15}N-labeled Tag-OBD. The changes in amide nitrogen chemical shifts of T199 (circles) and H203 (squares) in Tag are plotted against the ratio of Tag-OBD to RPA32C. The line through each curve represents a best fit to the standard single site binding equation.

amount of RPA32C attached to the beads was increased (Figure 17a, lanes 2, 4, 6). To further characterize the interaction, a series of ^{15}N-^{1}H heteronuclear single quantum correlation (HSQC) NMR spectra were acquired for a sample of ^{15}N-enriched Tag-OBD as unlabeled hRPA32C was titrated into the solution. Binding isotherms for two residues, derived from chemical shift changes induced in the Tag-OBD spectra upon addition of increasing amounts of hRPA32C (Figure 17b), were fit to a standard single-site binding equation using the approach described previously (Arunkumar et al., 2003). An average dissociation constant (Kd) of 60 ± 18 μM was obtained from all available data. This binding constant is similar to, but weaker than the Kd of 5-10 μM estimated for the interaction of hRPA32C with peptide fragments from the binding regions of the DNA repair factors XPA and UNG2 (Mer et al., 2000).

Structural model of the complex

The structures of free Tag-OBD (Luo et al., 1996) and hRPA32C (Mer et al., 2000) have been determined previously. These were used together with NMR chemical shift perturbations to identify the binding sites of interaction. Reciprocal titration experiments were carried out using ^{15}N-enriched RPA32C and unlabeled Tag-OBD and vice versa; the perturbed residues identify the binding surface on each molecule (Figures 18 and 19). To determine the structure of the complex, the chemical shift perturbations were used as input to guide a computational docking of the two molecules. The experimental data were sufficient to define a unique relative orientation for the two domains, and multiple refinements converged to an ensemble of conformers with a mean backbone root-mean-square deviation (RMSD) of 0.91 ± 0.17 Å (Table 2). Also, pairwise backbone RMSD

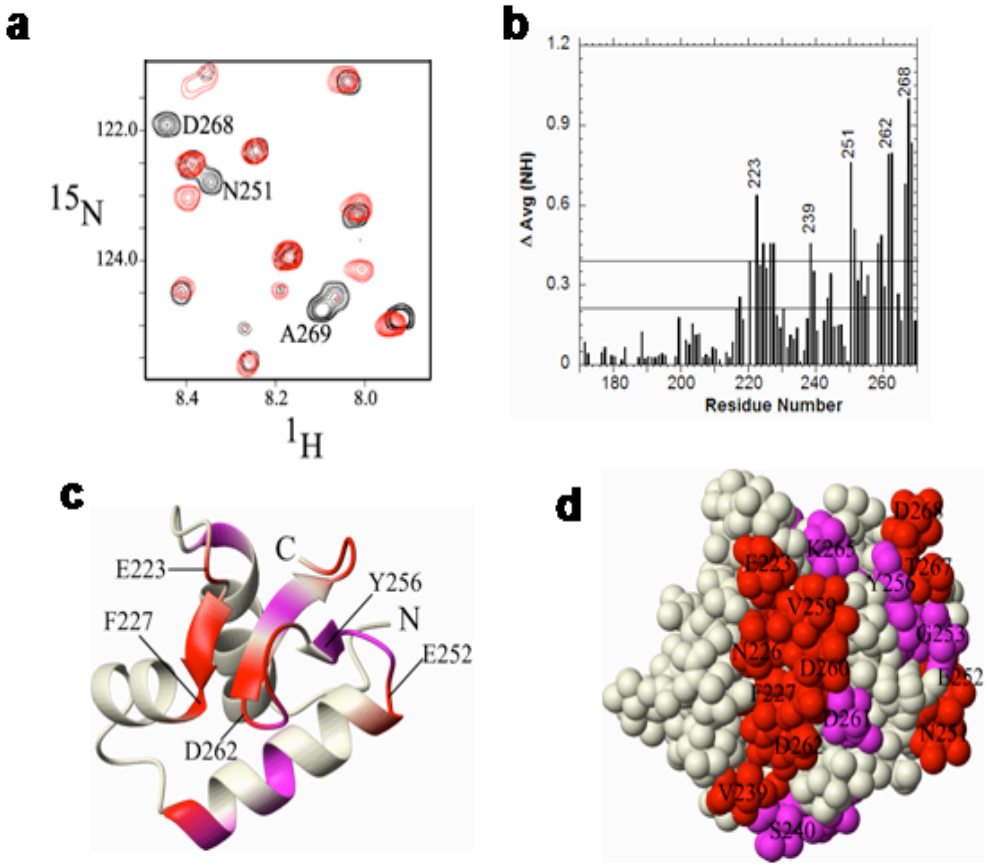

Figure 18: Mapping the Tag-OBD binding site of RPA32C. (a) ^{15}N-^{1}H HSQC spectra of RPA32C in the absence (black) and presence (red) of 2 molar equivalents of Tag-OBD. (b) Bar diagram showing the average chemical shift change (combined amide nitrogen and amide proton) upon addition of 2 molar equivalents of Tag-OBD versus the sequence of RPA32C. The lower bar represents the mean of the data and the upper bar represents the mean plus one standard deviation of the data. (c,d) Chemical shift perturbations mapped on the structure of RPA32C shown as a ribbon and a CPK model (A space-filling model represents the atoms as spheres whose radii are proportional to the atom's van der Waals radius), respectively. Red coloring indicates those residues that show changes above the mean plus one standard deviation. Magenta represents changes above the mean, but below the mean plus one standard deviation.

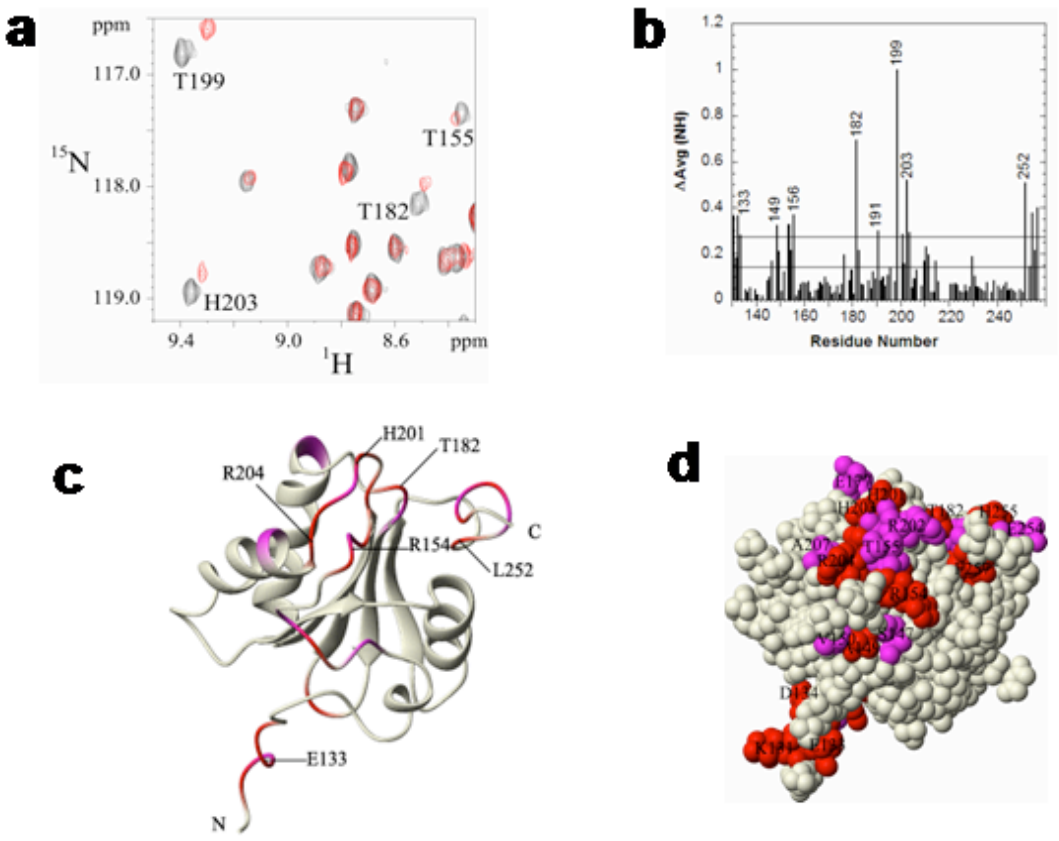

Figure 19: Mapping the RPA32C binding site of Tag-OBD. (a) ^{15}N-^{1}H HSQC spectra of Tag-OBD in the absence (black) and presence (red) of 2 molar equivalents of RPA32C. (b) Bar diagram showing the average chemical shift change (combined amide nitrogen and amide proton) upon addition of 2 molar equivalents of RPA32C *versus* the sequence of Tag-OBD. The lower bar represents the mean and the upper bar represents the mean plus one standard deviation. (c,d) Chemical shift perturbations mapped on the structure of Tag-OBD shown as a ribbon and a CPK model, respectively. Red highlights those residues that show changes above the mean plus one standard deviation, and magenta represents changes above the mean, but below the mean plus one standard deviation.

Table 2. Structural Statistics of the 20 best RPA32C/Tag-OBD model structures[a]

No. of residues used in chemical shift perturbation restraints	
From RPA32C	8
From Tag-OBD	8
Ramachandran analysis[b]	
Residues in the favored region (%)	83
Residues in other allowed regions (%)	16.5
Backbone rmsd (Å) with respect to mean	
All backbone	0.91 ± 0.17
Backbone rmsd (Å) with respect to starting structure	
NMR structure of RPA32C	0.64 ± 0.12
NMR structure of Tag-OBD	0.48 ± 0.13
Surface area buried at the inter-molecular interface ($Å^2$)	1151 ± 93

[a]Structural statistics of the 20 best structures of RPA32C/Tag-OBD complex obtained after flexible docking with HADDOCK followed by refinement in explicit water using ambiguous interaction restraints derived from chemical shift perturbation data. Cluster analysis of the structures was carried out as described in the HADDOCK manual (see Methods section).

[b]Ramachandran analysis was carried out using PROCHECK-NMR (Laskowski et al., 1996).

from the two starting structure of <1Å reveal that the structure of the two domains have not changed to any significant extent in the complex. The similarity of RMSD values for all residues versus those specifically in the interface region indicates the interface is as well defined as the rest of the structure. The absence of significant changes in the structure of the two domains is fully consistent with the modest binding-induced perturbations of the very sensitive NMR chemical parameter.

To validate the structural model, ^{15}N-^{1}H residual dipolar couplings ($^{1}D_{N-H}$) were measured by partially aligning the samples in strained polyacrylamide gels. The observed $^{1}D_{N-H}$ values varied from -3 to 5 Hz for RPA32C and from -5 to 7 Hz for Tag-OBD. The range was sufficiently large for both molecules to enable an accurate comparison to $^{1}D_{N-H}$ values back-calculated from the structure of the complex. There was a good fit between experimental and back-calculated data: the average RMSD for the 20 conformers over all 65 dipolar couplings was only 1.4 Hz. A plot of the experimentally measured values against the calculated values for the representative conformer shows a good correlation (Figure 20c).

Tag and DNA repair factors bind to the same site on RPA32C

In the model of the Tag-OBD/RPA32C complex, the binding surface of RPA32C includes β-strand II, β-strand III and the loop connecting helix III and β-strand II. There is a marked similarity between the RPA32C complex with Tag-OBD and that with the N-terminal binding region of the base excision repair factor UNG2 (Mer et al., 2000). Y256 is of particular note because it is a critical residue in the UNG2/RPA32C interface. The participation of Y256 in the Tag complex is clearly evident in ^{13}C-^{1}H HSQC NMR

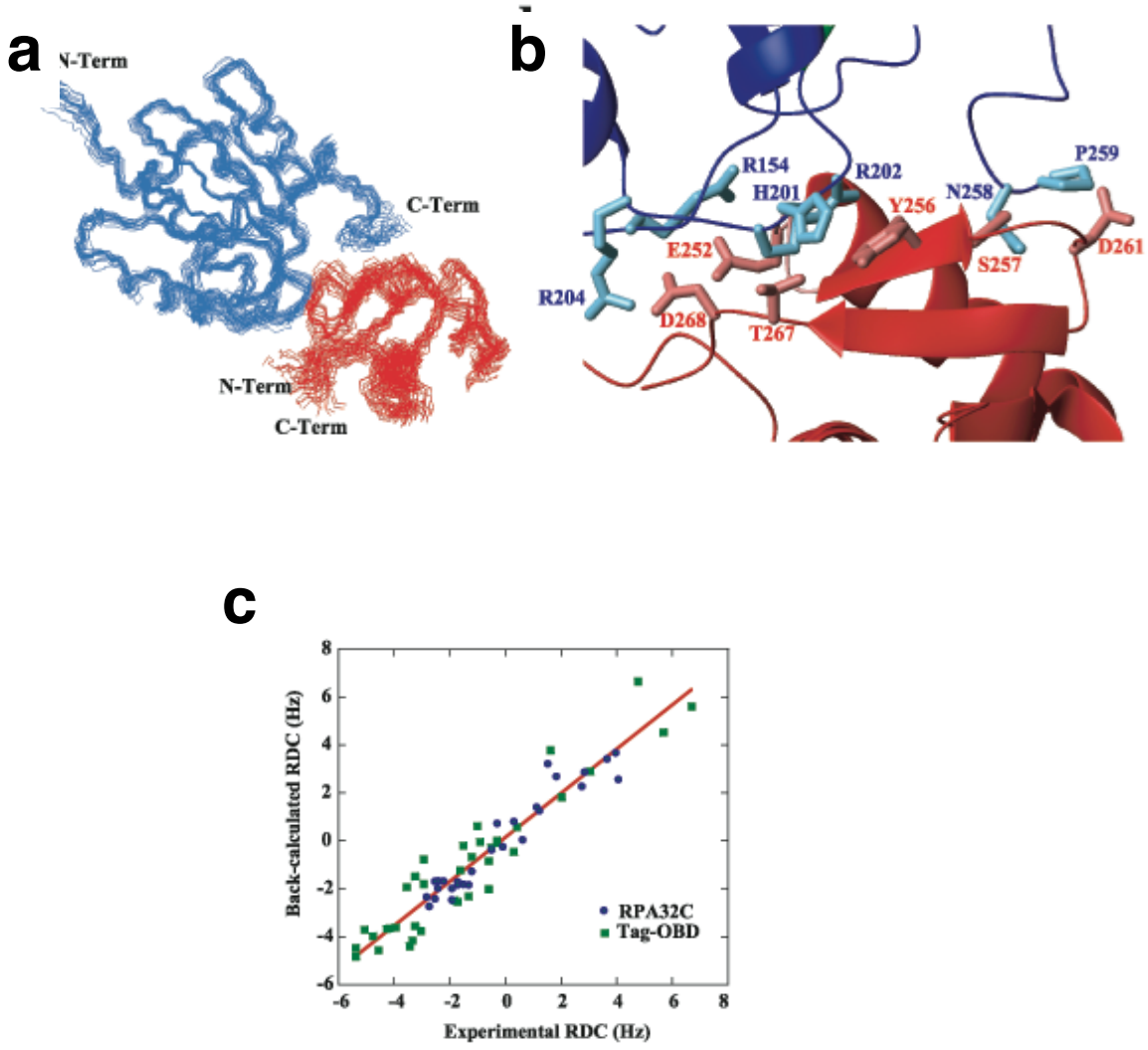

Figure 20: Analysis of Tag-OBD and RPA32C complex. (a) Ensemble of 20 lowest energy conformers of the complex of Tag (blue) and RPA32C (red). (b) Side chains in the binding interface of the representative Tag-OBD/RPA32C structure. Tag-OBD is blue and RPA32C is red. (c) Correlation between the experimentally measured $^{1}D_{NH}$ dipolar couplings (RPA32C, blue circles; Tag-OBD, green squares) versus the values back-calculated from the representative structure.

experiments, which reveal significant perturbations of the aromatic protons of Y256 upon binding to Tag-OBD (Figure 21). Thus, the similarity between the Tag-OBD and UNG2 complexes appears to extend to the specific details at the binding interface.

Although the structures of RPA32C in these complexes are so similar, the structure of the RPA32C-interacting region of Tag-OBD is distinct from those of the DNA repair factors. In particular, UNG2, XPA and RAD52 all interact with RPA32C through a single helix, whereas the Tag-OBD utilizes a compound surface composed of extended loops (Figure 20b). In addition to R154, R202, R204, N258, and P259, two histidines (H201 and H203) in Tag-OBD are in close contact with RPA32C. There is direct experimental evidence of the presence of the histidines in the binding interface: the resonances of the H201 and H203 side chains in the ^{13}C-^{1}H HSQC NMR spectrum are significantly perturbed upon addition of RPA32C to a solution of Tag-OBD (Figure 21). The distinctive character of the Tag-OBD binding site is reflected clearly in the absence of histidine residues in the RPA32C-binding sites of UNG2, XPA and Rad52 (Mer et al., 2000).

RPA32C binds to the same site on Tag-OBD as origin DNA

Detailed analysis of the structure of the complex revealed a significant overlap between the RPA32C-binding surface of Tag-OBD and the previously determined binding site for origin DNA. Three regions of the Tag-OBD (Phe151-Thr155, Phe183-His187, His203-Ala207) have been shown to be essential for origin DNA-specific recognition (Simmons et al., 1990a; Wun-Kim et al., 1993; Luo et al., 1996; Bradshaw et al., 2004). The first indication of similarity between the RPA32C and origin DNA binding sites was

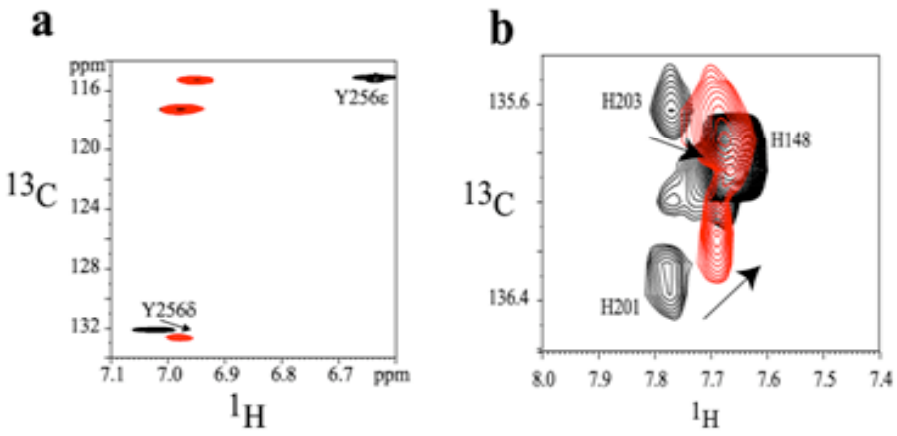

Figure 21: Side chains at the intermolecular interface. (a) Chemical shift changes in the tyrosine side chain of RPA32C in the aromatic region of the $^{13}C/^{1}H$ HSQC spectrum. (b) Chemical shift changes in the histidine side chain of Tag-OBD in the aromatic region of the $^{13}C/^{1}H$ HSQC spectra.

from the analysis of chemical shift perturbations, which showed that residues in these regions of Tag-OBD **s**hift upon addition of RPA32C. Inspection of the model of the Tag-OBD/RPA32C complex reveals that the proposed binding site for RPA32C extends over the top of the deep DNA binding site.

To further confirm the overlap of the Tag-OBD and origin DNA binding sites, a competitive binding experiment was done on the complex of ^{15}N-enriched RPA32C and unlabeled Tag-OBD. A duplex DNA oligomer containing the SV40 origin sequence recognized by Tag, where one strand is 5'-GCAGAGGCCGA-3', was titrated into this solution to see whether the DNA would compete RPA32C off of the OBD. The hRPA32C signals reverted back to the position of free RPA32C upon addition of a stoichiometric amount of DNA (compare Figure 22a and 22b). This experiment also shows that origin DNA binds more tightly to Tag than RPA32C, consistent with the reported K_d values for origin DNA (Titolo et al., 2003; Bradshaw et al., 2004) and that noted above for RPA32C.

Binding site mutations inhibit interaction

In test the importance of the interaction between the RPA32C domain and the Tag-OBD in SV40 replication, point mutations in RPA32C and Tag-OBD were designed based on the structure of the complex. Inspection of the surfaces of RPA32C and Tag-OBD reveals a significant electrostatic complementarity in their binding surfaces (Figure 23). The hRPA32C surface has an acidic character, contributed primarily by Glu252, Asp261, Asp262 and Asp268. Tag-OBD has three arginine residues (Arg154, Arg202, Arg204) contributing to a complementary basic surface. Salt bridges are found in the binding

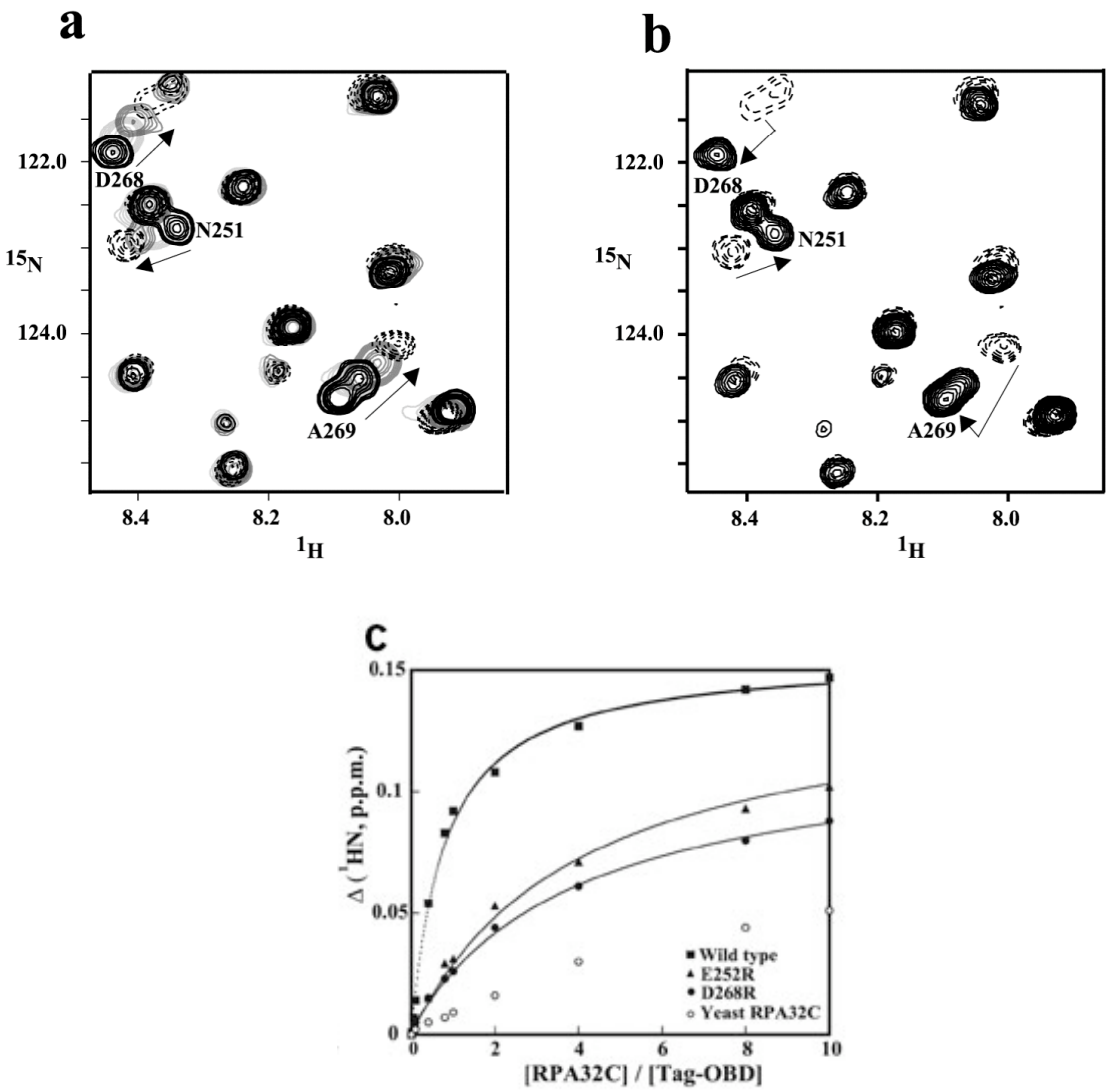

Figure 22: Effects of DNA binding and mutations on the interaction between RPA32C and Tag-OBD. Comparison of the binding of Tag-OBD to RPA32C in the absence (a) and presence (b) of origin DNA. Unlabeled Tag-OBD was titrated into a 100 mM solution of ^{15}N-enriched RPA32C and a series of ^{15}N,^{1}H HSQC NMR spectra were acquired. An overlay of a small region from these spectra is shown in panel a. A stoichiometric amount of origin DNA duplex was then titrated into the solution and an additional spectrum was acquired, as shown in panel b. Arrows are drawn to facilitate following the change in the location of the NMR signal. c) NMR 1H chemical shift titration curves for the binding of wild-type, E252R, E268R and yeast hRPA32C to 15N-labeled Tag-OBD. The changes in amide proton chemical shifts of Thr199 are plotted against the ratio of hRPA32C to Tag-OBD. The line through each curve represents a best fit to the standard single-site binding equation.

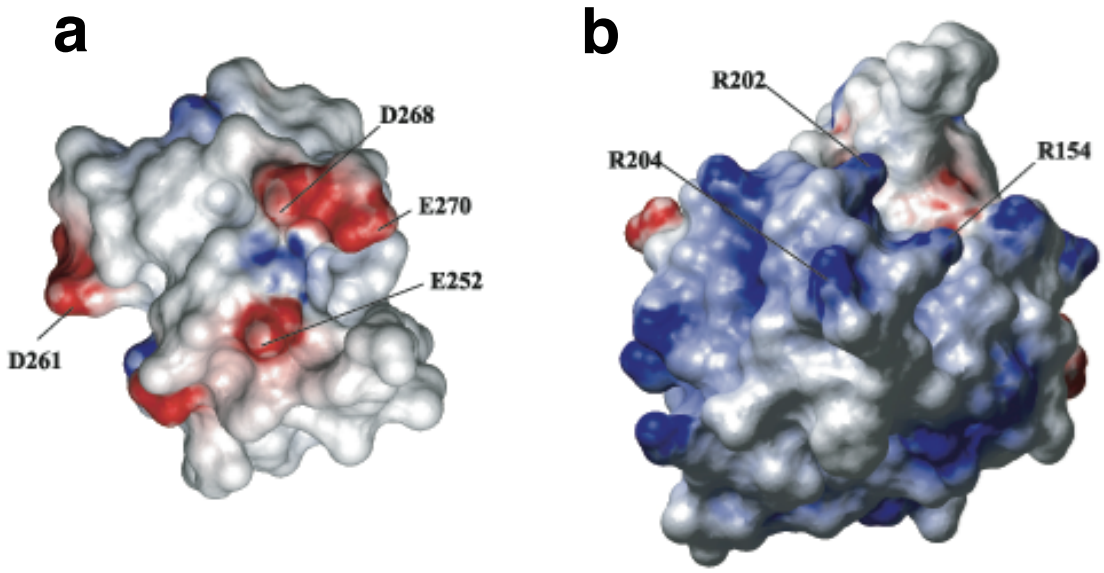

Figure 23: Electrostatic surfaces of the two molecules in the Tag-OBD/RPA32C complex. (a) RPA32C; (b) Tag-OBD. Red and blue colors correspond to negative and positive charge, respectively. Key residues in the binding interface are labeled.

interface, such as those involving Arg154, Arg204 of Tag-OBD with Glu252 and Asp268 of hRPA32C (Figure 20b). The strong electrostatic component of the interaction was confirmed by a salt titration, which revealed that the complex was completely dissociated in 250 mM NaCl. Consequently, the design of mutations was based on perturbing electrostatic interactions.

The effects of mutations were first assayed by biophysical methods to verify the stability, structural integrity and binding properties of the mutant hRPA32C proteins. Characterization of alanine substitutions of hRPA32C residues Glu252, Tyr256 and Asp268 showed that each mutant retained the structure of wild-type protein, but the effect on affinity for Tag-OBD was only very modest. We reasoned that charge neutralization was insufficient because electrostatic interactions are long-range and not highly directional, so the overall effect could be dispersed through the binding interface. A much more marked effect was anticipated for charge-reversal mutants that place an opposite charge in hRPA32C's acidic electrostatic field, and indeed, both E252R and D268R exhibited a more substantial effect on Tag-OBD binding. The binding curves for E252R and D268R demonstrate five- to ten-fold weaker binding compared with that of the wild-type hRPA32C (Kd ≅500 μM versus 60 μM; Figure 22c). These results were confirmed by similar charge-neutralization and charge-reversal mutations in Tag-OBD: a modest reduction in affinity for hRPA32C was observed for R154A but a much stronger effect for R154E (Figure 24). A further test of the proposed importance of electrostatic complementarity between Tag-OBD and hRPA32C involved examining the interaction of Tag-OBD with yRPA32C, which lacks several acidic residues in the hRPA32C-binding site for Tag-OBD (Figure 25). Titration of yRPA32C into Tag-OBD revealed a

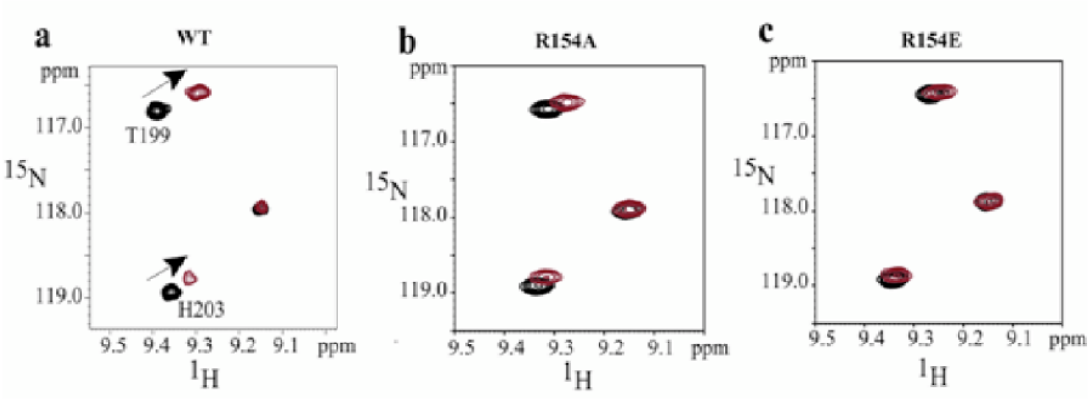

Figure 24: NMR chemical shift analysis of the interaction of wild type and mutant Tag-OBD with RPA32C. (a) Expanded region of the ^{15}N, ^{1}H HSQC NMR spectra of wild-type Tag-OBD in free (black) and in complex with 4 molar excess of RPA32C (red). (b) Expanded region of the ^{15}N, ^{1}H HSQC spectra of R154A mutant in free (black) and in complex with 4 molar excess of RPA32C (red). (c) Expanded region of the ^{15}N, ^{1}H HSQC spectra of R154E mutant in free (black) and in complex with 4 molar excess of RPA32C (red).

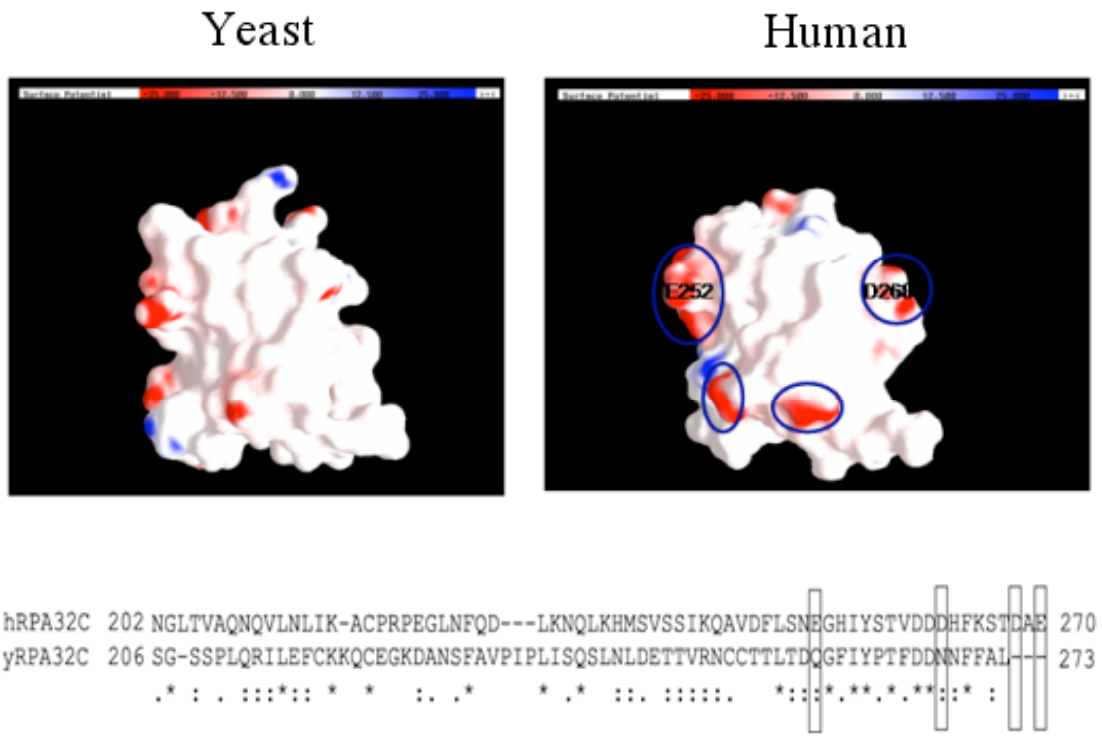

Figure 25: Comparative analysis of human and yeast RPA32C. Electrostatic surface representation of human and yeast RPA32C, generated using hRPA32C coordinates (PDB accession no: 1DPU). Negatively charged residues are red, positively charged—blue. The molecules are in the same orientation. Blue ovals mark the negatively charged patches on human RPA32C surface. Approximate location of the residues used to create charge-reversal point mutants investigated in this study is labeled accordingly. (c) Comparison of the primary sequences of the RPA32C domain from human and yeast. Residues that are important for the interaction with Tag-OBD are shown in boxes (Klimovich, Doctoral Dissertation).

substantially lower affinity than even the most perturbing of the hRPA32C charge-reversal mutations (Figure 22c). Indeed, binding was so weak that the Kd could not be determined, consistent with the considerably lower negative charge of the Tag-OBD binding surface (Figure 25).

RPA32C is required for initiation of SV40 DNA replication

To further assess the functional importance of the proposed Tag-OBD interaction with hRPA32C, hRPA heterotrimers with mutations in hRPA32C were tested in SV40 DNA replication assays using the monopolymerase assay as shown in Figure 26 (Matsumoto et al., 1990). Human RPA, used as a positive control in all assays, supported initiation (for example in Figure 26a, lanes 1 and 2). As expected, yRPA exhibited no activity (lanes 3 and 4). Negative control reactions lacking either Tag or pol-prim yielded no detectable products (lanes 5 and 6). A human-yeast chimera hRPAy32C containing the winged-helix-loop-helix domain from yeast RPA in place of the human domain retained ssDNA binding activity and its RPA70 subunit was active in binding to Tag (Figure 27). However, the initiation activity of hRPAy32C was diminished by an order of magnitude relative to that of hRPA in the same experiment (Figure 26b, compare lanes 1-4 and 5-8), correlating with the weak interaction of yRPA32C with Tag-OBD observed by NMR. Initiation activity increased dramatically in proportion to the amount of hRPA present in the reaction, while the corresponding amounts of hRPAy32C did not stimulate replication (Figure 27). The E252R mutation in RPA32C caused a modest reduction (~20%) in activity relative to wild type hRPA, whereas the D268R mutation substantially impaired initiation activity (~50%) (Figure 26c,d; compare lanes 1-4 and 5-8; Figure 28),

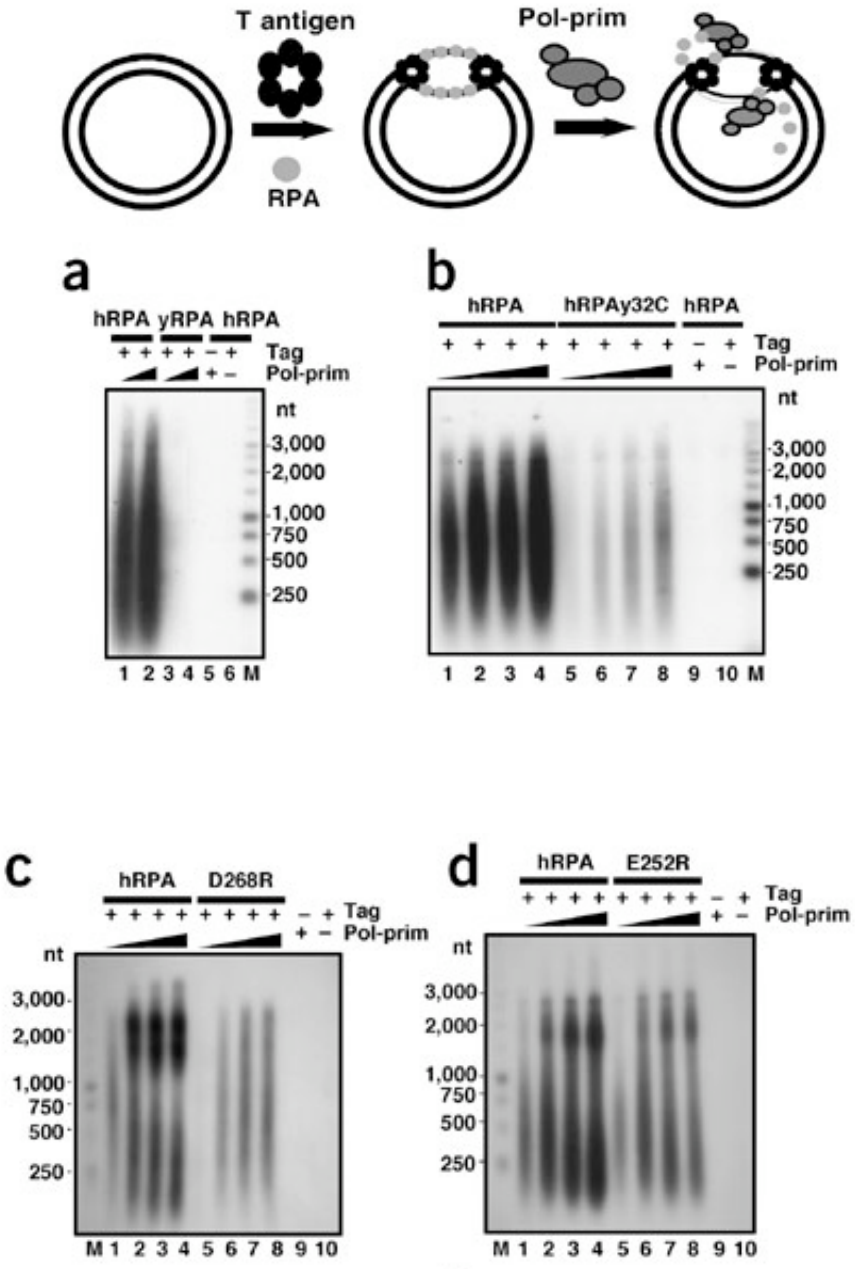

Figure 26: Mutations in hRPA32C that weaken interaction with Tag are defective in initiation of SV40 DNA replication. (a-d) Initiation of replication was tested in monopolymerase reactions containing 200 ng of the indicated hRPA and 300 or 400 (a), or 100-400 ng (b-d), of pol-prim as indicated. Control reactions contained hRPA but lacked either pol-prim or Tag as indicated (-). The products were resolved by alkaline agarose gel electrophoresis and visualized by autoradiography. DNA size markers are indicated (M).

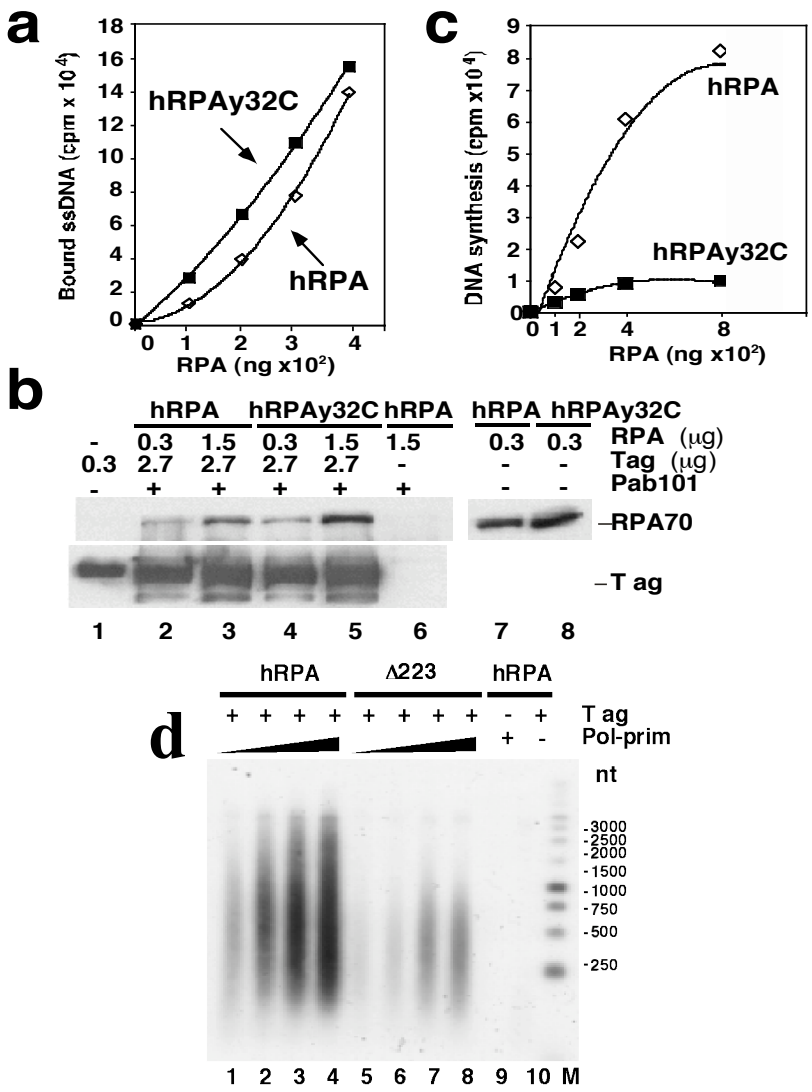

Figure 27: Characterization of the hRPA32C and hRPAy32C mutant proteins. (a) The indicated amounts of hRPA or hRPAy32C were incubated with 2.5 pmol of 32P-end-labeled oligo(dT)30 and bound DNA was quantified by filter-binding and scintillation counting. Diamonds, hRPA; filled squares, hRPAy32C. (b) The indicated amounts of purified hRPA or hRPAy32C were incubated with or without (-) Tag bound to Pab101-coupled Sepharose beads for 30 min at 4oC. After washing, proteins bound to the beads were analyzed by SDS-PAGE and western blotting with antibody against RPA70 (top panel) or Tag (bottom panel). Lanes 1, 7, 8: samples of the input proteins. (c) Initiation activity was tested as in Figure 26b except that the amount of hRPA or hRPAy32C wasvaried as indicated and 200 ng of pol-prim was present in each reaction. Acid-insolubleradiolabeled products in 4 ml of each reaction mix were quantified by scintillation counting. Diamonds, hRPA; filled squares, hRPAy32C. (d) SV40 DNA replication activity of hRPAΔ223 was compared with that of hRPA in monopolymerase reactions.

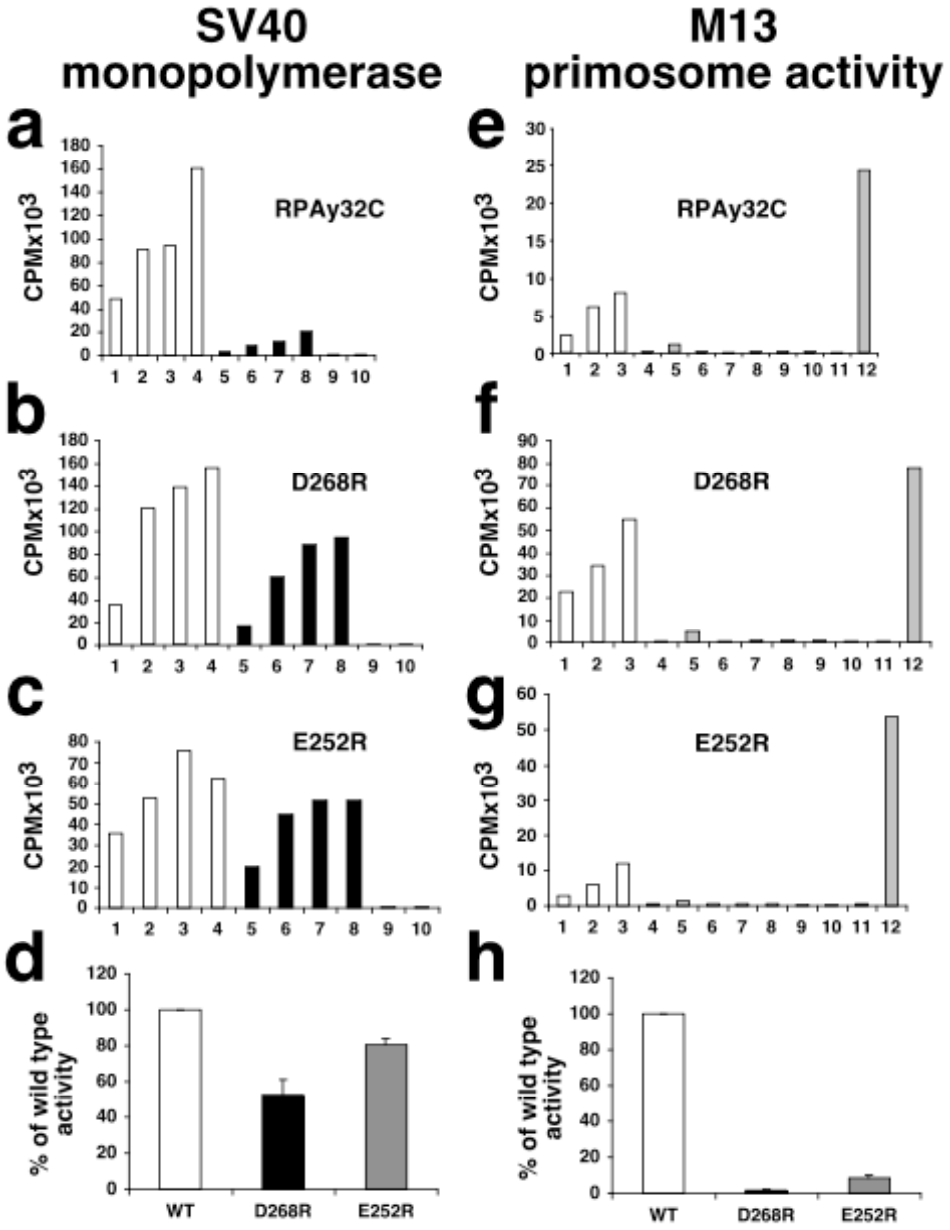

Figure 28: Quantitative comparison of wild type and mutant RPA in replication assays. (a-c) Quantification of typical SV40 monopolymerase assays as in Figures 26b,d (cpm, counts per minute determined by scintillation counting). White bars, wild type hRPA; black bars, mutant activity; gray bars, controls. (d) Mean results of at least two independent monopolymerase experiments showing mutant activity as a percentage of the wild type activity in the same experiment (the same concentration of proteins). Brackets represent standard error. (e-g) Quantification of typical primosome assays as in Figures 29a-e. White, wild type; black, mutant; gray, controls (h) Mean results of at least two experiments showing primosome activity with mutant RPA as a percentage of the wild type activity in the same experiment.

consistent with reduced binding of Tag-OBD to the corresponding RPA32C mutants. The results demonstrate that hRPA32C serves an important function in initiation of SV40 DNA replication, and provide strong support for the structural model of the Tag-OBD/RPA32C complex (Figures 17, 20 and 22).

RPA32C interaction with Tag promotes primer synthesis

Previous studies (Bullock, 1997), as well as the results presented in Figure 16, suggest that the Tag interaction with RPA is crucial for primer synthesis in initiation and in Okazaki fragment synthesis. To ask whether primer synthesis requires the Tag-RPA32C interaction, we first measured the ability of Tag to stimulate the synthesis of radiolabeled RNA primers (8-10 nt) in the SV40 monopolymerase reaction (Matsumoto et al., 1990) in the presence of wild type or mutant hRPA (Figure 29a). Tag stimulated primer synthesis in the presence of hRPA (lanes 3-5) but not chimeric RPA (lanes 6-8). Control reactions in the absence of Tag or pol-prim (lanes 1-2) yielded no primers. The hRPA32 point mutants E252R and D268R supported primer synthesis, but their activity was less than that of wild-type hRPA (Figure 29b). The results indicate that Tag interaction with hRPA32C promotes priming during initiation.

To test whether the Tag-RPA32C interaction is also needed for primer synthesis at a later step after origin DNA unwinding, ssDNA presaturated with hRPA, hRPAy32C chimera or a point mutant was used as the template for priming and elongation (Figure 30). In the presence of hRPA, Tag stimulated primer synthesis and extension into labeled DNA products (lanes 1-3), whereas little or no product was detected in the presence of any of the mutant hRPAs (lanes 6-8). Abundant products were detected in the

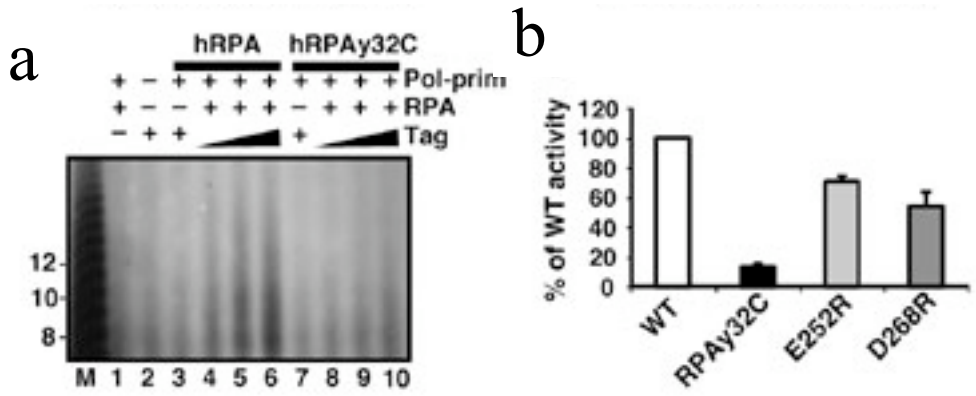

Figure 29: Mutations in hRPA32C that weaken interaction with Tag are defective in priming. (a) SV40 monopolymerase reactions containing radiolabeled CTP were carried out in the presence of 200 ng of the indicated hRPAs, 250 ng of pol-prim, and 250-750 ng of Tag as indicated. Control reactions lacking Tag, hRPA or pol-prim are indicated (-). Radiolabeled RNA products were resolved by electrophoresis on a polyacrylamide gel containing 20% (w/v) urea and visualized by autoradiography. M, radiolabeled oligonucleotide size marker dT (4-22). (b) Primer synthesis in the monopolymerase reaction was quantified and expressed as a percentage of wild-type activity. At least two reactions were used for quantification of each mutant. Brackets represent standard error.

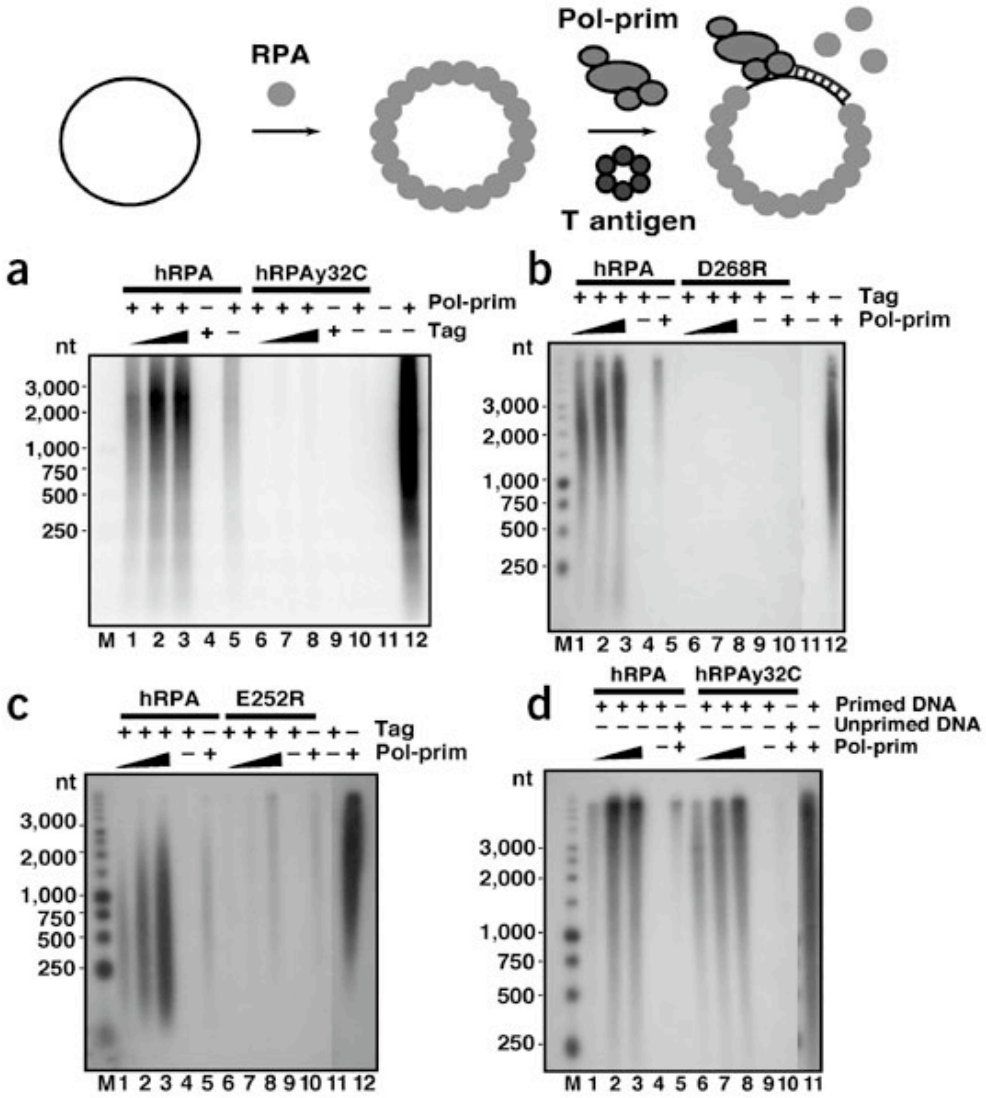

Figure 30: hRPA32C is needed for primosome activity, but not for primer extension. (a-c) Primer synthesis and extension was assayed on 100 ng M13 ssDNA precoated with 600 ng of hRPA or mutant hRPA as indicated. Reactions contained 250 ng of pol-prim and 250-750 ng of Tag as indicated. Control reactions lacked hRPA, pol-prim or Tag as indicated (-). Radiolabeled DNA products were resolved by alkaline agarose gel electrophoresis and visualized by autoradiography. M, DNA size markers as indicated. (d) Singly primed ssDNA (100 ng) precoated with 1,000 ng of the indicated hRPA was incubated with purified pol-prim (100, 150 and 250 ng) as indicated (+). Negative control reactions were done without pol-prim (lanes 4 and 9) or with unprimed template (lanes 5 and 10). Primer extension in the absence of hRPA is shown in lane 11.

positive controls without hRPA (lanes 12) and little or no products were observed in the absence of pol-prim (lanes 4, 9 and 11) or Tag (lanes 5 and 10). Quantification of primer synthesis and extension is shown in Figure 28. We conclude that interaction of Tag with hRPA32C, independent of origin DNA unwinding, is required for its ability to stimulate primer synthesis and elongation on hRPA-coated ssDNA.

The data above do not distinguish whether hRPA32C is required only for primer synthesis in the presence of Tag and pol-prim, or also for primer extension, which requires only pol-prim (Bullock, 1997; Yuzhakov et al., 1999a). This question was addressed by examining the activity of pol-prim on a pre-primed ssDNA template saturated with either the yeast RPA, chimera hRPAy32C or hRPA (Figure 30d). The primer elongation activity in the presence of human, yeast or chimeric RPA was nearly identical (lanes 1-3, 6-8). Primer extension was not detected in the absence of pol-prim or when unprimed DNA template was coated with the same amount of mutant RPA (lanes 4, 5, 9, 10). Primer elongation in the absence of RPA yielded products of smaller size (lane 11), consistent with previous evidence that RPA enhances the processivity of DNA synthesis (Kenny et al., 1990; Matsumoto et al., 1990; Dornreiter et al., 1992; Melendy & Stillman, 1993). We conclude that both hRPAs are capable of facilitating primer elongation by pol-prim.

Discussion

Taken together with the known interaction of Tag with RPA70 (Braun et al., 1997; Wold, 1997; Weisshart et al., 1998; Iftode et al., 1999), the evidence presented here suggests that each RPA heterotrimer has two binding surfaces for Tag, one in RPA70 and a

weaker one in RPA32C. Although the interaction of RPA32C with Tag-OBD is of moderate affinity, characterization of the complex by NMR enabled modeling of the structure at sufficient resolution to identify critical residues involved in the binding interface. The physical interaction of RPA32C with Tag-OBD is species specific. Despite strong homology between yRPA and hRPA, yRPA32C does not bind Tag-OBD or support SV40 DNA replication. Mutational analysis of hRPA32C strongly suggests that hRPA32C interaction with Tag-OBD allows pol-prim to gain access to hRPA-coated ssDNA for primer synthesis. The reduced replication activity of hRPA32C mutants is easily detectable as the amount of RPA is raised (Figure 27), but might not be obvious with lower amounts, providing an explanation for differences with observations reported previously (Lee & Kim, 1995; Braun et al., 1997). Other differences include the use of purified pol-prim and the monopolymerase and primosome assays, rather than the RPA-depleted human cell extracts used previously (Lee & Kim, 1995; Braun et al., 1997). Because hRPA is highly abundant *in vivo*, our results suggest that protein interactions of RPA32C with Tag are physiologically relevant. Notably, a conditional RPA32 mutant of yeast that lacks the RPA32C domain progresses through S phase, loses ARS plasmids at high frequency, and is synthetic lethal with a conditional pol-prim mutant at permissive temperature (Santocanale et al., 1995). These phenotypes imply that one or more steps in chromosomal replication may also depend on RPA32C interaction with protein partners.

hRPA32C uses a common binding site to interact with Tag-OBD and DNA repair factors (Mer et al., 2000). Like Tag, XPA and Rad52 have an additional binding site in RPA70 (Jackson et al., 2002; Daughdrill et al., 2003), although the relative importance of these contact points in DNA repair is not known. Notably, the RPA32C truncation mutant

of yeast displays mutator and hyper-recombination phenotypes, which does suggest a role for RPA32C in DNA repair (Santocanale et al., 1995). One of the common functions of RPA in these different DNA processing pathways lies in its ability to facilitate the exchange of proteins on ssDNA ("hand-off") (Kowalczykowski, 2000; Mer et al., 2000; Stauffer & Chazin, 2004b) as the pathway proceeds. The promiscuity of RPA32C in binding DNA processing proteins, while maintaining modest affinity for its binding partner, suggests that it serves as a facilitator in the hand-off mechanism. Characterization of structural mechanisms such as hand-off presents a significant challenge, but one which must be overcome to better understand fundamental DNA processing events such as replication.

Mechanism of Tag stimulation of primer synthesis?

Primer synthesis but not primer elongation on RPA-saturated ssDNA requires Tag (Matsumoto et al., 1990; Collins & Kelly, 1991; Melendy & Stillman, 1993; Yuzhakov et al., 1999a). The ability of Tag to mediate priming by pol-prim correlates with its ability to interact physically with the RPA bound to the template, strongly suggesting that physical interactions of Tag with RPA facilitate priming (Melendy & Stillman, 1993; Weisshart et al., 1998). The data presented in this report and previously (Lee & Kim, 1995) point to a functional role for RPA32C in Tag-mediated priming.

How might the physical interaction of Tag with RPA32C facilitate primer synthesis? We postulate that Tag interacts with RPA to facilitate its partial dissociation from ssDNA, thereby creating a short region of ssDNA accessible for primer synthesis (Figure 31). Based on all available evidence (Wold, 1997; de Laat et al., 1998; Iftode et

al., 1999; Yuzhakov et al., 1999a; Iftode & Borowiec, 2000; Bastin-Shanower & Brill, 2001; Ott et al., 2002; Arunkumar et al., 2003; Bochkarev & Bochkareva, 2004), we propose that a dual interaction of Tag with RPA32C and RPA70 allows it to remodel the structure of ssDNA-bound RPA, transiently shifting it from the high affinity, extended binding mode to a weaker, more compact binding mode (Figure 31a, b). hRPA binds to ssDNA with the high affinity DNA binding domains A and B at the 5' end of the occluded ssDNA, followed by the weaker binding domains C and D at the 3' end. The lower affinity of C and D implies that the 3' ssDNA would be transiently accessible. Binding of Tag to RPA32C might prolong the time window in which the 3' site is accessible. Because Tag binds to pol-prim through its helicase domain, a single Tag hexamer may bind concurrently to RPA and pol-prim (Fanning & Knippers, 1992; Bullock, 1997; Weisshart et al., 1998; Simmons, 2000; Stenlund, 2003). Given that Tag binding to both proteins is essential for priming (Weisshart et al., 1998), we propose that a Tag hexamer transiently associated with both RPA and pol-prim is poised to load pol-prim onto the accessible region of ssDNA (Figure 31b,c). Primase would thereby gain access to the free ssDNA template, permitting primer synthesis and leading to dissociation of a remodeled RPA molecule and Tag. Subsequent primer extension on RPA-ssDNA by pol-prim does not require Tag (Figure 31). The model proposed in Figure 31 is consistent with our results and a large body of published evidence, but much work remains to assess its validity.

To understand better the role(s) of RPA32C, it will be necessary to completely analyze all hRPA-Tag interactions. The objective is to understand their coordination action and how they are regulated through interactions with DNA and pol-prim. The

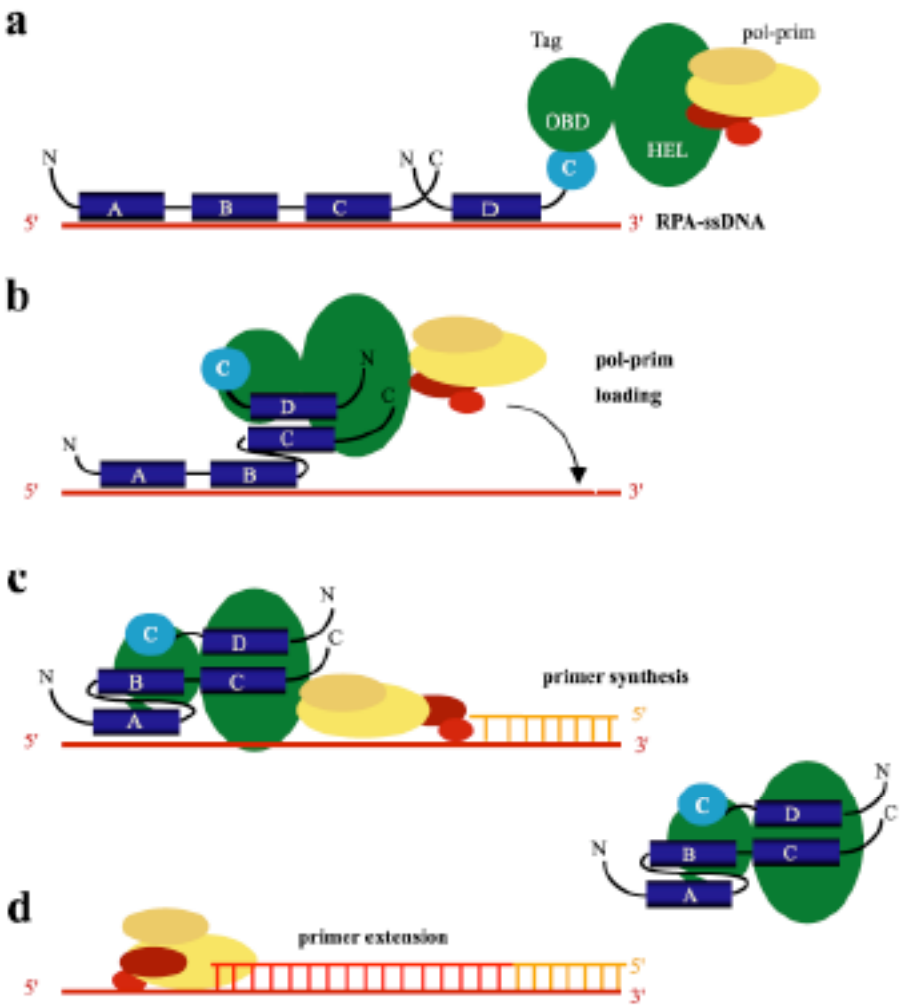

Figure 31: Model for SV40 primosome activity on RPA-coated ssDNA. (a) RPA (blue) is schematically depicted in the high affinity 28-30 nt binding mode with all four ssDNA binding domains (A-D) bound to ssDNA. RPA14 is omitted for simplicity. The helicase domain (HEL) of a Tag hexamer (green) can associate with a pol-prim heterotetramer (Koradi et al., 1996; Bullock, 1997). Antibodies against Tag that specifically inhibit either RPA binding to Tag-OBD or pol-prim binding to the helicase domain prevent primer synthesis (Weisshart et al., 1998). (b) We suggest that primosome assembly begins when Tag-OBD associates first with RPA32C and then with RPA70AB, transiently creating a short stretch of unbound ssDNA. (c) In concert with this RPA remodeling, pol-prim associated with the Tag hexamer would be poised to access the free ssDNA and begin primer synthesis. (d) Primer extension by pol-prim is likely coupled with RPA and Tag dissociation, and followed by the RFC/PCNA-mediated switch to DNA polymerase delta (Huang et al., 1998) (not shown).

increasingly detailed knowledge of the mode of action of modular, multifunctional because they provide an understanding of the fundamental molecular mechanisms of proteins, such as our studies of the SV40 replisome, are of considerable value DNA processing machineries and the role of hRPA in guiding the sucession of protein in each pathway.

Acknowledgments

We thank Shibani Bhattacharya, Brian Dattilo, Luke Douthitt, Gwen Hubbell, Jaison Jacob, Murthy Karra, Mark Kenny, Valentyna Klymovych, Susan Meyn, Carol Newlon, Charles Sanders, Libbey Schwertman, Eric M. Warren, Dewight Williams, and Marc Wold for valuable advice and assistance. Accelrys, Inc. (San Diego) is acknowledged for the generous gift of NMR software. Financial support is gratefully acknowledged from NIH for operating grants to EF and WJC and for facilities support to the Vanderbilt-Ingram Cancer Center and the Vanderbilt Center in Molecular Toxicology, as well as from the Howard Hughes Medical Institute Professors Program (to EF) and Vanderbilt University.

CHAPTER III

STRUCTRAL MECHANISM OF RPA LOADING ON DNA DURING ACTIVATION OF A SIMPLE PRE-REPLICATION COMPLEX[2]

Introduction

RPA is a conserved eukaryotic ssDNA binding protein that was discovered as an essential factor in the cell-free replication of simian virus 40 (SV40) DNA (Wold, 1997; Iftode et al., 1999; Bochkarev & Bochkareva, 2004). A large body of evidence now demonstrates that RPA is an obligatory participant in most eukaryotic DNA processing pathways, from DNA replication, repair, and recombination through somatic hypermutation in lymphocytes and DNA damage signaling (Zou & Elledge, 2003; Chaudhuri et al., 2004; Stauffer & Chazin, 2004b).

RPA is a highly flexible modular protein composed of three subunits (RPA70, RPA32, RPA14) that are stably associated with each other (Figure 32). Three-dimensional structures of each of the seven individual domains and several subassemblies are now available, but the quaternary structure(s) of RPA remains unknown (Bochkarev & Bochkareva, 2004; Stauffer & Chazin, 2004b). Four of the domains [DNA-binding domains (DBDs) A-D] bind to ssDNA with decreasing affinity from A to D (Figure 32). RPA binding to ssDNA occurs sequentially and with a defined polarity, beginning with DBD-A and B at the 5' end, yielding three different states that occlude 8-10, 12-23, or

[2] Jiang X.*, Klimovich V.*, Arunkumar A. I*, Hysinger E. B., Wang Y., Ott R. D., Guler G. D., Weiner B., Chazin W. J., Fanning E. (2006). Structural mechanism of RPA loading on DNA during activation of a simple pre-replication complex. EMBO J 25(23):5516-26. *These authors contributed equally to this work.

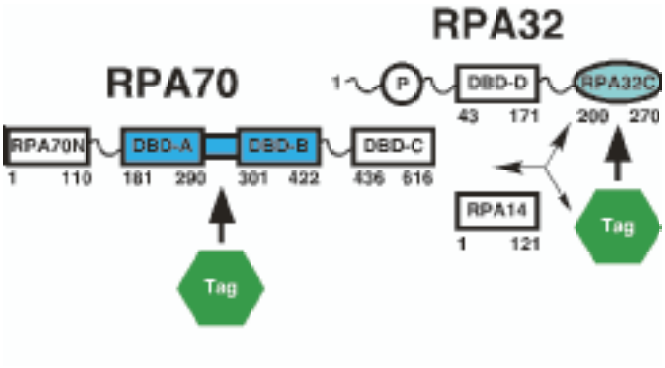

Figure 32: Domain organization of RPA with Tag binding regions shaded. Rectangles depict OB-folds, of which four are single-stranded DNA binding domains (DBDs A-D); an oval indicates the winged-helix-turn-helix of RPA32C (Mer et al., 2000); a circled P depicts the phosphorylated region of RPA32. A triple arrow symbolizes the association of subunits through a 3-helix bundle (Bochkareva et al., 2002), and hexagons denote Tag hexamers.

28-30 nucleotides (de Laat et al., 1998; Iftode & Borowiec, 2000; Bastin-Shanower & Brill, 2001; Arunkumar et al., 2003; Wyka et al., 2003). The three states of RPA are thought to co-exist in solution, in dynamic equilibrium with each other (Blackwell et al., 1996). Studies of free RPA70AB (residues 181-422) reveal that the linker peptide between domains A and B is flexible (Arunkumar et al., 2003), while RPA70AB bound to an 8-nucleotide ssDNA adopts a structure with domains A, B, and the linker in a fixed orientation (Bochkarev et al., 1997; Bochkareva et al., 2001; Arunkumar et al., 2003).

RPA also interacts directly with and modulates the activity of a large and growing number of factors that are required for proper processing of ssDNA (Iftode et al., 1999). The binding sites for these proteins have been mapped to regions in the RPA70N, 70A, 70B, and 32C domains (Figure 32). Notably, many of the DNA processing factors are, like RPA, modular multi-domain proteins, and in most instances, their interactions with RPA involve multiple contact points between two or more domains.

The viral replicative DNA helicase, SV40 T antigen (Tag), binds to RPA via its origin DNA binding domain (OBD, residues 131-259) and this interaction is essential for SV40 DNA replication (Dornreiter et al., 1992; Melendy & Stillman, 1993; Weisshart et al., 1998). The Tag binding regions of RPA have been mapped to RPA70 residues 169-327 (Braun et al., 1997) or RPA70A (Loo & Melendy, 2004; Park et al., 2005), and RPA32C (Lee & Kim, 1995). Although the physical interaction of Tag-OBD with RPA70 remains poorly understood, an important step forward was made possible by construction of a model of Tag-OBD and RPA32C from extensive NMR data (Arunkumar et al., 2005).

An understanding of how RPA functions in the progression of ssDNA processing pathways remains elusive. One proposal is that processing proteins successively compete with each other for RPA, allowing them to switch places on DNA as the pathway progresses toward completion (Yuzhakov et al., 1999a). This mechanism, termed hand-off, correlates with the increasing affinity of proteins for RPA during lagging strand SV40 DNA replication in vitro (Yuzhakov et al., 1999a). There is also evidence for a mechanism involving protein-mediated remodeling of RPA, from an extended conformation into a compact conformation that more readily dissociates from ssDNA, which allows incoming proteins to access ssDNA. For example, we recently demonstrated that Tag binding to RPA32C facilitates replacement of RPA on ssDNA by DNA polymerase alpha-primase to promote primer synthesis, and proposed that this transition is based on the ability of Tag to bind and remodel the ssDNA-binding mode of RPA (Arunkumar et al., 2005).

The ability of RPA-binding proteins to facilitate its displacement from ssDNA led us to consider whether RPA freely diffuses onto ssDNA or whether DNA processing proteins actively load RPA on ssDNA. Here, we demonstrate that the Tag double hexamer, which serves as a simple pre-replication complex on the viral origin, selectively loads human RPA on the emerging ssDNA at the origin. To define the structural basis for this loading reaction, we map the physical interaction surfaces of Tag and RPA70AB in detail and show that Tag forms a ternary complex with RPA70 domains A and B bound to a minimal ssDNA binding site of 8 nucleotides. However, in the presence of a 30-nucleotide oligomer, Tag was found to dissociate from the ternary complex. Our evidence suggests that the ternary complex initially couples activation of SV40 origin unwinding

by Tag helicase with RPA loading onto ssDNA, and then dissociates to enable RPA binding in an extended mode to the full ssDNA site.

Materials and methods

Protein and DNA

Human RPA70AB was expressed and purified as described (Arunkumar et al., 2003). $Tag_{131\text{-}259}$ (Tag-OBD), and recombinant trimeric human RPA, yeast RPA, and hRPAy32C chimera were expressed and purified as described (Arunkumar et al., 2005). SV40 Tag, DNA polymerase alpha-primase, and topoisomerase I were prepared as described (Ott et al., 2002). Monoclonal antibodies Pab101 against Tag (residues 696-708) (Weisshart et al., 2004) and 70C and 34A against hRPA (Kenny et al., 1990) were purified as described. HPLC pure oligo dT_{30}, dT_{15}, and dT_8 were purchased from Integrated DNA Technologies (Coralville, IA)

Uniformly enriched ^{15}N and ^{13}C, ^{15}N samples were prepared in minimal medium containing 1 g/L $^{15}NH_4Cl$ (CIL, Inc.) and 2g/L unlabeled or [$^{13}C_6$] glucose (CIL, Inc.), respectively. HPLC pure ssDNA, $d(C)_8$, was purchased from Midland Certified Co. (Midland, TX) and used without further purification.

NMR spectroscopy

All NMR experiments were performed on Bruker spectrometers operating at 600 MHz and 800 MHz. The buffer that was used for all the NMR experiments was 20 mM Tris-

d_{11} HCl containing 50 mM KCl, 10 mM $MgCl_2$, 2 mM DTT, and 0.01% NaN_3 at pH 7.2. All NMR experiments were recorded at 25 ºC. Two-dimensional, gradient-enhanced HSQC and TROSY-HSQC spectra were recorded with 4K complex data points in the ^1H and 200 complex points in ^{15}N dimension. All NMR spectra were processed and analyzed using Felix 2000 (Accelrys Inc., San Diego, CA). Complete backbone and side chain assignments for RPA70AB and Tag-OBD are reported elsewhere (Luo et al., 1996; Bhattacharya et al., 2004). Structures were visualized and figures were generated using MOLMOL (Koradi et al., 1996).

Limited proteolysis

Limited proteolysis of RPA70AB was carried out in the presence of trypsin at a molar ratio of 1:1000 (protease:protein) in the same buffer that was used in NMR studies. Free RPA70AB, binary complexes RP70AB/Tag-OBD and RPA70AB/$d(C)_8$, and the ternary RPA70AB/Tag-OBD/$d(C)_8$ complex were incubated in the presence of trypsin and aliquots were removed at various time points. The protease activity was quenched by addition of SDS-PAGE loading buffer followed by boiling for 3 min. The digestion products were separated and visualized by 4-17% SDS-PAGE and Coomassie staining.

Tag-RPA pull-down assays

Purified Tag was bound to monoclonal antibody Pab101 absorbed to protein G-agarose beads. Tag-bound beads were incubated with RPA or RPA70AB as indicated in the figure legends for 1 h at 4°C. After washing 3 times with washing buffer (30 mM

HEPES-KOH (pH 7.9), 50 mM KCl, 7 mM $MgCl_2$, 0.25% inositol, 0.05% NP-40), the beads were resuspended in the SDS sample buffer and analyzed by SDS-PAGE and western blotting with anti-RPA Mab70C and chemiluminescence. hRPA and RPA70AB binding to GST-Tag-OBD adsorbed to glutathione beads was assayed in a similar manner using anti-Tag Pab101.

In some experiments, increasing amounts of oligonucleotide dT_{30}, dT_{15} or dT_8 were added to the washed Tag/RPA complexes on beads and incubated for 1 h at 4°C. After washing again with washing buffer, bound hRPA was visualized by SDS-PAGE, immunoblotting with anti-RPA Mab70C (Kenny et al., 1990), and chemiluminescence.

ssDNA filter binding assays

Human RPA, yeast RPA or hRPAy32C was incubated with 3 pmol of 5' ^{32}P-end-labeled ssDNA (dT_{30}) in binding buffer (30 mM HEPES-KOH [pH7.9], 40 mM creatine phosphate, 7 mM $MgCl_2$, 4 mM ATP, 10 μM $ZnCl_2$) for 20 min at 37 ^{0}C. Reactions were spotted on alkaline-treated nitrocellulose filters (McEntee et al., 1980). The filters were washed five times with wash buffer (30 mM HEPES-KOH [pH7.9], 7 mM $MgCl_2$), dried, and analyzed by scintillation counting.

Native gel electrophoresis

Mobility shift reaction mixtures (15 μl) containing 3 pmol of 5' ^{32}P-end labeled ssDNA (dT_{30}) in binding buffer (30 mM HEPES-KOH [pH7.9], 40 mM creatine phosphate, 7 mM $MgCl_2$, 4 mM ATP, 0.01 mM $ZnCl_2$) were pre-incubated with 2-6 pmol of RPA

(human or yeast) as indicated in the figure legends at 25^{o}C for 10 min. Tag was added as indicated in the figure legends for 15 min at 37^{o}C. In some experiments, a purified monoclonal antibody was added 5 min later. The reaction products were analyzed after addition of loading buffer (2.5% w/v Ficoll 400, 0.05% w/v bromophenol blue, 0.05% w/v xylene cyanol) and electrophoresis on 7.5% polyacrylamide gels in 45 mM Tris, 45 mM boric acid, 0.01 mM $ZnCl_2$ for 2 h at 100 V. The gel was dried and complexes were detected by autoradiography. Bound proteins were quantified by densitometry using IPLabGel.

Initiation of SV40 DNA replication

Monopolymerase assays (Matsumoto et al., 1990) were carried out as described recently (Arunkumar et al., 2005) except that 750 ng of Tag was used and RPA was varied as indicated in the figure legends. Reactions were assembled at 4°C and incubated at 37°C for 90 min. Reaction products were purified on G-50 Sephadex columns (Roche Diagnostics Corp., Indianapolis, IN) and precipitated with 100% acetone. The washed and dried products were redissolved in loading buffer (45% formamide, 5 mM EDTA, 0.08% xylene cyanol FF, 0.08% bromophenol blue) and resolved by 1.2% alkaline (30 mM NaOH, 1 mM EDTA) agarose gel electrophoresis for 2 to 3 h at 100 V. The reaction products were visualized by autoradiography and quantified by scintillation counting.

Results

Selective loading of human RPA during unwinding of the SV40 replication origin

To determine whether origin DNA unwinding by Tag double hexamer is coupled to RPA recruitment and concomitant loading onto ssDNA, we asked whether Tag would selectively load human RPA onto emerging ssDNA in the presence of a competing ssDNA-binding protein that supports origin unwinding but not later steps in SV40 replication. Yeast RPA was chosen as the competitor in this experiment because it binds ssDNA with an affinity similar to human RPA (Figure 33a, b) and supports Tag-catalyzed unwinding of SV40 origin DNA, but it does not bind to Tag and does not support primer synthesis in SV40 replication (Brill & Stillman, 1989; Melendy & Stillman, 1993; Iftode & Borowiec, 1997; Sibenaller et al., 1998; Arunkumar et al., 2005). We reasoned that if yeast RPA can compete with human RPA for the emerging ssDNA, it should inhibit replication of the template DNA in a concentration-dependent manner.

To test this prediction, initiation of SV40 replication was monitored in a reaction containing supercoiled origin DNA, and purified proteins Tag, DNA polymerase alpha-primase, topoisomerase I, a limiting amount of human RPA, ribo- and deoxyribonucleotides, and radiolabeled dTTP. In this reaction, a low level of initiation (Figure 33d, lane 1) was detected, though clearly above that in negative control reactions (lanes 9-10). Additional human RPA stimulated robust initiation (lanes 2-4), confirming that the lowest level of human RPA was sub-saturating. As expected, no replication products were detected in a reaction that contained yeast RPA in place of human RPA (lane 11). Moreover, addition of yeast RPA in up to a 5-fold excess over the human RPA failed to reduce the initiation activity of human RPA (lanes 5-8). In fact, we note a weak

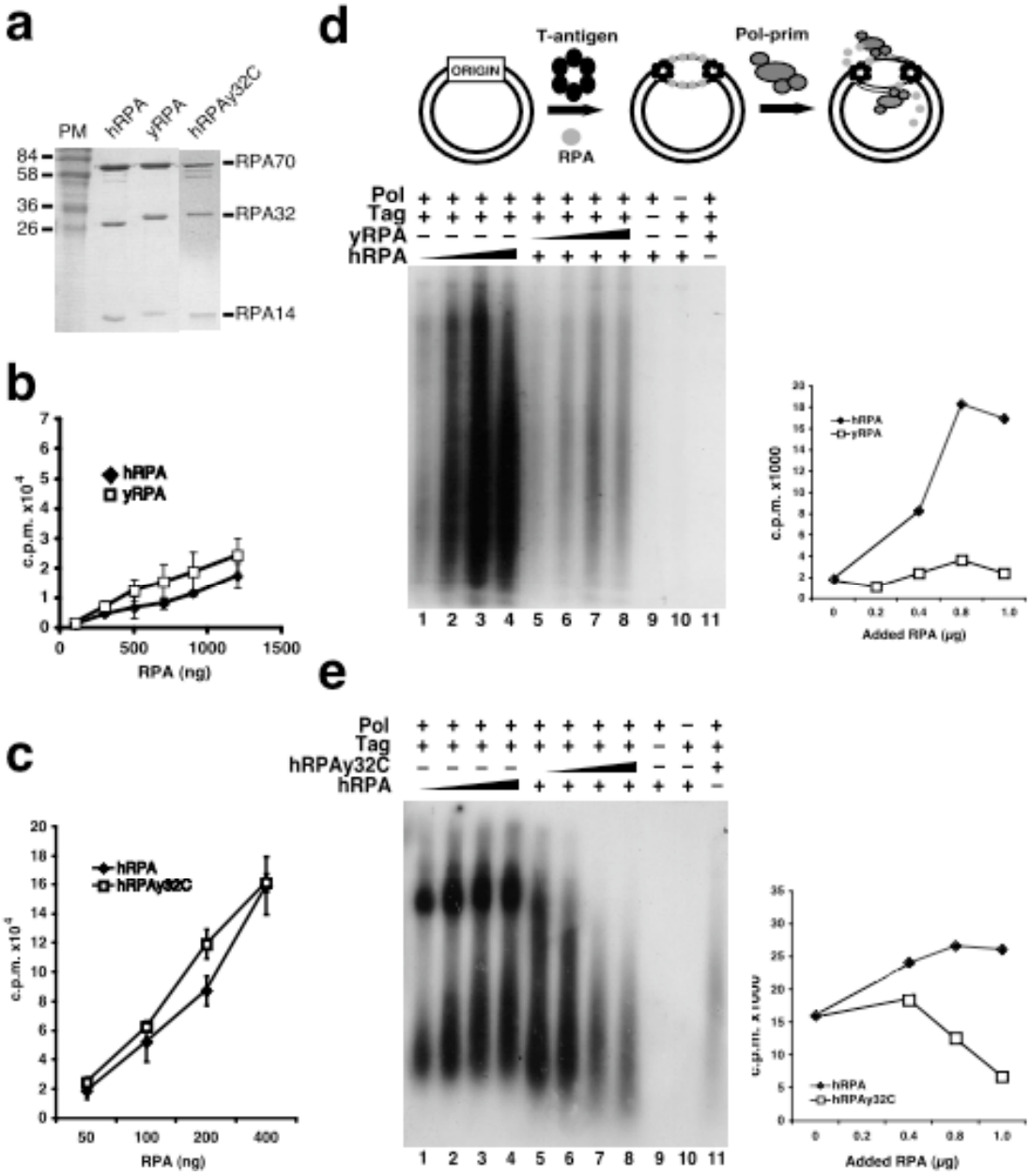

Figure 33: Tag interaction with RPA70AB actively loads human RPA onto ssDNA during initiation of SV40 DNA replication. (a) Purified hRPA, yRPA, and hRPAy32C chimera were visualized by SDS-PAGE and Coomassie stain. PM, protein mass marker. (b, c) Filter binding assays were used to compare the activity of the indicated RPAs in binding to radiolabeled dT_{30}. (d,e) SV40 monopolymerase assays were performed with a suboptimal amount of human RPA (0.2 mg) (lane 1) supplemented with up to 5-fold greater amounts of human RPA (lanes 2-5), and either (d) yeast RPA or (e) hRPAy32C (lanes 5-8) as indicated. Reaction products were visualized by denaturing gel electrophoresis and autoradiography (left), and quantified by scintillation counting (right). Negative control reactions lacked Tag, polymerase alpha-primase, or human RPA as indicated (lanes 9-11).

stimulation that, based on the absence of activity in lane 11, appears to be nonspecific. Together these results suggest that Tag selectively loaded human RPA onto ssDNA during origin unwinding, which prevents yeast RPA from gaining access to the template.

To confirm this interpretation, SV40 initiation was tested using limiting human RPA in the presence of increasing amounts of a chimeric RPA hRPAy32C, in which the yeast RPA32C domain replaced the human RPA32C domain. This chimeric RPA binds to ssDNA (Figure 33a,c) and to Tag, but does not support Tag-mediated primer synthesis (Arunkumar et al., 2005). As in Figure 33D, the low initiation activity with limiting human RPA (Figure 33e, lane 1) was stimulated by additional human RPA (lanes 2-4). However, in contrast to the results with excess yeast RPA (Figure 33d), increasing amounts of chimeric RPA inhibited initiation in a dose-dependent manner (Figure 33e, lanes 5-8), almost down to the level detected in a control reaction with chimeric RPA alone (lane 11). These results implicate physical interactions of Tag with the RPA70 subunit in selectively loading RPA onto ssDNA during unwinding. Taken together, the results in Figure 33 strongly suggest that origin unwinding is coupled with RPA loading directly onto the emerging ssDNA.

Domain mapping of interactions between Tag and RPA

The results in Figure 33 suggested that physical interaction between Tag and RPA could play an important role in coupling origin unwinding with RPA loading. Detailed mapping of the interactions between Tag and RPA70 was performed to confirm which domains of Tag and RPA70 are involved. Our first approach involved pull-down assays in which a constant amount of full length Tag or GST-fused Tag-OBD was titrated with purified

intact RPA or RPA70AB under buffer conditions similar to those used for cell-free SV40 DNA replication (Figure 34). RPA binding to purified Tag was easily detectable with small amounts of RPA (Figure 34b). When the same amount of Tag beads was incubated with RPA70AB, which lacks the known RPA32C interaction region, about 8-fold higher molar amounts were required to detect a level of binding comparable to that obtained with RPA heterotrimer (Figure 34c). Consistent with this observation, GST-OBD beads bound full length RPA quite well, and about 8-fold greater molar amounts of RPA70ABwere required to detect comparable binding (Figure 34d, e). These data confirm that RPA binds to Tag-OBD through RPA70AB, in addition to RPA32C, and that both interactions contribute to the overall binding affinity.

A second approach to characterize RPA70AB interactions with Tag-OBD involved proteolysis protection assays. In RPA70AB, the flexible linker between the two high affinity ssDNA binding domains A and B is sensitive to proteolysis (Gomes et al., 1996; Gomes & Wold, 1996). RPA70AB binding to ssDNA fixes the relative positions of the two domains and protects the linker against digestion (Gomes et al., 1996; Bochkarev et al., 1997). To gain insight into the interaction of RPA70AB with Tag-OBD, limited proteolysis of RPA70AB was carried out in the presence and absence of OBD. Without OBD, the linker between RPA70A and B was almost completely cleaved after digestion for 2 h (Figure 35a). In contrast, intact RPA70AB remained detectable for at least 15 h in the presence of OBD (Figure 35b). The stabilization of the linker strongly resembled that observed for RPA70AB digested in the presence of ssDNA (dC_8) (Figure 35c). These observations indicate that like ssDNA, OBD binds and stabilizes RPA70AB, but do not reveal whether the OBD binds to the same surface of RPA as ssDNA or a different one.

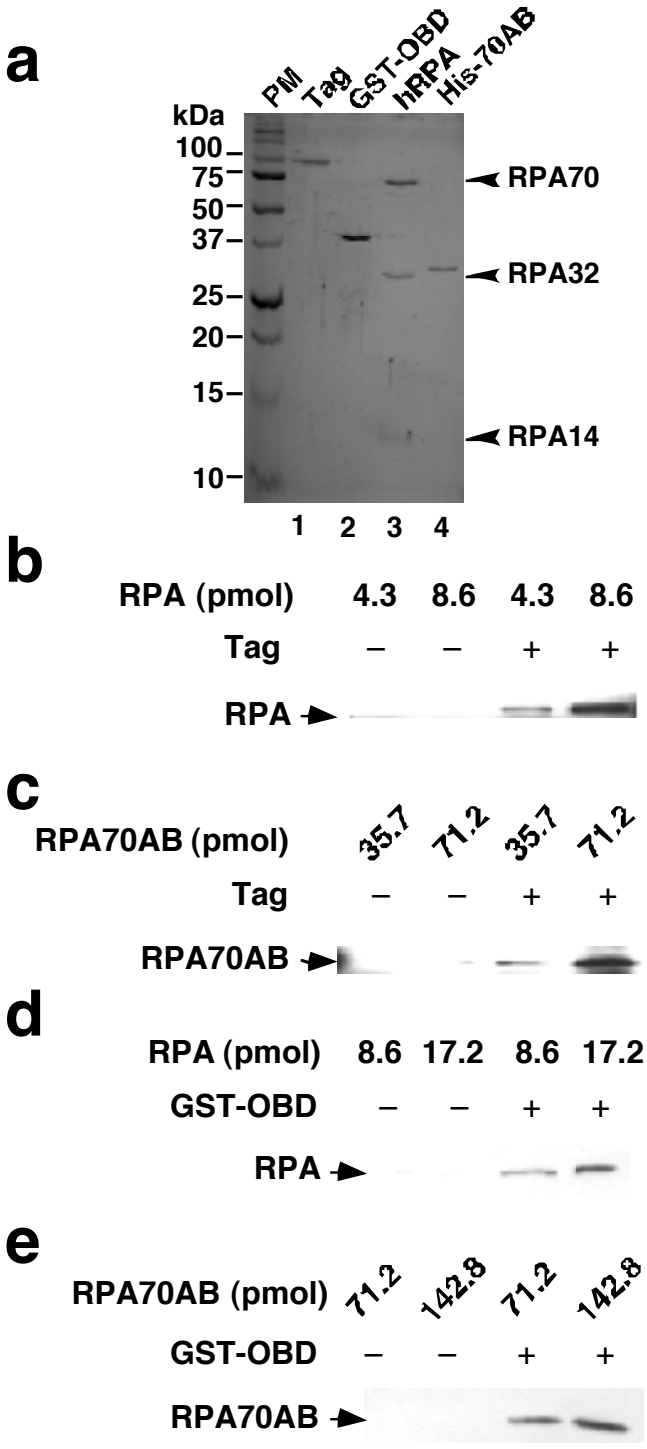

Figure 34: Tag-OBD binds to two regions of RPA. (a) Purified proteins used in panels B-E are shown at the right. (b, c) Tag bound to Pab101 beads and (d, e) GST-Tag-OBD bound to glutathione beads was incubated with the indicated amounts of RPA (b, d) or RPA70AB (c, e). After washing the beads, bound RPA was visualized by SDS-PAGE and western blotting with anti-RPA Mab70C.

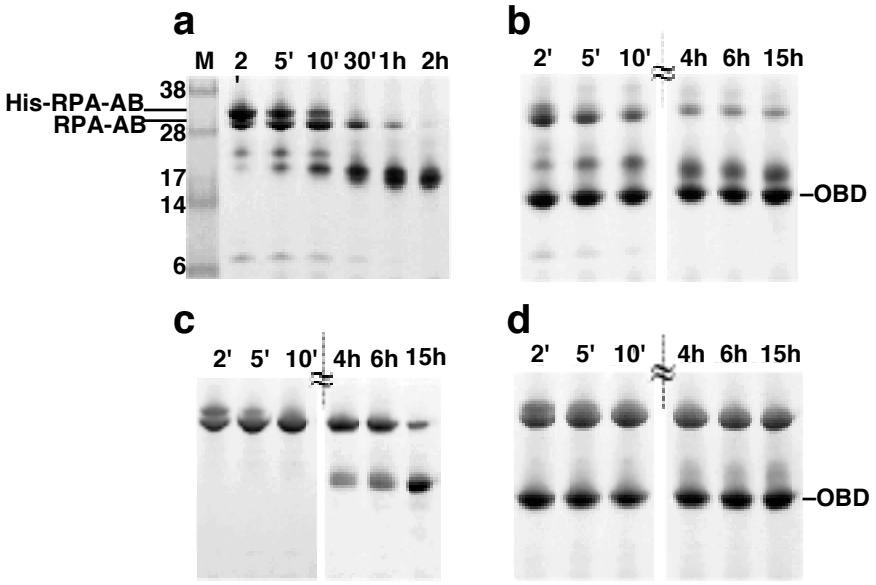

Figure 35: Tag-OBD protects RPA70AB from proteolytic digestion. RPA70AB was incubated with trypsin for the indicated time periods, either alone (a); or in the presence of Tag-OBD (b); $d(C)_8$ (c), or $d(C)_8$ and Tag-OBD (d). Digestion products were visualized by SDS-PAGE and Coomassie staining.

However, Figure 35d shows that RPA70AB was almost completely resistant to trypsin proteolysis in the presence of both ssDNA and OBD. The fact that ssDNA and OBD stabilized RPA70AB more effectively together than did either alone implies that a stable ternary complex is formed with discrete binding sites for each component.

RP70AB binds ssDNA and Tag-OBD at distinct sites

To determine the structural basis for the proposed coupling of origin unwinding to active RPA loading onto emerging ssDNA, heteronuclear NMR was used to directly map the Tag-OBD interacting surface of RPA70AB. The strategy involved monitoring perturbations of NMR signals as Tag-OBD is titrated into a solution of RPA70AB. This approach has proven valuable for mapping binding surfaces because the NMR chemical shift for each nucleus is extremely sensitive to its electronic environment. While perturbations will arise from direct binding as well as allosteric structural changes, binding sites can often be distinguished because a series of spatially proximate residues that form a contiguous surface is discernable from the ensemble of chemical shift data.

The experiments were performed by monitoring ^{15}N-^{1}H HSQC spectra of ^{15}N-enriched RPA70AB as unlabeled Tag-OBD was titrated because this allowed RPA70AB signals to be cleanly discriminated from those of Tag-OBD. A single set of signals was observed at all points during the titration, which indicates that RPA70AB is in fast exchange between its free and bound states, consistent with relatively weak binding in the micromolar range. Figure 36A shows the overlay of a portion of an HSQC spectrum of free RPA70AB and one obtained in the presence of 2 molar excess of Tag-OBD. Although most of the peaks were not affected by the presence of OBD, a subset of the

peaks progressively moved or broadened as the titration proceeded. Residues that displayed readily discernible changes in NMR chemical shift are labeled in the inset of Figure 36a. Mapping of the residues perturbed upon titration with Tag-OBD on the structure of RPA70AB revealed a contiguous surface along the linker and into both domains (Figure 36b). To confirm that this is a physically realistic surface for Tag-OBD binding, the RPA70AB and Tag-OBD structures were inspected to confirm that Tag-OBD is large enough to span across the linker and interact with both the A and B domains. Overall, these results imply Tag-OBD binds to RPA70AB at a site that is remote from the ssDNA binding sites.

To obtain further insight into the coupling of the binding of ssDNA and Tag-OBD to RPA70AB, additional NMR spectra were recorded for ^{15}N-enriched RPA70AB in the binary complex with ssDNA and the ternary complex with OBD and ssDNA (Figure 36c). Remarkably, the overall quality of the spectra was better for the larger ternary complex than for either of the binary complexes, a reflection of an increased structural stability of the ternary complex. Comparison of these spectra revealed three important points. First, the changes induced in the NMR spectrum by binding of ssDNA were mostly distinct from those induced by binding of Tag-OBD. For example, the changes in chemical shifts for D291 and Q299 are observed only when OBD is added to the solution, regardless of whether or not ssDNA is present (Figure 36c). Second, in addition to perturbations of RPA70AB chemical shifts, new peaks appear in the spectrum, which can be attributed to resonances from residues that are stabilized upon binding. Third, the spectrum of the ternary complex of RPA70AB, OBD and ssDNA contains all of the "new" peaks that appear in spectra of the binary complexes, as well a very small number

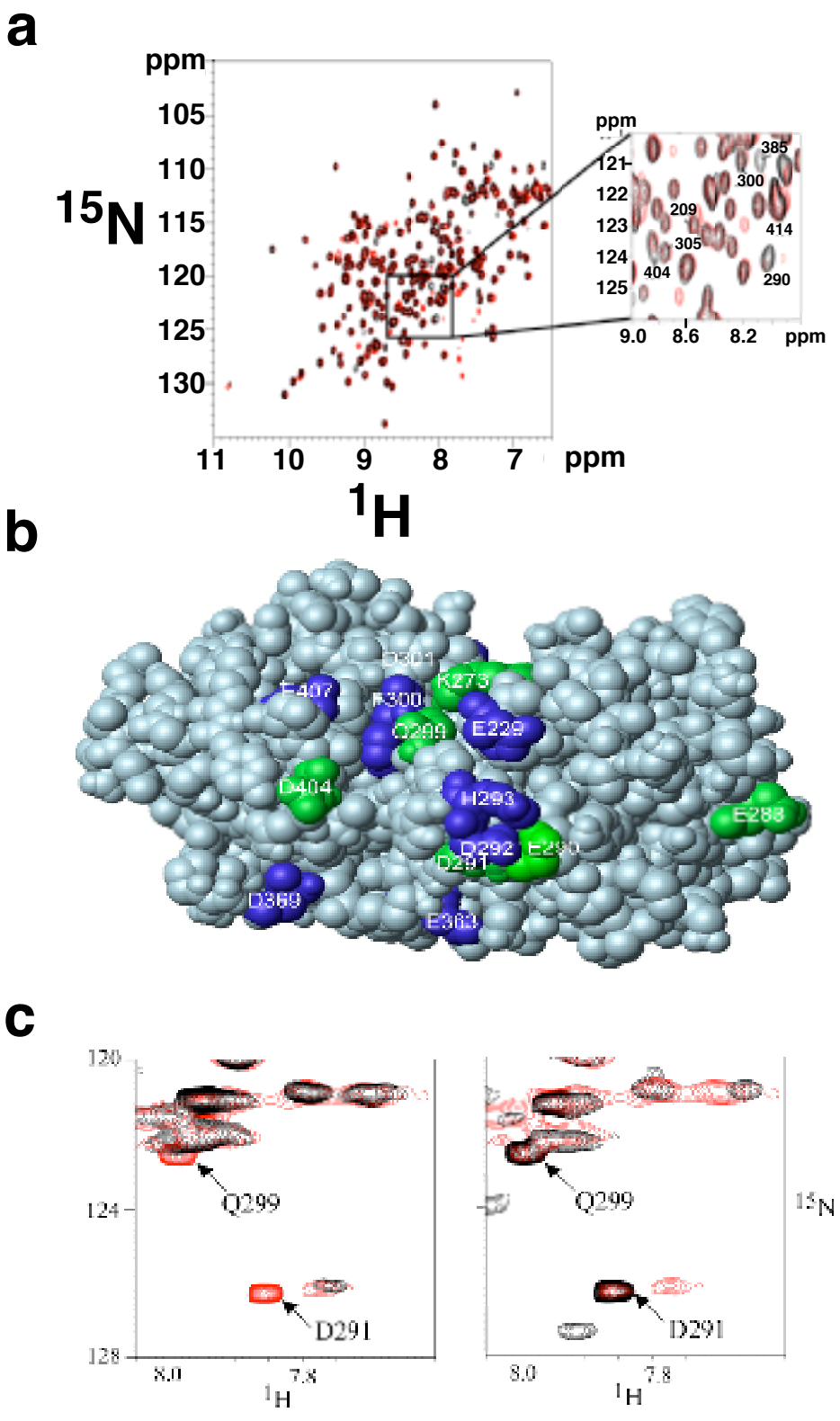

Figure 36: Structural mapping of RPA70AB binding site for Tag-OBD. (a) Chemical shift mapping of Tag-OBD binding site on RPA70AB. Overlay (to be continued)

(Figure 36-continued) of ^{15}N-^{1}H HSQC spectra of ^{15}N-enriched RPA70AB in the absence (black) and presence of Tag-OBD (red). The inset shows some of the residues that are perturbed or broadened upon interaction with Tag-OBD. (b) Molecular surface of RPA70AB with residues whose chemical shifts are perturbed upon binding of Tag-OBD colored in blue (strongest effects) and green (other significant effects). (c) Formation of a stable ternary complex of RPA70AB with $d(C)_8$ and Tag-OBD. The left panel shows a region from the ^{15}N-^{1}H HSQC spectra of the binary complex of ^{15}N-enriched RPA70AB with $d(C)_8$ in the absence (black) and presence of Tag-OBD (red). The right panel shows a region from the ^{15}N-^{1}H HSQC spectra of the binary complex of ^{15}N-enriched RPA70AB with Tag-OBD in the absence (black) and presence of $d(C)_8$ Tag-OBD (red).

of additional peaks. Thus, in addition to revealing that Tag-OBD binds to a surface of RPA70AB that is remote from the ssDNA-binding site, these observations provide evidence of the energetic coupling of the binding of the two different ligands (ssDNA and Tag-OBD) to RPA70AB, which suggests the possibility of function through an allosteric structural mechanism (vide infra).

Tag-OBD associates with RPA70AB through electrostatic interactions

To deepen our understanding of the structural basis for the interaction between RPA70AB and Tag-OBD, the NMR-based strategy was used to map the region of Tag-OBD that binds to RPA70AB. To this end, ^{15}N-enriched Tag-OBD was titrated with unlabeled RPA70AB and chemical shift perturbations were monitored (Figure 37a). The most significant effect detected was the perturbation of residues from three regions that together form a contiguous binding surface on Tag-OBD (F151-T155, F183-H187, H203-A207) (Figure 37B, circle). This surface has a significant basic character arising primarily from three prominent surface residues: R154, R202 and R204.

These results, combined with the analysis of the RPA70AB binding site, indicate there is a significant electrostatic component to the interaction of Tag-OBD with RPA70AB. In particular, the basic residues on the Tag-OBD binding surface are complemented by the highly acidic nature of the RPA70AB binding surface, in which residues E290, D291, D292, D404 and D407 form a dense negatively charged surface on the opposite side of RPA70AB from the ssDNA binding surface (Figure 37c). To verify the importance of the electrostatic complementarity observed in the RPA70AB-Tag-OBD binding interface, charge reversal mutations were designed in Tag-OBD at the RPA-

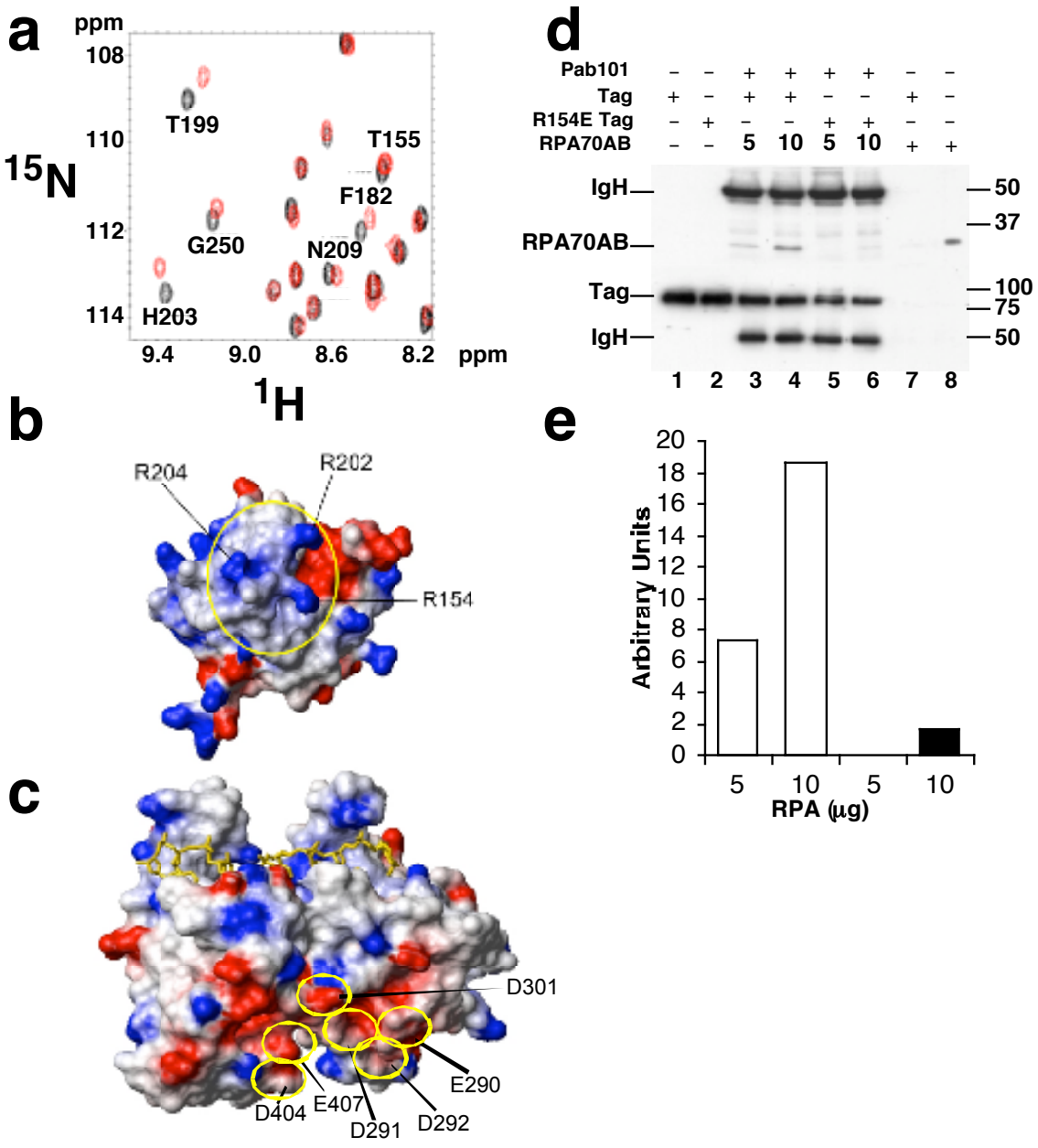

Figure 37: Structural mapping of Tag-OBD binding site for RPA70AB. (a) Chemical shift perturbation analysis of the Tag-OBD binding site on RPA70AB. Overlay of ^{15}N-^{1}H HSQC spectra of ^{15}N-enriched Tag-OBD in the absence (black) and presence of RPA70AB (red). The inset shows an expansion of a small region highlighting some of the residues that are perturbed or broadened upon interaction with RPA70AB. (b,c) Molecular surface diagrams of the electrostatic potential of Tag-OBD and RPA70AB, respectively, with blue for positive charge and red for negative charge. The large yellow circle in (b) highlights the contiguous binding region composed of regions F151-T155, F183-H187 and H203-A207. The three prominent Arg residues providing the bulk of the basic character of this region are labeled. The small yellow circles in (c) highlight the six acidic residues that provide the acidic character to the Tag-OBD (to be continued)

(Figure 37- continued) binding site on RPA70AB. The ssDNA in the RPA70AB structure is colored yellow. (d) A charge reversal mutation in Tag-OBD reduces Tag binding to RPA70AB. Wild type (lanes 1, 3, 4) and R154E mutant Tag (lanes 2, 5, 6) adsorbed to antibody beads were incubated with 5 or 10 μg of RPA70AB as indicated. Proteins bound to the beads were separated by SDS-PAGE and visualized by western blotting with Mab70C against RPA (top panel) or Pab101 against Tag (lower panel). Antibody beads lacking Tag did not bind RPA70AB (lane 7). Lane 8 shows 200 ng of input RPA70AB. (e) Quantification of bound RPA70AB in lanes 3-6 of panel D after subtraction of background in lane 7.

binding interface with the goal of weakening the interaction with RPA70AB. Indeed, RPA70AB binding of purified full-length Tag containing the R154E mutation was 8 to 10-fold weaker than of wild type Tag (Figure 37d, lanes 3-6), confirming the importance of the electrostatic character of the interaction surface. As a control, the mutant Tag-OBD was subjected to biophysical/structural analysis, which showed that the reduction in binding affinity did not arise from perturbation of the structure (Figure 38).

Physical interaction with Tag-OBD stimulates ssDNA binding of RPA

The finding that Tag-OBD and ssDNA bind to different sites in RPA70AB led us to ask whether full length Tag can also form a ternary complex with trimeric RPA and ssDNA. To examine this possibility, RPA complexes were pre-formed with Tag adsorbed to antibody beads, and after unbound RPA was removed, ssDNA was titrated into the complexes. The lengths of ssDNA chosen for this experiment (8, 15, or 30 nucleotides) correspond to those bound by RPA in its three different binding modes (see Introduction). The complexes were incubated with ssDNA for one hour and then analyzed by SDS-PAGE and western blotting to detect bound RPA (Figure 39a). In the absence of ssDNA, RPA remained stably bound to the Tag beads for at least one hour after removal of the free RPA (lanes 3). When the Tag-RPA complexes were exposed to an 8-nucleotide ssDNA (upper panel) or, as a negative control, to duplex DNA (not shown), the complexes remained stable. In the presence of a 15-mer, most of the RPA remained bound to the Tag beads except when exposed to the highest amounts of ssDNA (middle panel, lanes 8, 9). Remarkably, in the presence of a 30-mer, most of the bound RPA was dissociated from Tag (lower panel, lanes 4-9). These findings indicate that the length of

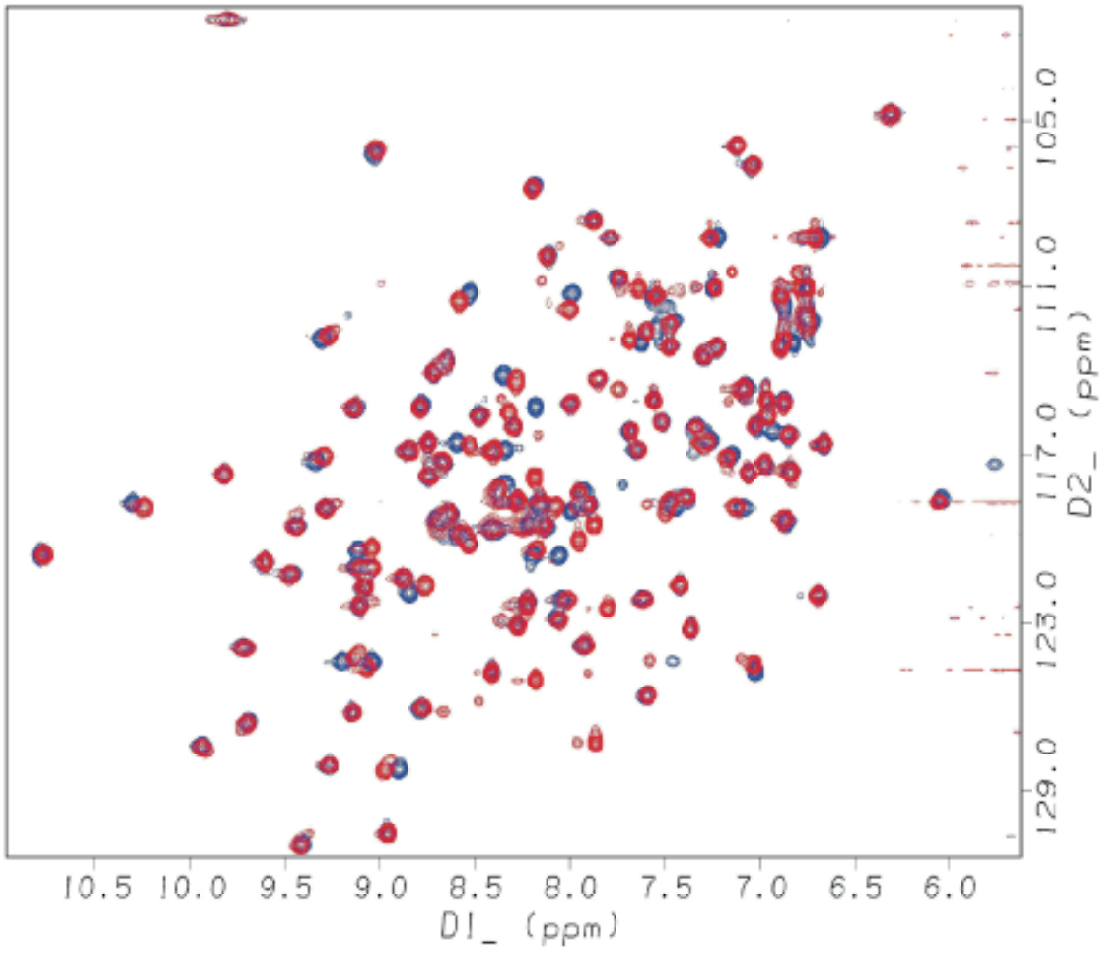

Figure 38: Similarity of NMR chemical shifts reveals that the R154E mutation in Tag-OBD does not significantly affect protein structure. Overlay of the 600 MHz 15N-1H HSQC NMR spectra of wild-type (blue) and R154E (red) Tag-OBD.

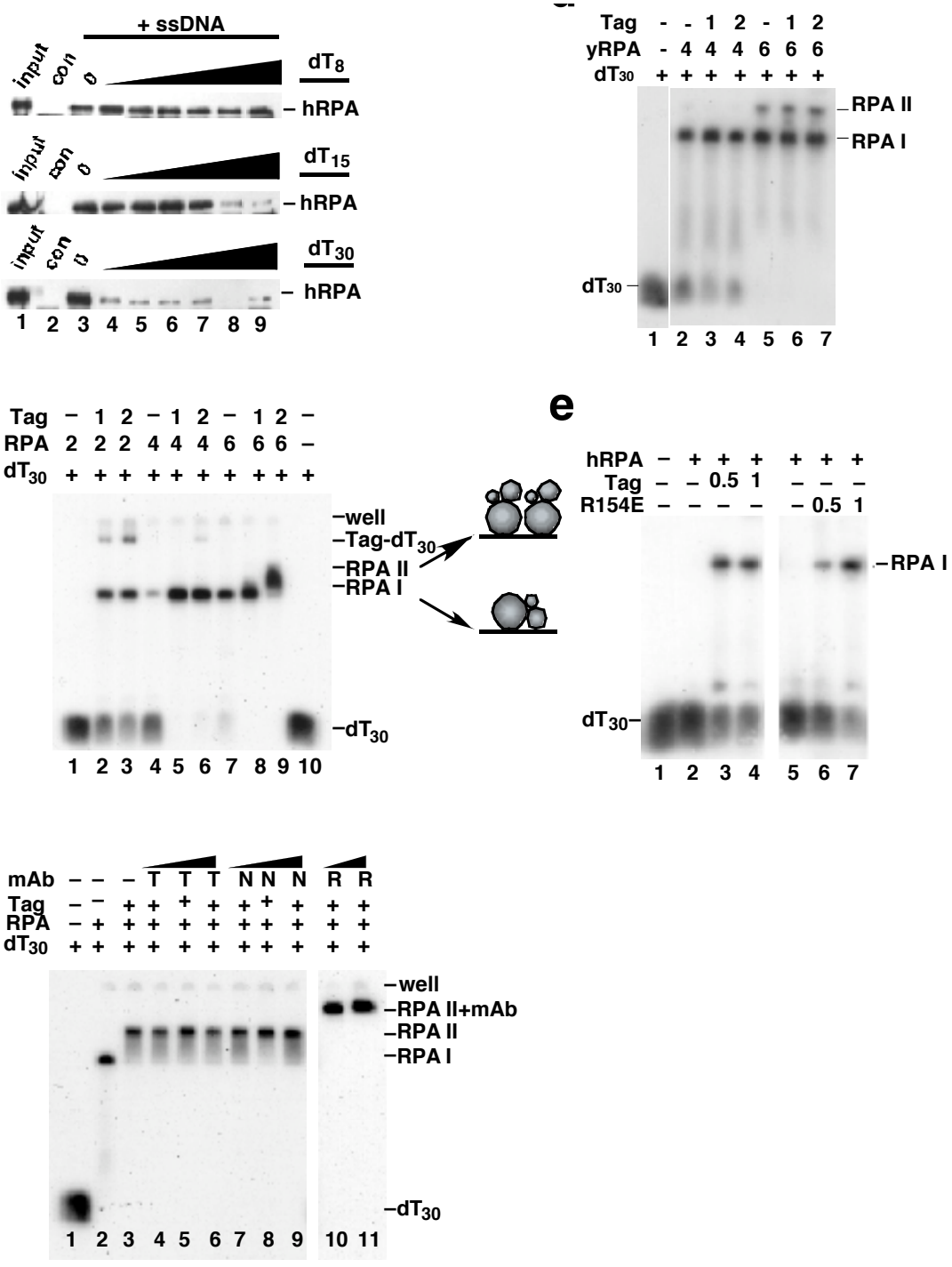

Figure 39: Transient Tag binding to RPA facilitates ssDNA binding of RPA. (a) Tag bound to Pab101-protein G beads was incubated with RPA (8.6 pmol) or without RPA (con). After washing the beads, increasing amounts of oligonucleotides dT_{30}, dT_{15}, or dT_8 (0, 1, 2, 4, 9, 17, or 34 pmol) were added. After 1 h, the amount of (to be continued)

(Figure 39-continued) RPA that remained bound to Tag was visualized by SDS-PAGE and western blot with anti-RPA70 antibody. Input: 5% of the RPA added to samples. (b) RPA in the indicated amounts (pmol) was pre-incubated with ~3 pmol of radiolabeled dT_{30} for 10 min at 25°C and then, after addition of the indicated amounts of Tag (pmol of hexamer), for another 15 min at 37°C. Protein-DNA complexes were detected by native gel electrophoresis and autoradiography. The migration of Tag-dT_{30} complex (Figure 40) is indicated. W, wells of the gel. (c) RPA (9 pmol) was incubated with ~3 pmol of dT_{30}, followed by addition of 3.5 pmol of Tag hexamer and, after 5 min, monoclonal antibody (0.5, 2.5, or 5 μg) against Tag (T), influenza hemagglutinin (N), or RPA32C (R). Complexes were visualized as in (b). (d) The indicated amounts (pmol) of yeast RPA (yRPA) were incubated with ~ 3pmol of radiolabeled dT_{30} in the presence of Tag hexamer (pmol) as indicated. Complexes were analyzed as in (b). (e) Increasing amounts (0.5 or 1 pmol of hexamer) of wild type (lanes 3 and 4) or mutant R154E Tag (lanes 6 and 7) were added to RPA (2 pmol) that had been preincubated with radiolabeled dT_{30} as indicated, and protein-DNA complexes were analyzed by native gel electrophoresis and autoradiography as in (b).

ssDNA bound to RPA affects its ability to exist in a stable complex with Tag. One possible interpretation of the data is that RPA in its compact binding mode with an 8-mer forms a stable ternary complex with Tag, but that RPA in its extended binding mode with a 30-mer binds more weakly to Tag, leading to its dissociation from Tag. This correlates with the greater affinity of RPA for a 30-mer than for shorter oligonucleotides.

To gain further insight into the interaction of RPA with ssDNA in the presence and absence of Tag, electrophoretic mobility shift assays were performed. In the absence of Tag, RPA bound to radiolabeled ssDNA (dT_{30}) with the expected 1:1 stoichiometry of RPA:ssDNA (RPA I) (Figure 39b, lanes 1, 4, 7). Importantly, when Tag was added to the same amount of RPA that had been pre-incubated with labeled dT_{30}, the stoichiometry remained 1:1 but the abundance of the RPA:ssDNA complex clearly increased (lanes 2, 3, 5, 6). Hence, Tag stimulated RPA binding to the 30-nucleotide ssDNA, even though there is no evidence of Tag being present in the complex along with RPA and ssDNA.

A novel slower migrating, diffuse species was observed at the highest concentration of RPA when Tag was present (RPAII, Figure 39b, lanes 8, 9). To characterize the composition of this complex, the mobility shift experiment was repeated in the presence of monoclonal antibody against RPA or Tag. When a saturating amount of RPA was incubated with radiolabeled ssDNA (Figure 39c, lanes 2, 3), addition of Tag was seen to lead to formation of a slowly migrating ssDNA complex (RPAII) (lane 3). When purified monoclonal antibody against the extreme C-terminus of Tag was titrated into the binding reaction, the mobility of the ssDNA complex remained unchanged (lanes 4-6). Two other antibodies that recognize epitopes remote from the Tag-OBD and do not

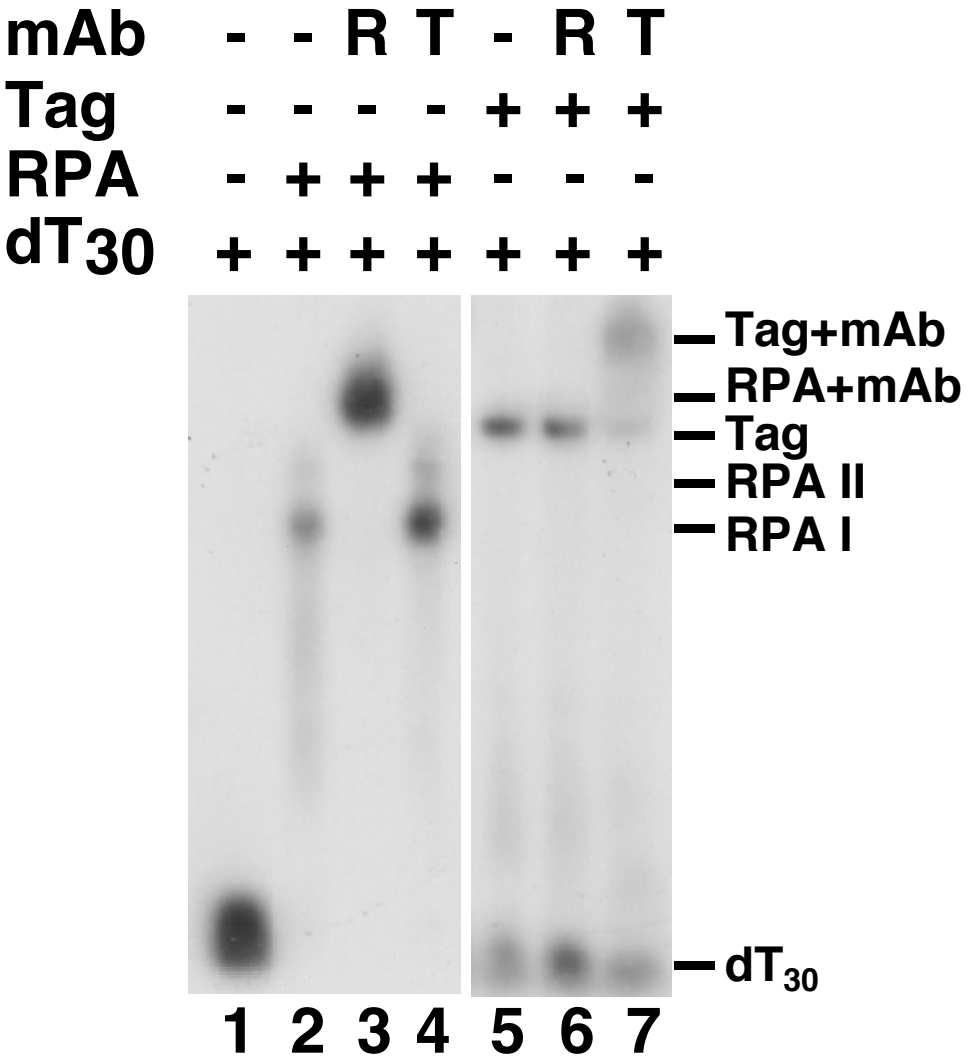

Figure 40: Migration of RPA- and Tag-ssDNA complexes in native gel electrophoresis. Radiolabeled dT_{30} (3 pmol) was incubated in the presence (+) or absence (-) of RPA (7 pmol) as indicated for 10 min at 37^0C (lane 1 to lane 4). Radiolabeled dT_{30} (3 pmol) was incubated with Tag (3.5 pmol hexamer) for 30 min at 37^0C (lane 5 to lane 7). Purified monoclonal antibody (mAb) (2.5 μg) against RPA (Ab 34A) (R) or against Tag (PAb101) (T) was added and incubated for 10 min at 37^0C. The total reaction volume was 15 μl. Samples were analyzed by native gel electrophoresis and autoradiography as in Figure 39b.

interfere with RPA:Tag complex formation (Weisshart et al., 1998) yielded identical results (not shown). These results indicated that Tag is not present in RPAII. The mobility of the RPAII complex was also unaffected by addition of control antibody against influenza hemagglutinin (lanes 7-9), but was supershifted to a slower mobility in the presence of antibody against RPA32C (lanes 10, 11). We conclude that the RPAII complex observed at high RPA concentrations is not a ternary complex with Tag. We believe that RPAII may contain 2 or 3 RPA molecules bound to the 30-mer in a compact binding mode (Blackwell et al., 1996).

Since Tag did not appear to form a stable ternary complex with RPA and a 30-mer ssDNA, we asked whether direct physical interaction between Tag and RPA was necessary to stimulate ssDNA binding to RPA. To address this question, additional mobility shift assays were carried out with RPA from budding yeast, which binds ssDNA but not Tag (Melendy & Stillman, 1993). In these experiments, ssDNA binding of yeast RPA was unaffected by Tag (Figure 39d, lanes 2-7), arguing that at least a transient Tag interaction with RPA is required to enhance RPA binding to a 30-mer. To further assess the role of Tag-RPA interaction in facilitating RPA binding to ssDNA, the previously discussed mutant Tag (R154E) with reduced affinity for RPA70AB (Figure 37d) was tested in mobility shift experiments (Figure 39e). Tag R154E retained the ability to stimulate RPA binding to dT_{30}, but its activity was clearly reduced (Figure 39e, compare lanes 3 and 6). The results in Figures 39d and e indicate that the ability of Tag to facilitate RPA binding to a 30-nucleotide ssDNA correlates with Tag-RPA affinity.

Discussion

We have shown here for the first time that during activation of a simple model pre-replication complex, origin DNA unwinding is directly coupled to RPA loading on the emerging ssDNA, and that physical interaction of the pre-replication protein Tag with RPA70AB, but not RPA32C, is required for this novel coupling (Figure 33). The interaction surfaces of Tag-OBD and RPA70AB have been mapped, revealing a strong electrostatic component. Formation of a stable ternary complex composed of RPA, an 8-mer ssDNA, and Tag has been demonstrated (Figures 35-37,39). However, RPA binding to a 15 to 30-mer ssDNA was shown to lead to dissociation of Tag from the ternary complex (Figure 39), completing the RPA loading process.

The structural perspective provided in this study significantly advances our understanding of the complex interplay between RPA and Tag during DNA unwinding. The ability of RPA to bind simultaneously to Tag and an 8-mer ssDNA in a ternary complex demonstrates that Tag and ssDNA do not compete directly for RPA. Our evidence suggests that dissociation of Tag from the ternary complex in the presence of 15-30 nucleotide ssDNA involves allosteric remodeling of RPA quaternary structure from a compact 8-nucleotide binding mode into an extended ssDNA binding mode that weakens Tag binding. The precise nature of these conformational changes is currently under investigation.

The ternary complex: A coupling device for protein-mediated RPA loading during DNA unwinding

Our new results suggest a simple two-step model for Tag-mediated RPA loading on ssDNA as it emerges from the active helicase (Figure 41a). Once the Tag hexamer is active, it moves 3' to 5' on ssDNA, displacing the complementary strand. Based on the recent crystal structure of the closely related papillomavirus E1 helicase domain in complex with ssDNA (Enemark & Joshua-Tor, 2006), the displaced strand would emerge close to the Tag-OBD (Figure 41a, top). Our model suggests that the basic RPA70AB-binding surface of a Tag-OBD would be exposed to the exterior as the helicase moves, positioning it to bind RPA. An exposed basic surface of Tag-OBD was recently noted in the crystal structure of hexameric Tag-OBD in an open spiral (Meinke et al., 2006). Based on our findings, formation of the ternary complex would occur upon the extrusion of 8-10 nucleotides of ssDNA. Continued helicase action (~200 nucleotides per min) (Murakami & Hurwitz, 1993), would rapidly generate a 30 nucleotide stretch of ssDNA, allowing RPA to bind in an extended ssDNA binding mode that weakens binding to Tag-OBD and leads to Tag release (Figure 41a, bottom). This simple model depicts an initial and a final step in loading each RPA molecule, but is not meant to rule out the possible existence of intermediate steps.

During initiation of SV40 DNA replication (Bullock, 1997; Simmons, 2000; Fanning & Pipas, 2006), a similar structural mechanism may couple origin DNA unwinding with RPA loading on the emerging ssDNA, as depicted in Figure 41B. SV40 DNA replication begins with the assembly of a simple pre-replication complex, the Tag double hexamer, in the presence of ATP on the central palindrome of the viral origin, nucleated by sequence-specific contacts of two subunits in each hexamer with the four pentanucleotides in the palindrome (arrows in Figure 41b). Assembly of the double

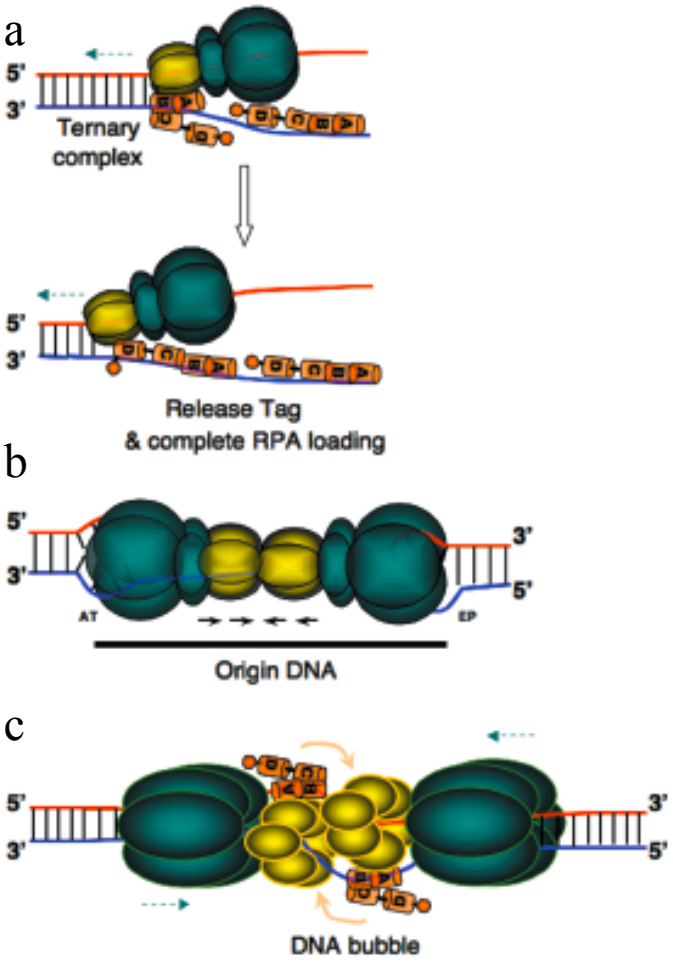

Figure 41: Proposed mechanism for coupling activation of the SV40 pre-replication complex with RPA loading on ssDNA. (a) An active Tag hexamer (OBD and N-terminus in gold; helicase domains in turquoise) translocating 3' to 5' on the red strand (dotted line) and displacing the blue strand is proposed to form a ternary complex, in which Tag-OBD binds to RPA70AB (orange) associated with 8-10 nucleotides of ssDNA. As more DNA is unwound, RPA extends into the 30-nucleotide binding mode on ssDNA and releases Tag-OBD. (b) Tag monomers recognize four specific binding sites (black arrows) in the origin DNA, nucleating double hexamer assembly and inducing an ssDNA bubble at the flanking EP sequence and distortion at AT. The depicted path of DNA through the Tag double hexamer is speculative (Li et al., 2003; Gai et al., 2004b; Valle et al., 2006). (c) Remodeling of the Tag N-terminus and Tag-OBD (Meinke et al., 2006; Valle et al., 2006) in the presence of human RPA is proposed to facilitate formation of a ternary complex composed of RPA70AB bound to an ssDNA bubble and to a basic OBD surface exposed on the exterior of each hexamer, analogous to that shown in (a). As the helicase translocates (dotted lines) and more ssDNA emerges, RPA would extend into the 30-nucleotide binding mode on ssDNA (orange arrows) and dissociate from Tag, completing the loading cycle.

hexamer is accompanied by remodeling of contacts between Tag subunits, both in the helicase domain and in the N-terminal and OBD domains (Smelkova & Borowiec, 1998; Weisshart et al., 1999; Li et al., 2003; Gai et al., 2004a; Gai et al., 2004b; Weisshart et al., 2004; Meinke et al., 2006; Valle et al., 2006). This remodeling gives rise to distortion of the duplex DNA, generating an 8-nucleotide bubble in the EP region and an untwisted AT region at the opposite end of the origin (Figure 41b) (Borowiec & Hurwitz, 1988). The single-stranded bubble thus represents an early intermediate in the unwinding reaction catalyzed by the double hexamer and marks the origin of bidirectional replication from which the two leading strands initiate and diverge (Hay & DePamphilis, 1982).

Interestingly, the ability of heterologous ssDNA-binding proteins to bind to a synthetic 8-nucleotide ssDNA-bubble substrate correlates with their ability to support SV40 origin DNA unwinding by Tag (Iftode & Borowiec, 1997; Iftode & Borowiec, 1998), suggesting a possible role for RPA binding to such a bubble during unwinding. We propose that origin distortion leads to extrusion of an ssDNA bubble near the OBDs and to exposure of at least one OBD surface from each hexamer (Gai et al., 2004b; Meinke et al., 2006; Valle et al., 2006), enabling the formation of a ternary complex of RPA and Tag-OBD with the ssDNA bubble (Figure 41c). Thus, as noted for RPA loading on emergent ssDNA from the active helicase, the ternary complex would physically couple origin unwinding with RPA loading. As origin DNA unwinding progresses, more ssDNA would be extruded from the double hexamer (Wessel et al., 1992; Murakami & Hurwitz, 1993; Fanning, 1994; Smelkova & Borowiec, 1998; Alexandrov et al., 2002). Repetition of the unwinding and RPA loading cycle to generate enough template for

replisome assembly would set the stage for Tag-mediated RPA displacement and DNA polymerase alpha-primase loading to initiate leading strand synthesis (Arunkumar et al., 2005).

Although this model is speculative, it allows several previously unexplained observations to be rationalized. For example, excess yeast RPA is unable to compete effectively with human RPA in SV40 initiation (Figure 33D), which can be explained by the fact that the ssDNA-bubble complex bound to yeast RPA could not be stabilized in a ternary complex with Tag. Our model also offers an explanation for the previously puzzling observation that a monoclonal antibody against RPA70 (Mab70C) inhibits SV40 origin DNA unwinding even though Mab70C does not inhibit ssDNA binding of RPA (Kenny et al., 1990). Notably, Mab70C binds to the same region of RPA70AB that interacts with Tag-OBD (Gomes & Wold, 1996) and presumably inhibits ternary complex formation with Tag, thereby inhibiting origin unwinding.

Our proposal of a ternary complex of RPA70AB, Tag, and an 8-mer as the initial step in protein-mediated RPA loading on ssDNA is fully consistent with the sequential binding mechanism of RPA domains A-D to ssDNA that was proposed for purified RPA (Bochkareva et al., 2002; Arunkumar et al., 2003; Wyka et al., 2003). Protein-mediated RPA loading on emerging ssDNA offers obvious advantages over diffusion-mediated loading on pre-existing ssDNA, since the ssDNA would be continuously protected from nucleases and potential hairpin formation from the time of its creation until the restoration of the duplex structure. Moreover, protein-mediated RPA loading on ssDNA offers the potential to create a regular, ordered array of RPA on ssDNA that may facilitate subsequent DNA processing more effectively than diffusion-mediated RPA

loading on free ssDNA. The structural resemblance of the simple SV40 pre-replication complex to MCM double hexamers in the more elaborate eukaryotic pre-replication complex (Forsburg, 2004; Sclafani et al., 2004) is intriguing in this context. Our results provide strong motivation to determine whether DNA unwinding at cellular pre-replication complexes may also be coupled with RPA loading.

Acknowledgments

We thank S. Bhattacharya, A. Bochkarev, P.A. Bullock, X.S. Chen, M.R. Ehrhardt, E. Enemark, J. Ferguson, K. Hinson, D.L. Kaplan, M.K. Kenny, A.R. Nager, E. Petrova, P. Shindiapina, D. Williams, M.S. Wold, and K. Zhao for helpful discussions, valuable advice and assistance. Financial support is gratefully acknowledged from the US National Institutes of Health for operating grants (GM65484 to W.J.C. and GM52948 to E.F.) and support to the Vanderbilt-Ingram Cancer Center (P30 CA68485) and the Vanderbilt Center in Molecular Toxicology (P50 ES00267), as well as from the Howard Hughes Medical Institute Professors Program (to E.F.) and Vanderbilt University.

CHAPTER IV

CONCLUSION AND DISCUSSION

Summary of RPA dynamics during DNA replication initiation

Our studies of interaction between T antigen and RPA demonstrate the dynamic behavior of RPA during DNA replication initiation. Detailed understanding of the physical interaction of T antigen-OBD with two separate domains of RPA has been revealed as discussed in Chapter II and III.

Although T antigen-OBD interaction with RPA70 has been known for a long time (Weisshart et al., 1998), the details of this interaction were unknown. With the structural data made available by our collaborators, we find that T antigen-OBD interacts with RPA70AB primarily through electrostatic interaction as discussed in Chapter III (Jiang et al., 2006). Charge reversal mutations weaken the interaction. The T antigen-binding site on RPA70AB is distal from the surface that contributes to the high affinity ssDNA binding of RPA70AB. Importantly T antigen-OBD forms a ternary complex with RPA70AB-8-mer-ssDNA, as revealed by NMR studies and by partial proteolysis of RPA70AB in complex with T antigen in the presence or absence of ssDNA. In the presence of longer ssDNA (i.e. 30-mer), intact T antigen dissociates from the RPA-ssDNA complex. Although T antigen cannot form a stable complex with RPA and 30-mer ssDNA, it facilitates RPA binding to 30-mer ssDNA as a T antigen mutant that has weaker interaction with RPA is defective in this stimulation of RPA binding to ssDNA. To test the hypothesis that T antigen interaction with RPA directly loads RPA onto

ssDNA, we used yeast RPA and a human/yeast RPA chimera to compete with human RPA in SV40 DNA replication initiation assays. It turns out that yeast RPA that doesn't interact with T antigen but binds ssDNA cannot compete with human RPA for ssDNA binding during initiation of DNA replication. Chimera RPA that interacts with T antigen and binds ssDNA can compete with human RPA for ssDNA binding. The data strongly suggest that T antigen binding to RPA70AB selectively loads RPA onto ssDNA as the viral origin DNA is unwound. Thus the ternary complex seems to be an intermediate in T antigen-mediated RPA loading. We propose that as longer ssDNA emerges from the T antigen double hexamer, RPA likely undergoes a conformational change from a compact form to an extended form, which weakens the interaction between T antigen and RPA. T antigen then dissociates from RPA-ssDNA complex, which completes the loading process.

A detailed structural model of T antigen-OBD interaction with RPA32C was established based on a series of NMR experiments as discussed in Chapter II (Arunkumar et al., 2005). There were controversial opinions about the role of RPA32C in SV40 DNA replication. Our biochemical and structural data demonstrate that T antigen interacts with RPA32C through electrostatic binding. Charge reversal mutations weaken the interaction between RPA32C and T antigen-OBD, confirming the electrostatic interaction model. Charge reversal mutations were also introduced into intact T antigen and RPA to figure out the role of RPA32C-T antigen interaction in SV40 replication initiation. Our results demonstrate that T antigen-mediated priming by pol-prim on RPA–coated ssDNA, a crucial step in initiation, requires T antigen interaction with RPA32C. These data suggest that T antigen binding of RPA32C induces remodeling of RPA on ssDNA from a tightly

bound extended mode to a more weakly bound compact mode. When pol-prim is bound concurrently to the T antigen helicase domain, pol-prim can gain access to the transiently exposed ssDNA and subsequently synthesize an RNA primer.

How does RPA associate with newly exposed ssDNA?

Our data suggest a dynamic model for RPA in initiation of DNA replication, but it is unclear where ssDNA emerges from T antigen double hexamer. As we discussed before (Figure 6), T antigen assembles as a double hexamer around origin DNA, which is the active form of T antigen during DNA replication (Mastrangelo et al., 1989; Valle et al., 2000). The isolated helicase domain of T antigen (aa 251-627) can form hexamers (Li et al., 2003). In the intact protein, the OBD and helicase domains are involved in hexamer formation, but the helicase domain is the primary site of hexamerization (Li et al., 2003). According to the structural data of T antigen-OBD and DNA complex, the first four T antigen molecules bind to the origin DNA asymmetrically (Bochkareva et al., 2006). On the other hand, the EM structures showed a symmetric double hexamer of T antigen (Valle et al., 2000; Gomez-Lorenzo et al., 2003; Bochkareva et al., 2006; Valle et al., 2006). This difference can be explained by the flexible nature of the N-terminus of the double hexamer. The J domain and the OBD of T antigen are flexible within a single hexamer even in the presence of origin DNA (Valle et al., 2006). The formation of a double hexamer reorganizes the J domain and OBD to form a middle body (Figure 41, yellow parts) between two helicase domains of double hexamer (Valle et al., 2006).

T antigen-OBD forms a left handed spiral with an inner channel of 30Å having six subunits per turn during in the crystal, which might represent the hexamer assembly

of OBD around DNA as shown in Figure 42 (Meinke et al., 2006). The inner channel is positively charged and includes residues known to bind DNA. At least three residues of T antigen-OBD that bind DNA have also been shown to bind RPA (Arunkumar et al., 2005; Jiang et al., 2006). Since the structure of the middle body is very flexible, one or more of the OBDs may rotate out from the central ring so as to more fully expose their RPA interaction surface (Valle et al., 2006; Meinke et al., 2007). While the spiral already provides a "gap" for the ssDNA stand to exit the ring, such a rotation of OBDs away from the DNA would allow both easier access for accessory proteins such as hRPA and easier egress for ssDNA (Meinke et al., 2007).

Significance and future direction

The significance of studying RPA dynamics

RPA is a modular protein involved in almost all aspects of DNA metabolism. It interacts physically and functionally with a variety of other DNA processing proteins. Those interactions are thought to transiently order and guide the parade of proteins that "trade places" on ssDNA (a model known as 'hand off'), as the processing pathway proceeds (Stauffer & Chazin, 2004b; Arunkumar et al., 2005; Fanning et al., 2006). How this hand-off mechanism works remains poorly understood. Our studies of RPA dynamics suggest a novel mechanism by which proteins may trade places on ssDNA by binding to RPA and mediating conformational changes that alter the ssDNA-binding properties of RPA.

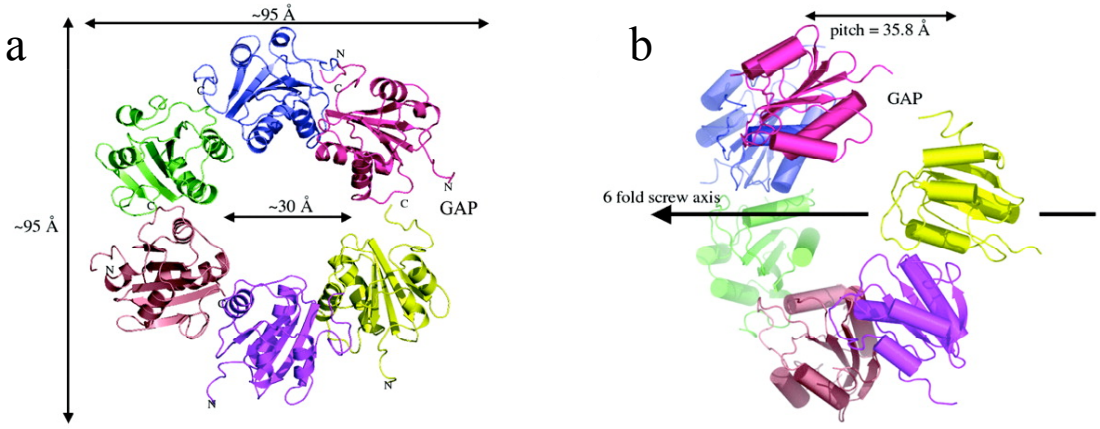

Figure 42: The structure of T antigen origin binding domain. (a) Ribbon diagram of six spirally arranged T antigen-OBD molecules. The six-fold screw axis is perpendicular to the page. Each monomer is colored differently. The inner diameter of the channel is ~30 Å. These six T antigen-OBD's form an "open ring" or spiral, and the position of the gap is shown. (b) Ribbon diagram of the spiral shown in side view to visualize the gap and the screw translation. Each monomer is colored as in A. The black line through the center of the spiral represents the six-fold screw axis (panel A rotated by ~90°). The pitch of the spiral is 35.8 Å. The opening or gap between the first molecule (yellow) and the last molecule (red) is indicated (Meinke et al., 2006).

Our studies of RPA interaction with T antigen suggest a dynamic model of RPA function in DNA processing, in which successive protein-mediated remodeling of RPA facilitates its binding to and its dissociation from ssDNA upon completion of a processing step as reviewed by Fanning et al., 2006. The basis of this dynamic model is that RPA exists in three different binding modes characterized by the length of ssDNA that is occupied by RPA and their relative affinities for ssDNA (Fanning et al., 2006). When a DNA processing protein interacts with free RPA, it remodels RPA into a compact binding mode that can form a ternary complex with a short length of ssDNA (10-mer ssDNA). If a longer ssDNA is available, the ternary complex is destabilized since RPA binds to longer ssDNA with an extended mode and higher affinity. Thus the DNA processing protein dissociates from the ternary complex and RPA binds to ssDNA with an extended mode. On the other hand, once RPA binds to ssDNA in a high affinity, extended mode, we suggest that a DNA processing protein can bind to RPA-ssDNA and remodel RPA into a lower affinity, compact mode that can be easily displaced or exchanged for a new incoming protein delivered by the RPA-associated protein. RPA offers only a limited number of distinct binding sites for DNA processing proteins. Patches of charged surface residues play a prominent role in T antigen-RPA interaction (Arunkumar et al., 2005; Jiang et al., 2006), but it is not clear yet whether electrostatic interaction are a general feature of RPA-protein interaction.

The hand-off model appears to be widely involved in RPA dynamics during DNA replication, repair and recombination. As discussed in Chapter I, in homologous recombination, RPA assembles at double stranded DNA breaks, either through diffusion or a protein-mediated mechanism, preventing formation of secondary structure (Wang &

Haber, 2004). Rad51 has to displace RPA to generate a recombinogenic Rad51-ssDNA filament (Fanning et al., 2006). In yeast, Rad52 forms a ternary complex with RPA-ssDNA and interacts with Rad51 with a separate domain (Sugiyama & Kowalczykowski, 2002). This is very similar to T antigen remodeling RPA binding modes to load pol-prim onto ssDNA, although the detailed mapping of Rad52 interaction with Rad51 and RPA is needed to further test if Rad52 remodels RPA binding mode to remove it from ssDNA. In human, the interactions among Rad52, Rad51, and RPA have been mapped. Both RPA70AB and RPA32C interact with the same site on Rad52 (aa 218-303), which is analogous to the interaction between RPA and T antigen (Jackson et al., 2002). However, RPA32C interacts with Rad52 with higher affinity compared with RPA32C interaction with T antigen. Despite the similarity between T antigen-RPA and Rad52-RPA interaction, human Rad52 doesn't remove RPA from ssDNA by remodeling RPA binding modes. Although human Rad52 interacts with Rad51, the association of Rad51 with Rad52 only helps to increase the local concentration of Rad51. Human Rad51N interacts with RPA70 ssDNA binding surfaces to compete with RPA for ssDNA binding directly (Stauffer & Chazin, 2004a).

It has been speculated that RPA interaction with some DNA helicases may enable them to actively place RPA on ssDNA as it emerges from the helicase complex (Fanning et al., 2006). Interaction of the Werner and Bloom syndrome helicases with RPA70 stimulates their unwinding activity on long duplexes, perhaps by facilitating RPA binding to ssDNA (Shen et al., 2003; Doherty et al., 2005). Whether these helicases can also displace RPA from ssDNA to mediate loading of an incoming DNA processing protein is

not known. If so, one or more features of the protein–ssDNA complex must determine whether RPA is loaded or displaced (Fanning et al., 2006).

The hand-off model is also found in other protein dynamics in DNA metabolism. For example, during pol-prim to polymerase δ switch and Okazaki fragment maturation, the clamp PCNA serves as a platform for the exchange of many DNA binding proteins. Our studies of RPA dynamics may help to understand the hand-off mechanism in other processes. Our detailed model of RPA dynamics in DNA replication further confirms that proteins don't exist in a pre-assembled complex, but assemble/disassemble when needed (Kowalczykowski, 2000).

Future directions

Although our studies laid the groundwork to understand RPA dynamics during the initiation steps of SV40 DNA replication, additional steps of DNA replication are thought to involve RPA dynamics. During the elongation step of DNA replication, pol-prim removes RPA from ssDNA without T antigen. In addition, the primase dimer can transiently stimulate RPA binding to a 30-mer ssDNA in a manner similar to T antigen (Jiang and Fanning, unpublished data; Figure 39). This result suggests that primase modulates RPA-ssDNA binding from an extended mode to a compact mode to unload RPA from ssDNA. Detailed mapping of interaction domains between primase and RPA is needed to answer this question.

Further studies of RPA mutants will greatly help to confirm the RPA loading model in SV40 DNA replication. RPA70 mutants that are defective in T antigen binding should be impaired in the RPA loading process. Yeast RPA should compete with RPA70

mutants in viral DNA replication initiation assays. However, currently there is no RPA70 mutant available that is stable in solution and defective in T antigen binding.

Whether the RPA dynamics *in vivo* corresponds to the *in vitro*-derived models proposed in chapters II and III is unknown. To answer this question, RPA32 mutants can be introduced into SV40-infected human cells with greatly reduced level of endogenous RPA32 (Vassin et al., 2004). T antigen, RPA32 mutants, and endogenous replication factors can be examined in SV40-infected cells by immunofluorescence to test if RPA mutants localize in the viral replication centers. The viral replication products can be extracted from infected human cells and quantitified by Real-time Polymerase Chain Reaction (PCR). If the *in vitro* model for primosome function (Figure 31) applies *in vivo*, RPA32C mutants should not support the initiation of SV40 DNA replication. Thus RPA mutants transfected cells should have fewer replication products than WT RPA transfected cells. Conversely, it should be possible that a mutant T antigen that does not bind to RPA32 fails to replicate, but so far this experiment has not been performed. Although there are many T antigen mutants available, the residues of T antigen involved in RPA binding also interact with SV40 origin (Luo et al., 1996; Arunkumar et al., 2005). Thus it is difficult to find a T antigen mutant that is defective only in RPA binding.

RPA dynamics in eukaryotic DNA replication initiation

The rationale for studying SV40 DNA replication was to develop an understanding of the mechanism of human DNA replication, since the initiation of eukaryotic DNA replication is far more complicated. I hypothesize that RPA dynamics also happens in eukaryotic replication. Although T antigen is responsible for both loading and unloading RPA

during viral replication, there may be one or more cellular proteins that play these roles during eukaryotic DNA replication. The protein/ protein complex candidate needs to interact with the helicase and RPA for the loading process. It has to interact with RPA and pol-prim for the RPA unloading process. MCM (minichromosome maintenance) might be the candidate responsible for RPA loading in eukaryotes. MCM2-7 is the helicase in eukaryotic DNA replication (Costa & Onesti, 2008). Although MCM2-7 doesn't have the origin-binding domain, it has an N-terminal domain that is capable of binding both ssDNA and dsDNA (Costa & Onesti, 2008). T antigen-OBD is required for helicase activity after origin recognition. T antigen-OBD residues that are involved in non-specific contacts with DNA are essential for helicase activity (Simmons et al., 1990b). T antigen-OBD has ssDNA binding activity (Reese et al., 2006). All these similarities suggest that the N-terminus of MCM2-7 might be involved in loading RPA onto ssDNA. However, there is so far no evidence showing that MCM2-7 interacts with RPA. To further test if MCM2-7 is involved in the loading process, MCM2-7 interaction with RPA needs to be investigated. EMSA can be used to test if MCM2-7 stimulates RPA binding to ssDNA *in vitro*.

Since the functions of eukaryotic DNA replication proteins have been specialized, there might be a specific protein/proteins involved in unloading RPA. MCM10, the first protein that associates with cellular pre-replication complexes in S phase, recruits pol-prim to origins of replication (Fien et al., 2004; Ricke & Bielinsky, 2004; Ricke & Bielinsky, 2006). Recent studies demonstrate that p180 interacts with two different sites on MCM10 (Robertson et al., 2008). MCM10 also interacts with MCM2-7, the DNA helicase in budding yeast (Izumi et al., 2000). Thus MCM10 might be involved in

unloading RPA via interacting with the helicase and pol-prim. However, it is unknown whether MCM10 interacts with RPA or interacts with another protein able to remodel RPA-ssDNA binding. Pull down experiments can be used to test if MCM10 interacts with RPA. The potential candidates for unloading RPA should interact with RPA on one or both binding sites and stimulate RPA binding to ssDNA in an EMSA assay. With more and more proteins discovered in eukaryotic DNA replication, there might be more candidates for loading and unloading RPA. Those studies would greatly enhance our understanding of the initiation of human DNA replication. In summary, our studies elucidate the mechanism of RPA dynamics during initiation of SV40 DNA replication, which broadens our knowledge about protein dynamics and implies the mechanism of RPA dynamics in many other aspects of DNA metabolism.

APPENDIX

TOPBP1 INTERACTS WITH T ANTIGEN AND DNA POLYMERASE α-PRIMASE

Introduction

Simian Virus 40 (SV40) is a small DNA virus with a 5.2 kb genome that assembles as a mini-chromosome (Fanning et al., 2008). SV40 DNA replication requires only one viral protein, large T antigen (Challberg & Kelly, 1989; Stillman, 1989; Hurwitz et al., 1990). T antigen recruits additional required replication proteins from host cells. With many years of studies, 10 host proteins were identified and found essential for viral replication *in vitro* as shown in Table 1 (Waga & Stillman, 1998). SV40 has been used as a model system to study human replication since SV40 DNA replication is thought to mimic the host chromosomal replication as discussed in Chapter I.

Despite many similarities, big differences exist between viral and host DNA replication. Replication of the host chromosome is regulated to ensure that DNA replication occurs only once per cell cycle. In contrast, viral replication is very productive and results in replication of thousands of daughter genomes per cell cycle (Tegtmeyer, 1972; Chou et al., 1974; Botchan et al., 1979). The interaction of T antigen with Nbs1 is proposed to disrupt the cell cycle control to achieve multiple viral and host replications per cell cycle (Wu et al., 2004). Moreover, SV40 DNA replication is correlated with ATM activation and phosphorylation of T antigen (Shi et al., 2005). Recent studies in our lab suggest that SV40 DNA replicates in a DNA damage signaling active environment

and that ATM activity is required for viral replication (Zhao et al., 2008). ATM recruits other DNA damage signaling proteins such as Mre11-Rad50-Nbs1 (MRN) complex to the viral replication center. This recruitment is important for proteasome-dependent degradation of MRN complex through T antigen interaction with Cul7 ubiquitin ligase (Zhao et al., 2008). A mutant virus with T antigen mutant defective in Cul7 binding produces fewer virus progeny compared with WT virus. Thus SV40 re-programs the ATM damage-signaling pathway to facilitate its own replication. In host cells, DNA replication stops once DNA damage signaling pathways become active, and DNA damage repair system is thought to repair any damaged DNA. Interestingly, the ten host proteins essential for viral replication are also involved in DNA repair processes (Waga & Stillman, 1998). These observations suggest that SV40 viral DNA replication represents a damage- or stress-adapted pathway that utilizes mechanisms related to host DNA repair or replication fork recovery after damage.

T antigen has four functional domains: a Dna J chaperone domain, an origin DNA-binding domain, a helicase domain, and a host range domain. Interactions of T antigen with the p53 tumor suppressor, retinoblastoma family proteins, the Hsc70 chaperone protein, the mitotic spindle checkpoint protein Bub1, and the ubiquitin ligase CUL7 protein contribute to oncogenic cell transformation (Cotsiki et al., 2004; Ahuja et al., 2005; Kasper et al., 2005; Gjoerup et al., 2007). T antigen interacts with the N-terminus of Nbs1 to disrupt the cell cycle regulation of host DNA replication (Wu et al., 2004). T antigen also interacts with RPA, DNA pol-prim and Topoisomerase I for viral DNA replication (Dornreiter et al., 1992; Simmons et al., 1996; Weisshart et al., 1998).

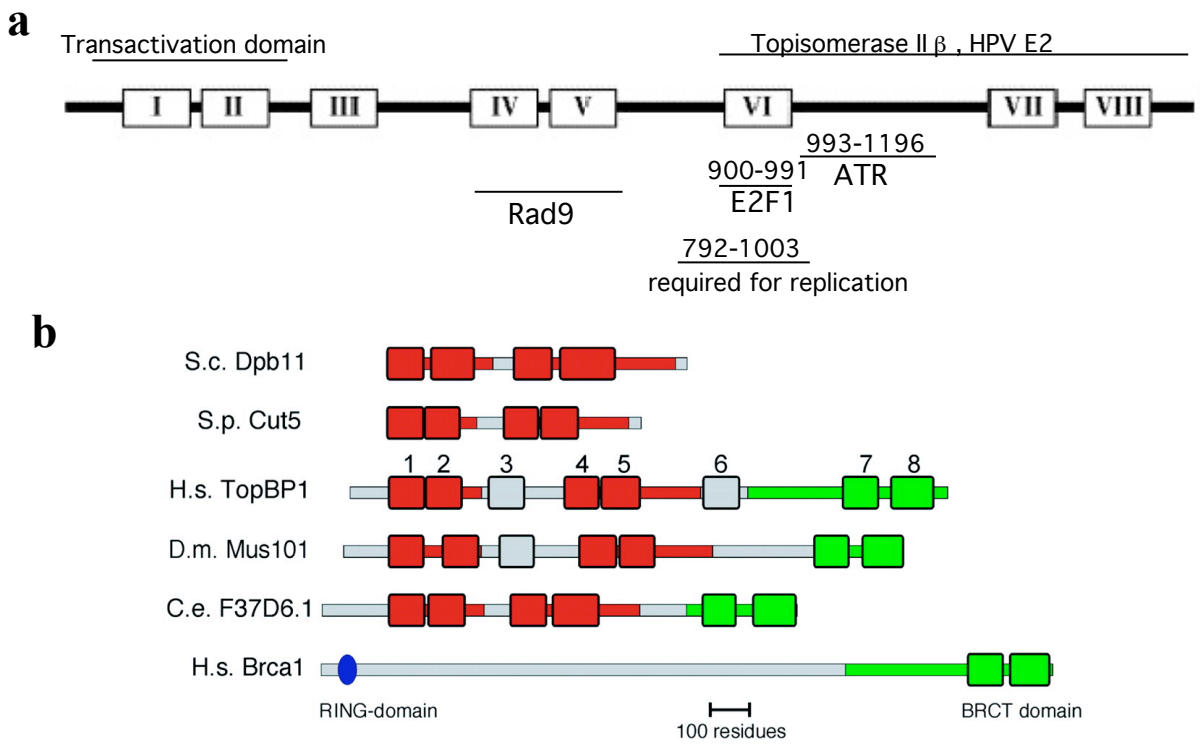

Figure 43: Schematic drawing of human TopBP1 and its homology in other species. (a) Human TopBP1 has eight BRCT domains (I-VIII) shown in boxes. Its interacting proteins and binding sites are shown in the drawing. (b) TopBP1 homology in different species and compared with human Brca1(Makiniemi et al., 2001).

Recent studies show that human TopBP1 (Topoisomerase IIβ binding protein 1) might be involved in SV40 DNA replication (personal communication with Dr. Matthew Michael at Harvard University). TopBP1 has eight BRCT (BRCA1 carboxyl terminus) repeats (Figure 43a). TopBP1-related proteins have been found in diverse eukaryotic species (Garcia et al., 2005) and all TopBP1 orthologs have the BRCT repeats (Figure 43b). BRCT is a structural domain similar to the Brca1 C-terminus (Figure 43b) that often binds phosphoproteins (Manke et al., 2003; Yu et al., 2003). BRCT-containing proteins are known for forming large protein complexes involved in the surveillance of DNA integrity (Larsen et al., 2003). Like other BRCT proteins, TopBP1 is a multiple functional protein that is involved in DNA replication, stalled replication forks, DNA damage detection, and DNA damage checkpoint activation (Garcia et al., 2005).

TopBP1 has dual roles in DNA replication and DNA damage signaling. It is essential for loading of cdc45 and DNA polymerases α and ε in the *Xenopus* DNA replication initiation process (Van Hatten et al., 2002; Hashimoto & Takisawa, 2003) and for activation of ATR/ATRIP in DNA damage in *Xenopus* extract (Kumagai et al., 2006; Lee et al., 2007; Yoo et al., 2007). TopBP1 in association with other proteins, is vital to stimulate ATR kinase activity, which is both sufficient and necessary for ATR activation of checkpoint response in *Xenopus* cell extract (Kumagai et al., 2006). TopBP1, as the activation factor, transiently interacts with ATR to activate ATR kinase activity (Kumagai et al., 2006).

The detailed mechanisms by which TopBP1 activates ATR differ depending upon the types of DNA damage. In response to double stranded DNA break (DSB), in *Xenopus* extract ATM stably associates with TopBP1 and phosphorylates Ser1131 (Yoo et al.,

2007). This phosphorylated isoform of TopBP1 has increased affinity for ATR/ATRIP, resulting in activation of the ATR/ATRIP pathway. TopBP1 phosphorylation is also required for chk1 phosphorylation at DSBs (Yoo et al., 2007). It appears that stalled replication forks adopt a different mechanism to activate ATR/ATRIP through TopBP1. At stalled replication forks, the Rad9-Hus1-Rad1 checkpoint clamp gets loaded onto the stalled replication site. TopBP1 BRCT domains I and II interact with the Rad9-Hus1-Rad1 checkpoint clamp through the phosphorylated C-terminus of Rad9 (Lee et al., 2007). This interaction is necessary for activation of ATR through ATR/ATRIP binding of TopBP1 and for phosphorylation of chk1 at the stalled DNA replication fork (Lee et al., 2007). Thus TopBP1 is necessary to activate two DNA damage-signaling pathways.

There are other lines of evidences that TopBP1 is involved in DNA damage signaling pathways. PML bodies are subnuclear structures that contain promyelocytic leukaemia (PML) proteins and they are involved in the regulation of gene expression, apoptosis, p53 function, senescence, DNA repair, the interferon response and viral infection (Everett, 2006). PML bodies are found near sites of DNA damage (Everett, 2006) and are correlated with viral replication (Maul et al., 1996). SV40 DNA replication foci juxtapose with PML bodies and viral DNA replication is preferentially located in close association with PML bodies (Maul et al., 1996; Zhao & Fanning, unpublished data). These observations are consistent with the idea that viral DNA replication is related to DNA repair pathways. TopBP1 co-localizes in foci with PML, ATM, Rad50 and Rad9 after ionizing radiation (IR) (Xu et al., 2003). PML can stabilize TopBP1 after IR (Xu et al., 2003). Data from our lab also show that TopBP1 co-localizes with T antigen in viral replication center in virus-infected cells (Zhao & Fanning, unpublished data), suggesting

that TopBP1 might play a role in viral replication. In addition, TopBP1 might directly interact with replication proteins since it associates with ORC and is required for host DNA replication initiation in *Xenopus* extracts (Van Hatten et al., 2002; Hashimoto & Takisawa, 2003).

TopBP1 is involved in viral replication in human papillomavirus (HPV) (Boner & Morgan, 2002; Boner et al., 2002). TopBP1 interacts with HPV E2 proteins (Boner & Morgan, 2002; Boner et al., 2002), serves as a transcription cofactor of HPV16 E2 protein (Boner et al., 2002), and stimulates the E2-mediated DNA replication of HPV16 (Boner et al., 2002). E2 is a transcription regulator essential for the life cycle of HPV (Ham et al., 1991). HPV E1 and E2 together are functionally similar to T antigen, as T antigen also regulates its own gene transcription. These similarities led me to hypothesize that TopBP1 is involved in SV40 viral replication. In addition, the involvement of TopBP1 in the ATR/ATRIP signaling pathway suggests that SV40 infection may re-program the ATR/ATRIP checkpoint pathway.

To test these hypotheses, the localization of TopBP1, T antigen and endogenous replication factors were examined in SV40-infected cells by immunoflueorescence (Zhao & Fanning, unpublished data). These studies revealed that TopBP1 co-localizes with T antigen, RPA and DNA polymerase α-primase, consistent with possibility that TopBP1 is involved in viral DNA replication in vivo. SV40 DNA replication assays reconstituted *in vitro* with purified proteins is stimulated by TopBP1 (Zhang & Fanning, unpublished data). In this chapter, I tested if TopBP1 interacts directly with T antigen as HPV16 E2 does. The co-immunoprecipitation (co-IP) experiments show that TopBP1 interacts with T antigen and DNA pol-prim.

Material and Methods

Protein purification

T antigen was purified from Hi-5 cells infected with a recombinant baculovirus that expresses T antigen as described (Jiang et al., 2006). Pol-prim was purified from Hi-5 cells co-infected with baculoviruses expressing p180, p68, p58, p48 (Ott et al., 2002). Purified TopBP1 and fragments used in this chapter were gifts from Daniel Mordes and Gloria Glick in Dr. David Cortez' lab at Vanderbilt University. Full length his-tagged TopBP1 was expressed in Hi-5 cells and purified over nickel-nitrilotriacetic acid column. GST-tagged full length TopBP1 [the construct is a gift from Dr. Weei-chin Lin at University of Alabama at Birmingham, (Liu et al., 2006)] and fragments (the proteins are a gift from Dr. David Cortez's lab at Vanderbilt University) were expressed in bacterial BL21 cells and purified with glutathione beads.

Co-immunoprecipitation Assays

20 μl of protein A agarose beads was incubated with 7.5 μg SJK132-20 anti-polα antibody (Bensch et al., 1982) or 15 μg PAb101 α-T antigen antibody (Fanning et al., 1981) for an hour in binding buffer [30 mM HEPES–KOH (pH 7.9), 10 mM KCl, 7 mM $MgCl_2$] at 4 ^{0}C with end-over-end rotation. Beads were briefly washed to remove unbound antibody. 5 μg purified pol-prim or 10 μg purified T antigen was added to the beads and the mixture was incubated at 4 ^{0}C for an hour in binding buffer. Beads were briefly washed to remove unbound proteins. Varying amounts of purified TopBP1 or

fragments of TopBP1 were added and reactions were incubated for an hour at 4 ^{0}C in binding buffer. The reactions were washed twice with binding buffer and three times with washing buffer [30 mM HEPES–KOH (pH 7.9), 50 mM KCl, 7 mM $MgCl_2$, 0.25% inositol, 0.05% NP-40]. The beads were heated to 95 ^{0}C for 2 minutes in 20 μl of 4x SDS-PAGE loading buffer. The proteins bound to the beads were separated by 12.5% SDS-PAGE and visualized by using different antibodies, TopBP1 antibody BL893 (Bethyl Laboratories, Inc.) for full length TopBP1 and the GST-tagged fragments of TopBP1, Pab101 antibody for T antigen, and 2CT25 for p180 (Dornreiter et al., 1990).

Results

T antigen binds to the C-terminal region of TopBP1

Since TopBP1 plays a dual role in DNA replication and repair and the preliminary data from our lab suggest that TopBP1 stimulates viral DNA replication *in vitro* (Zhang & Fanning, unpublished data), I wondered whether TopBP1 could interact with T antigen. Co-IP assays were used to address this question. Purified T antigen bound to antibody beads was incubated with two different amounts of purified his-tagged full length TopBP1 and bound TopBP1was analyzed by 12.5% SDS –PAGE gel and western blotting (Figure 44). Lanes 1 and 5 show input controls with T antigen and TopBP1 respectively. In the absence of T antigen, there was no band corresponding to the molecular weight of TopBP1 (lane 4). T antigen pulled down TopBP1 in a concentration-

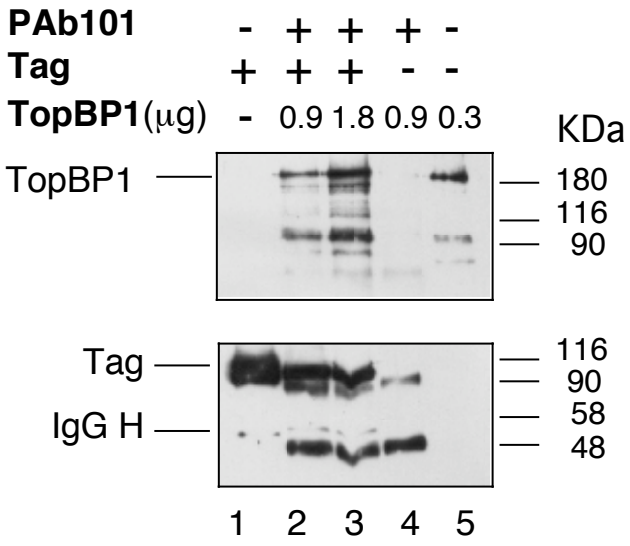

Figure 44: T antigen interacts with TopBP1. T antigen (lanes 2 and 3) adsorbed to PAb101 antibody beads were incubated with 0.9 μg (lane 2) or 1.8 μg (lane 3) of TopBP1 as indicated. Proteins bound to the beads were separated by 12.5% SDS-PAGE and visualized by western blotting with α-TopBP1 antibody (top panel) or PAb101 against T antigen (lower panel). Antibody beads without T antigen didn't bind TopBP1 (lane 4). Lanes 1 and 5 show 0.5 μg of input T antigen and the input of his-tagged TopBP1 respectively. IgG H represents IgG heavy chain.

dependent manner (compare lanes 2 and 3). The results in Figure 44 show that T antigen interacts with TopBP1 directly and specifically.

Next, I attempted to map which region of TopBP1 binds to T antigen using the same assay with GST-tagged fragments of TopBP1. The negative control in lane 4 of Figure 45 shows that TopBP1 (aa 541-1522) doesn't bind to the beads or Pab101 antibody non-specifically. Input controls (lanes 1 and 5) shows where T antigen and TopBP1 (aa 541-1522) run on 12.5% SDS-PAGE gel. TopBP1 (aa 541-1522) binds T antigen in a concentration-dependent manner too (compare lanes 2 with 3). The data suggest that the N-terminus deletion mutant of TopBP1, TopBP1 (aa 541-1522) interacts with T antigen directly and specifically. Similar results were obtained using a C-terminal fragment of TopBP1, TopBP1 (aa 978-1522) (Figure 46). Lanes 1 and 5 show the input control of T antigen and TopBP1 (aa 978-1522). Lane 4 shows that TopBP1 (aa 978-1522) didn’t associate with the beads without T antigen. Lanes 2 and 3 showed that increasing amounts of TopBP1 (aa 978-1522) bound T antigen. The results implied that the shorter deletion mutant, TopBP1 (aa 978-1522), could still bind T antigen directly and specifically.

The co-IP data show that TopBP1 directly and specifically interacts with T antigen. The C-terminus from aa 978-1522 of TopBP1 is sufficient for T antigen binding. TopBP1 (aa 541-1522) binding T antigen is comparable to that of full length TopBP1 (Figures 44 and 45). But the fraction of input TopBP1 (aa 978-1522) bound to T antigen appears to be smaller compared with the bound fraction of full length TopBP1 and TopBP1 (aa 541-1522) (compare Figure 46 with Figures 44 and 45). These data suggest that the residues between aa 541 to 978 contribute to the binding. Since the N-terminal

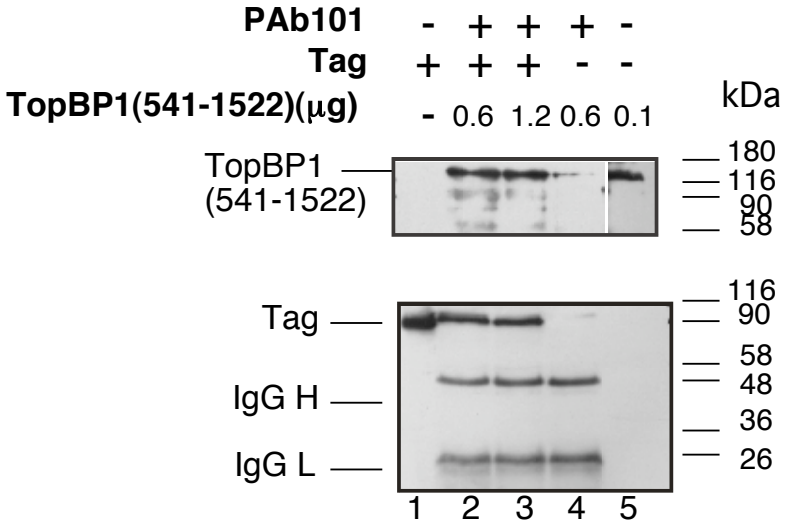

Figure 45: T antigen interacts with TopBP1(aa 541-1522) fragment. T antigen (lanes 2 and 3) bound PAb101 antibody beads were incubated with 0.6 μg (lane 2) or 1.2 μg TopBP1(aa 541-1522) (lane 3) as indicated. Proteins bound to the beads were separated by 12.5% SDS-PAGE and visualized by western blotting with α-TopBP1 antibody against TopBP1(aa 541-1522) (top panel) or PAb101 against T antigen (lower panel). The molecular weight of GST-tagged TopBP1 (aa 541-1522) is 134 kDa. Antibody beads without T antigen didn't bind TopBP1(aa 541-1522) (lane 4). Lanes 1 and 5 show 0.5 μg of input T antigen and the input control of GST-tagged TopBP1 (aa 541-1522) respectively. IgG H and IgG L represent IgG heavy and light chains respectively.

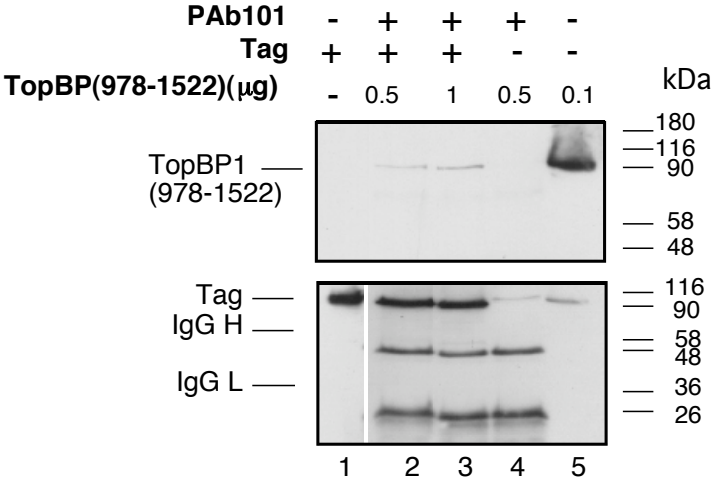

Figure 46: T antigen interacts with TopBP1(aa 978-1522) fragment. T antigen (lanes 2 and 3) adsorbed to PAb101 antibody beads were incubated with 0.5 μg (lane 2) or 1.0 μg TopBP1(aa 978-1522) (lane 3) as indicated. Proteins bound to the beads were separated by 12.5% SDS-PAGE and visualized by western blotting with α-TopBP1 antibody against TopBP1(aa 978-1522) (top panel) or PAb101 against T antigen (lower panel). The molecular weight of GST-tagged TopBP1(aa 978-1522) is 86 kDa. Antibody beads without T antigen didn't bind TopBP1(aa 978-1522) (lane 4). Lanes 1 and 5 show 0.5 μg of input T antigen and the input control of GST-tagged TopBP1 (aa 978-1522) respectively. IgG H and IgG L show IgG heavy and light chains respectively.

fragments of TopBP1 haven't been tested in the co-IP assay, there might be other sites on TopBP1 for T antigen binding.

TopBP1 interacts with pol-prim

Studies in *Xenopus* cell-free replication assays show that TopBP1 is important for recruitment of cdc45 and DNA polymerases to the pre-initiation complex (Hashimoto & Takisawa, 2003). Since TopBP1 stimulates SV40 DNA replication initiation *in vitro*, I hypothesize that TopBP1 also physically interacts with host proteins that participate in initiation, such as pol-prim. To address this hypothesis, similar Co-IP was done using pol-prim antibody and pol-prim instead of T antigen antibody and T antigen. The bound proteins were analyzed by 12.5% SDS-PAGE and western blotting. Lanes 1 and 5 in Figure 47 are input controls for pol-prim and TopBP1 respectively. Lane 4 is negative control without pol-prim added to the reaction. In lanes 2 and 3, two different amounts of TopBP1 were added to the reaction with constant amount of pol-prim. The result in lane 4 indicates that TopBP1 didn't associate with the beads in the absence of pol-prim. The data in lanes 2 and 3 suggest that TopBP1 bound specifically to pol-prim.

Discussion

In this chapter, I present evidence that TopBP1 interacts directly with both T antigen and pol-prim. TopBP1 binds weakly to the C-terminus of TopBP1 (aa 978-1522) and more strongly to a larger fragment (aa 541-1522).

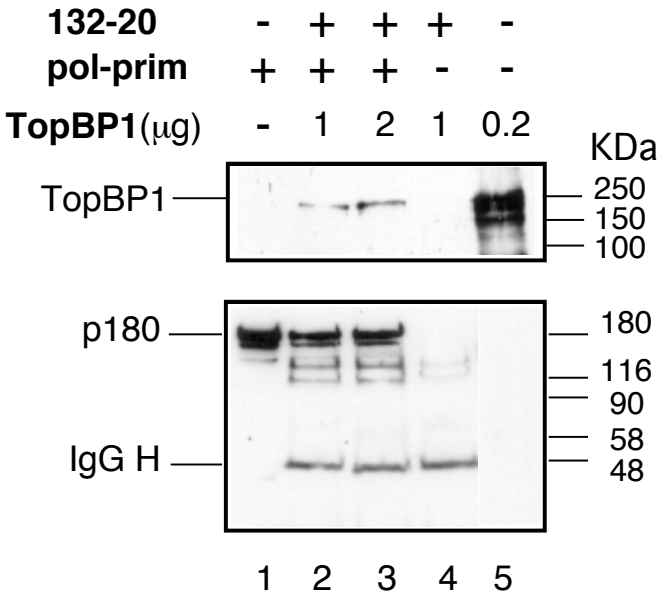

Figure 47: Pol-prim interacts with TopBP1. Pol-prim (lanes 2 and 3) adsorbed to SJK 132-20 antibody beads were incubated with 1 μg (lane 2) or 2 μg (lane 3) of TopBP1 as indicated. Proteins bound to the beads were separated by 12.5% SDS-PAGE and visualized by western blotting with the antibody against TopBP1 (top panel) or 2CT25 against p180 (lower panel). Antibody beads without pol-prim didn't bind TopBP1 (lane 4). Lanes 1 and 5 show 0.75 μg of input pol-prim and the input of his-tagged TopBP1 respectively. IgG H represents IgG heavy chain.

The functional importance of interaction between T antigen/pol-prim and TopBP1 must be further tested. Those interactions may be important for viral DNA replication, as the interaction of TopBP1 with HPV16 E2 promotes E2-mediated HPV16 DNA replication (Boner et al., 2002). Since TopBP1 interacts with both T antigen and pol-prim, it might help to recruit pol-prim to the replication origin bound by the T antigen double hexamer, thereby stimulating SV40 DNA replication in vitro.

The interaction between T antigen and TopBP1 might help to re-program the ATR/ATRIP pathway for viral replication, since viral DNA replication is closely linked to DNA damage signaling pathways. Recent studies in our lab and others suggest that T antigen reprograms the ATM signaling pathways to facilitate viral DNA replication and that ATM activity is required for SV40 replication *in vivo* (Shi et al., 2005; Zhao et al., 2008). Although ATM and ATR pathways respond to different DNA damage stimuli, they are not independent of each other (Hurley & Bunz, 2007). There is cross talk between these two important pathways. At stalled replication forks, ATR/ATRIP can directly phosphorylate ATM to stimulate its kinase activity (Stiff et al., 2006). Conversely, at DSBs, ATM indirectly activates the ATR/ATRIP pathway through phosphorylation of TopBP1 (Yoo et al., 2007). In *Xenopus* egg extract, ATM stably associates with phosphorylated TopBP1 upon induction of DSBs and phosphorylates TopBP1 (Yoo et al., 2007). Phosphorylated TopBP1 has increased affinity for ATR/ATRIP, and thus activates the ATR/ATRIP pathway (Yoo et al., 2007). Human TopBP1 is also phosphorylated on Ser1138 at DSBs, suggesting that the same activities that happen in *Xenopus* egg extracts may also happen in human cells. Thus in SV40-infected cells, since ATM pathway is active after infection, ATM may phosphorylate

TopBP1 to activate ATR/ATRIP pathway. In this chapter, I show that T antigen directly interacts with TopBP1 (aa 978-1522). Interestingly, this fragment overlaps with the ATR/ATRIP binding site on TopBP1 (aa 993-1196). This opens the possibility that T antigen might inactivate the ATR/ATRIP signaling pathway by disrupting binding between ATR/ATRIP and TopBP1 through direct competition. Thus TopBP1 might play other roles besides stimulation of viral replication. The exact mapping of the interaction sites between T antigen and TopBP1 and competition assay will be required to figure out whether T antigen competes with ATR/ATRIP for TopBP1 binding directly or blocks the ATR/ATRIP binding site. Further experiments will be needed to test ATR/ATRIP activation by phosphorylated TopBP1 in the presence of T antigen *in vitro*. *In vivo* experiments are needed to test if T antigen down-regulates the ATR/ATRIP signaling by interacting with TopBP1.

REFERENCES

Ahuja D, Saenz-Robles MT, Pipas JM (2005) SV40 large T antigen targets multiple cellular pathways to elicit cellular transformation. *Oncogene* **24**(52)**:** 7729-7745

Alexandrov AI, Botchan MR, Cozzarelli NR (2002) Characterization of simian virus 40 T-antigen double hexamers bound to a replication fork. The active form of the helicase. *J Biol Chem* **277**(47)**:** 44886-44897

Arezi B, Kuchta RD (2000) Eukaryotic DNA primase. *Trends Biochem Sci* **25**(11)**:** 572-576

Arthur AK, Hoss A, Fanning E (1988) Expression of simian virus 40 T antigen in Escherichia coli: localization of T-antigen origin DNA-binding domain to within 129 amino acids. *J Virol* **62**(6)**:** 1999-2006

Arunkumar AI, Klimovich V, Jiang X, Ott RD, Mizoue L, Fanning E, Chazin WJ (2005) Insights into hRPA32 C-terminal domain-mediated assembly of the simian virus 40 replisome. *Nat Struct Mol Biol* **12**(4)**:** 332-339

Arunkumar AI, Stauffer ME, Bochkareva E, Bochkarev A, Chazin WJ (2003) Independent and coordinated functions of replication protein A tandem high affinity single-stranded DNA binding domains. *J Biol Chem* **278**(42)**:** 41077-41082

Bastin-Shanower SA, Brill SJ (2001) Functional analysis of the four DNA binding domains of replication protein A. The role of RPA2 in ssDNA binding. *J Biol Chem* **276**(39)**:** 36446-36453

Bax A (2003) Weak alignment offers new NMR opportunities to study protein structure and dynamics. *Protein Sci* **12**(1)**:** 1-16

Bensch KG, Tanaka S, Hu SZ, Wang TS, Korn D (1982) Intracellular localization of human DNA polymerase alpha with monoclonal antibodies. *J Biol Chem* **257**(14)**:** 8391-8396

Bhattacharya S, Arunkumar AI, Sullivan SL, Botuyan MV, Arrowsmith CH, Chazin WJ (2004) 1H, 13C and 15N assignments of single-stranded DNA binding domains from the 70 kDa subunit of human replication protein A. *J Biomol NMR* **28**(2)**:** 195-196

Binz SK, Lao Y, Lowry DF, Wold MS (2003) The phosphorylation domain of the 32-kDa subunit of replication protein A (RPA) modulates RPA-DNA interactions. Evidence for an intersubunit interaction. *J Biol Chem* **278**(37)**:** 35584-35591

Blackwell LJ, Borowiec JA (1994) Human replication protein A binds single-stranded DNA in two distinct complexes. *Mol Cell Biol* **14**(6)**:** 3993-4001

Blackwell LJ, Borowiec JA, Masrangelo IA (1996) Single-stranded-DNA binding alters human replication protein A structure and facilitates interaction with DNA-dependent protein kinase. *Mol Cell Biol* **16**(9)**:** 4798-4807

Bochkarev A, Bochkareva E (2004) From RPA to BRCA2: lessons from single-stranded DNA binding by the OB-fold. *Curr Opin Struct Biol* **14**(1)**:** 36-42

Bochkarev A, Bochkareva E, Frappier L, Edwards AM (1999) The crystal structure of the complex of replication protein A subunits RPA32 and RPA14 reveals a mechanism for single-stranded DNA binding. *EMBO J* **18**(16)**:** 4498-4504

Bochkarev A, Pfuetzner RA, Edwards AM, Frappier L (1997) Structure of the single-stranded-DNA-binding domain of the replication protein A bound to DNA. *Nature* **385:** 176-181

Bochkareva E, Belegu V, Korolev S, Bochkarev A (2001) Structure of the major single-stranded DNA-binding domain of replication protein A suggests a dynamic mechanism for DNA binding. *EMBO J* **20**(3)**:** 612-618

Bochkareva E, Kaustov L, Ayed A, Yi GS, Lu Y, Pineda-Lucena A, Liao JC, Okorokov AL, Milner J, Arrowsmith CH, Bochkarev A (2005) Single-stranded DNA mimicry in the p53 transactivation domain interaction with replication protein A. *Proc Natl Acad Sci U S A* **102**(43)**:** 15412-15417

Bochkareva E, Korolev S, Bochkarev A (2000) The role for zinc in replication protein A. *J Biol Chem* **275**(35)**:** 27332-27338

Bochkareva E, Korolev S, Lees-Miller SP, Bochkarev A (2002) Structure of the RPA trimerization core and its role in the multistep DNA-binding mechanism of RPA. *EMBO J* **21**(7)**:** 1855-1863

Bochkareva E, Martynowski D, Seitova A, Bochkarev A (2006) Structure of the origin-binding domain of simian virus 40 large T antigen bound to DNA. *EMBO J* **25**(24)**:** 5961-5969

Boner W, Morgan IM (2002) Novel cellular interacting partners of the human papillomavirus 16 transcription/replication factor E2. *Virus Res* **90**(1-2)**:** 113-118

Boner W, Taylor ER, Tsirimonaki E, Yamane K, Campo MS, Morgan IM (2002) A Functional interaction between the human papillomavirus 16 transcription/replication factor E2 and the DNA damage response protein TopBP1. *J Biol Chem* **277**(25)**:** 22297-22303

Borowiec JA, Hurwitz J (1988) Localized melting and structural changes in the SV40 origin of replication induced by T-antigen. *EMBO J* **7**(10)**:** 3149-3158

Botchan M, Topp W, Sambrook J (1979) Studies on simian virus 40 excision from cellular chromosomes. *Cold Spring Harb Symp Quant Biol* **43 Pt 2:** 709-719

Bradshaw EM, Sanford DG, Luo X, Sudmeier JL, Gurard-Levin ZA, Bullock PA, Bachovchin WW (2004) T antigen origin-binding domain of simian virus 40: determinants of specific DNA binding. *Biochemistry* **43**(22)**:** 6928-6936

Braun KA, Lao Y, He Z, Ingles CJ, Wold MS (1997) Role of protein-protein interactions in the function of replication protein A (RPA): RPA modulates the activity of DNA polymerase alpha by multiple mechanisms. *Biochemistry* **36**(28)**:** 8443-8454

Brill SJ, Stillman B (1989) Yeast replication factor-A functions in the unwinding of the SV40 origin of DNA replication. *Nature* **342**(6245)**:** 92-95

Brunger AT, Adams PD, Clore GM, DeLano WL, Gros P, Grosse-Kunstleve RW, Jiang JS, Kuszewski J, Nilges M, Pannu NS, Read RJ, Rice LM, Simonson T, Warren GL (1998) Crystallography & NMR system: A new software suite for macromolecular structure determination. *Acta Crystallogr D Biol Crystallogr* **54**(Pt 5)**:** 905-921

Bullock PA (1997) The initiation of simian virus 40 DNA replication in vitro. *Crit Rev Biochem Mol Biol* **32**(6)**:** 503-568

Burckhardt CJ, Greber UF (2008) Redox rescues virus from ER trap. *Nat Cell Biol* **10**(1)**:** 9-11

Challberg MD, Kelly TJ (1989) Animal virus DNA replication. *Annu Rev Biochem* **58:** 671-717

Chaudhuri J, Khuong C, Alt FW (2004) Replication protein A interacts with AID to promote deamination of somatic hypermutation targets. *Nature* **430**(7003)**:** 992-998

Chen S, Paucha E (1990) Identification of a region of simian virus 40 large T antigen required for cell transformation. *J Virol* **64**(7)**:** 3350-3357

Chen XS, Stehle T, Harrison SC (1998) Interaction of polyomavirus internal protein VP2 with the major capsid protein VP1 and implications for participation of VP2 in viral entry. *EMBO J* **17**(12)**:** 3233-3240

Chou JY, Avila J, Martin RG (1974) Viral DNA synthesis in cells infected by temperature-sensitive mutants of simian virus 40. *J Virol* **14**(1)**:** 116-124

Christensen JB, Imperiale MJ (1995) Inactivation of the retinoblastoma susceptibility protein is not sufficient for the transforming function of the conserved region 2-like domain of simian virus 40 large T antigen. *J Virol* **69**(6)**:** 3945-3948

Collins KL, Kelly TJ (1991) Effects of T antigen and replication protein A on the initiation of DNA synthesis by DNA polymerase alpha-primase. *Mol Cell Biol* **11**(4)**:** 2108-2115

Copeland WC, Wang TS (1993) Enzymatic characterization of the individual mammalian primase subunits reveals a biphasic mechanism for initiation of DNA replication. *J Biol Chem* **268**(35)**:** 26179-26189

Costa A, Onesti S (2008) The MCM complex: (just) a replicative helicase? *Biochem Soc Trans* **36**(Pt 1)**:** 136-140

Cotsiki M, Lock RL, Cheng Y, Williams GL, Zhao J, Perera D, Freire R, Entwistle A, Golemis EA, Roberts TM, Jat PS, Gjoerup OV (2004) Simian virus 40 large T antigen targets the spindle assembly checkpoint protein Bub1. *Proc Natl Acad Sci U S A* **101**(4)**:** 947-952

Daniels R, Sadowicz D, Hebert DN (2007) A Very Late Viral Protein Triggers the Lytic Release of SV40. *PLoS Pathog* **3**(7)**:** e98

Daughdrill GW, Ackerman J, Isern NG, Botuyan MV, Arrowsmith C, Wold MS, Lowry DF (2001) The weak interdomain coupling observed in the 70 kDa subunit of human replication protein A is unaffected by ssDNA binding. *Nucleic Acids Res* **29**(15)**:** 3270-3276

Daughdrill GW, Buchko GW, Botuyan MV, Arrowsmith C, Wold MS, Kennedy MA, Lowry DF (2003) Chemical shift changes provide evidence for overlapping single-stranded DNA- and XPA-binding sites on the 70 kDa subunit of human replication protein A. *Nucleic Acids Res* **31**(14)**:** 4176-4183

de Laat WL, Appeldoorn E, Sugasawa K, Weterings E, Jaspers NG, Hoeijmakers JH (1998) DNA-binding polarity of human replication protein A positions nucleases in nucleotide excision repair. *Genes Dev* **12**(16)**:** 2598-2609

Dean FB, Borowiec JA, Eki T, Hurwitz J (1992) The simian virus 40 T antigen double hexamer assembles around the DNA at the replication origin. *J Biol Chem* **267**(20)**:** 14129-14137

Dean FB, Borowiec JA, Ishimi Y, Deb S, Tegtmeyer P, Hurwitz J (1987) Simian virus 40 large tumor antigen requires three core replication origin domains for DNA unwinding and replication in vitro. *Proc Natl Acad Sci U S A* **84**(23)**:** 8267-8271

Deb S, DeLucia AL, Baur CP, Koff A, Tegtmeyer P (1986a) Domain structure of the simian virus 40 core origin of replication. *Mol Cell Biol* **6**(5)**:** 1663-1670

Deb S, DeLucia AL, Koff A, Tsui S, Tegtmeyer P (1986b) The adenine-thymine domain of the simian virus 40 core origin directs DNA bending and coordinately regulates DNA replication. *Mol Cell Biol* **6**(12)**:** 4578-4584

Deb S, Tsui S, Koff A, DeLucia AL, Parsons R, Tegtmeyer P (1987) The T-antigen-binding domain of the simian virus 40 core origin of replication. *J Virol* **61**(7)**:** 2143-2149

Deb SP, Tegtmeyer P (1987) ATP enhances the binding of simian virus 40 large T antigen to the origin of replication. *J Virol* **61**(12)**:** 3649-3654

DeLucia AL, Deb S, Partin K, Tegtmeyer P (1986) Functional interactions of the simian virus 40 core origin of replication with flanking regulatory sequences. *J Virol* **57**(1)**:** 138-144

Dickmanns A, Zeitvogel A, Simmersbach F, Weber R, Arthur AK, Dehde S, Wildeman AG, Fanning E (1994) The kinetics of simian virus 40-induced progression of quiescent cells into S phase depend on four independent functions of large T antigen. *J Virol* **68**(9)**:** 5496-5508

Doherty KM, Sommers JA, Gray MD, Lee JW, von Kobbe C, Thoma NH, Kureekattil RP, Kenny MK, Brosh RM, Jr. (2005) Physical and functional mapping of the replication protein A interaction domain of the Werner and Bloom syndrome helicases. *J Biol Chem* **280**(33)**:** 29494-29505

Dominguez C, Boelens R, Bonvin AM (2003) HADDOCK: a protein-protein docking approach based on biochemical or biophysical information. *J Am Chem Soc* **125**(7)**:** 1731-1737

Dornreiter I, Erdile LF, Gilbert IU, von Winkler D, Kelly TJ, Fanning E (1992) Interaction of DNA polymerase alpha-primase with cellular replication protein A and SV40 T antigen. *EMBO J* **11**(2)**:** 769-776

Dornreiter I, Hoss A, Arthur AK, Fanning E (1990) SV40 T antigen binds directly to the large subunit of purified DNA polymerase alpha. *EMBO J* **9**(10)**:** 3329-3336

Dutta A, Stillman B (1992) cdc2 family kinases phosphorylate a human cell DNA replication factor, RPA, and activate DNA replication. *EMBO J* **11**(6)**:** 2189-2199

Enemark EJ, Joshua-Tor L (2006) Mechanism of DNA translocation in a replicative hexameric helicase. *Nature* **442**(7100)**:** 270-275

Everett RD (2006) Interactions between DNA viruses, ND10 and the DNA damage response. *Cell Microbiol* **8**(3)**:** 365-374

Fairman MP, Stillman B (1988) Cellular factors required for multiple stages of SV40 DNA replication in vitro. *EMBO J* **7**(4)**:** 1211-1218

Fanning E (1994) Control of SV40 DNA replication by protein phosphorylation: a model for cellular DNA replication? *Trends Cell Biol* **4**(7)**:** 250-255

Fanning E, Burger C, Gurney EG (1981) Comparison of T antigen-associated host phosphoproteins from SV40-infected and -transformed cells of different species. *J Gen Virol* **55**(Pt 2)**:** 367-378

Fanning E, Klimovich V, Nager AR (2006) A dynamic model for replication protein A (RPA) function in DNA processing pathways. *Nucleic Acids Res* **34**(15)**:** 4126-4137

Fanning E, Knippers R (1992) Structure and function of simian virus 40 large tumor antigen. *Annu Rev Biochem* **61:** 55-85

Fanning E, Pipas JM (2006) *DNA Replication and Human Disease*, Cold Spring Harbor: Cold Spring Harbor Laboratory Press.

Fanning E, Zhao X, Jiang X (2008) *Polyomavirus Life Cycle*: Springer Science and Business Media.

Fien K, Cho YS, Lee JK, Raychaudhuri S, Tappin I, Hurwitz J (2004) Primer utilization by DNA polymerase alpha-primase is influenced by its interaction with Mcm10p. *J Biol Chem* **279**(16)**:** 16144-16153

Fiers W, Contreras R, Haegemann G, Rogiers R, Van de Voorde A, Van Heuverswyn H, Van Herreweghe J, Volckaert G, Ysebaert M (1978) Complete nucleotide sequence of SV40 DNA. *Nature* **273**(5658)**:** 113-120

Fisher PA, Korn D (1981) Properties of the primer-binding site and the role of magnesium ion in primer-template recognition by KB cell DNA polymerase alpha. *Biochemistry* **20**(16)**:** 4570-4578

Foiani M, Marini F, Gamba D, Lucchini G, Plevani P (1994) The B subunit of the DNA polymerase alpha-primase complex in Saccharomyces cerevisiae executes an essential function at the initial stage of DNA replication. *Mol Cell Biol* **14**(2)**:** 923-933

Forsburg SL (2004) Eukaryotic MCM Proteins: Beyond Replication Initiation. *Microbiol Mol Biol Rev* **68**(1)**:** 109-131

Gai D, Li D, Finkielstein CV, Ott RD, Taneja P, Fanning E, Chen XS (2004a) Insights into the Oligomeric States, Conformational Changes, and Helicase Activities of SV40 Large Tumor Antigen. *J Biol Chem* **279**(37)**:** 38952-38959

Gai D, Zhao R, Li D, Finkielstein CV, Chen XS (2004b) Mechanisms of conformational change for a replicative hexameric helicase of SV40 large tumor antigen. *Cell* **119**(1)**:** 47-60

Garcia V, Furuya K, Carr AM (2005) Identification and functional analysis of TopBP1 and its homologs. *DNA Repair (Amst)* **4**(11)**:** 1227-1239

Garg P, Burgers PM (2005) DNA polymerases that propagate the eukaryotic DNA replication fork. *Crit Rev Biochem Mol Biol* **40**(2)**:** 115-128

Gately DP, Hittle JC, Chan GK, Yen TJ (1998) Characterization of ATM expression, localization, and associated DNA-dependent protein kinase activity. *Mol Biol Cell* **9**(9)**:** 2361-2374

Gjoerup OV, Wu J, Chandler-Militello D, Williams GL, Zhao J, Schaffhausen B, Jat PS, Roberts TM (2007) Surveillance mechanism linking Bub1 loss to the p53 pathway. *Proc Natl Acad Sci U S A* **104**(20)**:** 8334-8339

Goddard TD, Kneller DG Sparky 3. *University of California, San Francisco*

Goetz GS, Dean FB, Hurwitz J, Matson SW (1988) The unwinding of duplex regions in DNA by the simian virus 40 large tumor antigen-associated DNA helicase activity. *J Biol Chem* **263**(1)**:** 383-392

Gomes XV, Henricksen LA, Wold MS (1996) Proteolytic mapping of human replication protein A: evidence for multiple structural domains and a conformational change upon interaction with single-stranded DNA. *Biochemistry* **35**(17)**:** 5586-5595

Gomes XV, Wold MS (1996) Functional domains of the 70-kilodalton subunit of human replication protein A. *Biochemistry* **35**(32)**:** 10558-10568

Gomez-Lorenzo MG, Valle M, Frank J, Gruss C, Sorzano CO, Chen XS, Donate LE, Carazo JM (2003) Large T antigen on the simian virus 40 origin of replication: a 3D snapshot prior to DNA replication. *EMBO J* **22**(23)**:** 6205-6213

Greene MK, Maskos K, Landry SJ (1998) Role of the J-domain in the cooperation of Hsp40 with Hsp70. *Proc Natl Acad Sci U S A* **95**(11)**:** 6108-6113

Ham J, Dostatni N, Gauthier JM, Yaniv M (1991) The papillomavirus E2 protein: a factor with many talents. *Trends Biochem Sci* **16**(11)**:** 440-444

Hamdan SM, Marintcheva B, Cook T, Lee SJ, Tabor S, Richardson CC (2005) A unique loop in T7 DNA polymerase mediates the binding of helicase-primase, DNA binding protein, and processivity factor. *Proc Natl Acad Sci U S A* **102**(14)**:** 5096-5101

Hashimoto Y, Takisawa H (2003) Xenopus Cut5 is essential for a CDK-dependent process in the initiation of DNA replication. *EMBO J* **22**(10)**:** 2526-2535

Hay RT, DePamphilis ML (1982) Initiation of SV40 DNA replication in vivo: location and structure of 5 ' ends of DNA synthesized in the ori region. *Cell* **28**(4)**:** 767-779

Henricksen LA, Umbricht CB, Wold MS (1994) Recombinant replication protein A: expression, complex formation, and functional characterization [published erratum appears in J Biol Chem 1994 Jun 10;269(23):16519]. *J Biol Chem* **269**(15)**:** 11121-11132

Huang SG, Weisshart K, Gilbert I, Fanning E (1998) Stoichiometry and mechanism of assembly of SV40 T antigen complexes with the viral origin of DNA replication and DNA polymerase alpha-primase. *Biochemistry* **37**(44)**:** 15345-15352

Hubscher U, Maga G, Spadari S (2002) Eukaryotic DNA polymerases. *Annu Rev Biochem* **71:** 133-163

Hurley PJ, Bunz F (2007) ATM and ATR: components of an integrated circuit. *Cell Cycle* **6**(4)**:** 414-417

Hurwitz J, Dean FB, Kwong AD, Lee SH (1990) The in vitro replication of DNA containing the SV40 origin. *J Biol Chem* **265**(30)**:** 18043-18046

Iftode C, Borowiec JA (1997) Denaturation of the simian virus 40 origin of replication mediated by human replication protein A. *Mol Cell Biol* **17**(7)**:** 3876-3883

Iftode C, Borowiec JA (1998) Unwinding of origin-specific structures by human replication protein A occurs in a two-step process. *Nucl Acids Res* **26**(24)**:** 5636-5643

Iftode C, Borowiec JA (2000) 5' --> 3' molecular polarity of human replication protein A (hRPA) binding to pseudo-origin DNA substrates. *Biochemistry* **39:** 11970-11981

Iftode C, Daniely Y, Borowiec JA (1999) Replication protein A (RPA): the eukaryotic SSB. *Crit Rev Biochem Mol Biol* **34**(3)**:** 141-180

Ito N, Nureki O, Shirouzu M, Yokoyama S, Hanaoka F (2003) Crystal structure of the Pyrococcus horikoshii DNA primase-UTP complex: implications for the mechanism of primer synthesis. *Genes Cells* **8**(12)**:** 913-923

Izumi M, Yanagi K, Mizuno T, Yokoi M, Kawasaki Y, Moon KY, Hurwitz J, Yatagai F, Hanaoka F (2000) The human homolog of Saccharomyces cerevisiae Mcm10 interacts

with replication factors and dissociates from nuclease-resistant nuclear structures in G(2) phase. *Nucleic Acids Res* **28**(23)**:** 4769-4777

Jackson D, Dhar K, Wahl JK, Wold MS, Borgstahl GEO (2002) Analysis of the human replication protein A:Rad52 complex: evidence for crosstalk between RPA32, RPA70, Rad52 and DNA. *J Mol Biol* **321**(1)**:** 133-148

Jacobs DM, Lipton AS, Isern NG, Daughdrill GW, Lowry DF, Gomes X, Wold MS (1999) Human replication protein A: Global fold of the N-terminal RPA-70 domain reveals a basic cleft and flexible C-terminal linker. *J Biomol NMR* **14**(4)**:** 321-331

Jao CC, Weidman MK, Perez AR, Gharakhanian E (1999) Cys9, Cys104 and Cys207 of simian virus 40 Vp1 are essential for inter-pentamer disulfide-linkage and stabilization in cell-free lysates. *J Gen Virol* **80:** 2481-2489

Jares P, Blow JJ (2000) Xenopus cdc7 function is dependent on licensing but not on XORC, XCdc6, or CDK activity and is required for XCdc45 loading. *Genes Dev* **14**(12)**:** 1528-1540.

Jiang X, Klimovich V, Arunkumar AI, Hysinger EB, Wang Y, Ott RD, Guler GD, Weiner B, Chazin WJ, Fanning E (2006) Structural mechanism of RPA loading on DNA during activation of a simple pre-replication complex. *EMBO J* **25**(23)**:** 5516-5526

Joo WS, Luo X, Denis D, Kim HY, Rainey GJ, Jones C, Sreekumar KR, Bullock PA (1997) Purification of the simian virus 40 (SV40) T antigen DNA-binding domain and characterization of its interactions with the SV40 origin. *J Virol* **71**(5)**:** 3972-3985

Kasper JS, Kuwabara H, Arai T, Ali SH, DeCaprio JA (2005) Simian virus 40 large T antigen's association with the CUL7 SCF complex contributes to cellular transformation. *J Virol* **79**(18)**:** 11685-11692

Kelley WL, Landry SJ (1994) Chaperone power in a virus? *Trends Biochem Sci* **19**(7)**:** 277-278

Kelman Z, Yuzhakov A, Andjelkovic J, O'Donnell M (1998) Devoted to the lagging strand-the subunit of DNA polymerase III holoenzyme contacts SSB to promote processive elongation and sliding clamp assembly. *EMBO J* **17**(8)**:** 2436-2449

Kenny MK, Schlegel U, Furneaux H, Hurwitz J (1990) The role of human single-stranded DNA binding protein and its individual subunits in simian virus 40 DNA replication. *J Biol Chem* **265**(13)**:** 7693-7700

Kim A, Park JS (2002) Involvement of subcomplexes of 32 and 14 kDa subunits in RPA's DNA binding activity through redox change. *Mol Cells* **13**(3)**:** 493-497

Kim H-Y, Ahn B-Y, Cho Y (2001) Structural basis for the inactivation of retinoblastoma tumor suppressor by SV40 large T antigen. *EMBO J* **20**(1)**:** 295-304

Koradi R, Billeter M, Wuthrich K (1996) MOLMOL: a program for display and analysis of macromolecular structures. *J Mol Graph* **14**(1)**:** 51-55, 29-32

Kowalczykowski SC (2000) Some assembly required. *Nat Struct Biol* **7**(12)**:** 1087 - 1089

Kress M, de Vaux Saint Cyr C, Girard M (1978) The molecular weight of SV40 T-antigen. *Colloq INSERM* **69:** 79-92

Kumagai A, Lee J, Yoo HY, Dunphy WG (2006) TopBP1 activates the ATR-ATRIP complex. *Cell* **124**(5)**:** 943-955

Larsen AK, Escargueil AE, Skladanowski A (2003) From DNA damage to G2 arrest: the many roles of topoisomerase II. *Prog Cell Cycle Res* **5:** 295-300

Laskowski RA, Rullmannn JA, MacArthur MW, Kaptein R, Thornton JM (1996) AQUA and PROCHECK-NMR: programs for checking the quality of protein structures solved by NMR. *J Biomol NMR* **8**(4)**:** 477-486

Lee J, Kumagai A, Dunphy WG (2007) The Rad9-Hus1-Rad1 checkpoint clamp regulates interaction of TopBP1 with ATR. *J Biol Chem* **282**(38)**:** 28036-28044

Lee S-H, Kim DK (1995) The role of the 34-kDa subunit of human replication protein A in simian virus 40 DNA replication in vitro. *J Biol Chem* **270**(21)**:** 12801-12807

Li D, Zhao R, Lilyestrom W, Gai D, Zhang R, DeCaprio JA, Fanning E, Jochimiak A, Szakonyi G, Chen XS (2003) Structure of the replicative helicase of the oncoprotein SV40 large tumour antigen. *Nature* **423**(6939)**:** 512-518

Li JJ, Peden KW, Dixon RA, Kelly T (1986) Functional organization of the simian virus 40 origin of DNA replication. *Mol Cell Biol* **6**(4)**:** 1117-1128

Liddington RC, Yan Y, Moulai J, Sahli R, Benjamin TL, Harrison SC (1991) Structure of simian virus 40 at 3.8-A resolution. *Nature* **354**(6351)**:** 278-284

Lilyestrom W, Klein MG, Zhang R, Joachimiak A, Chen XS (2006) Crystal structure of SV40 large T-antigen bound to p53: interplay between a viral oncoprotein and a cellular tumor suppressor. *Genes Dev* **20**(17)**:** 2373-2382

Lin YL, Shivji MK, Chen C, Kolodner R, Wood RD, Dutta A (1998) The evolutionarily conserved zinc finger motif in the largest subunit of human replication protein A is required for DNA replication and mismatch repair but not for nucleotide excision repair. *J Biol Chem* **273**(3)**:** 1453-1461

Liu K, Paik JC, Wang B, Lin FT, Lin WC (2006) Regulation of TopBP1 oligomerization by Akt/PKB for cell survival. *EMBO J* **25**(20)**:** 4795-4807

Liu VF, Weaver DT (1993) The ionizing radiation-induced replication protein A phosphorylation response differs between ataxia telangiectasia and normal human cells. *Mol Cell Biol* **13**(12)**:** 7222-7231

Loeber G, Stenger JE, Ray S, Parsons RE, Anderson ME, Tegtmeyer P (1991) The zinc finger region of simian virus 40 large T antigen is needed for hexamer assembly and origin melting. *J Virol* **65**(6)**:** 3167-3174

Loo Y-M, Melendy T (2004) Recruitment of replication protein A by the papillomavirus E1 protein and modulation by single-stranded DNA. *J Virol* **78**(4)**:** 1605-1615

Luo X, Sanford DG, Bullock PA, Bachovchin WW (1996) Solution structure of the origin DNA-binding domain of SV40 T-antigen. *Nat Struct Biol* **3**(12)**:** 1034-1039

Maga G, Villani G, Tillement V, Stucki M, Locatelli GA, Frouin I, Spadari S, Hubscher U (2001) Okazaki fragment processing: modulation of the strand displacement activity of DNA polymerase delta by the concerted action of replication protein A, proliferating cell nuclear antigen, and flap endonuclease-1. *Proc Natl Acad Sci U S A* **98**(25)**:** 14298-14303

Makiniemi M, Hillukkala T, Tuusa J, Reini K, Vaara M, Huang D, Pospiech H, Majuri I, Westerling T, Makela TP, Syvaoja JE (2001) BRCT domain-containing protein TopBP1 functions in DNA replication and damage response. *J Biol Chem* **276**(32)**:** 30399-30406

Manke IA, Lowery DM, Nguyen A, Yaffe MB (2003) BRCT repeats as phosphopeptide-binding modules involved in protein targeting. *Science* **302**(5645)**:** 636-639

Mastrangelo IA, Hough PV, Wall JS, Dodson M, Dean FB, Hurwitz J (1989) ATP-dependent assembly of double hexamers of SV40 T antigen at the viral origin of DNA replication. *Nature* **338**(6217)**:** 658-662

Matsumoto T, Eki T, Hurwitz J (1990) Studies on the initiation and elongation reactions in the simian virus 40 DNA replication system. *Proc Natl Acad Sci U S A* **87**(24)**:** 9712-9716

Maul GG, Ishov AM, Everett RD (1996) Nuclear domain 10 as preexisting potential replication start sites of herpes simplex virus type-1. *Virology* **217**(1)**:** 67-75

McEntee K, Weinstock GM, Lehman IR (1980) recA protein-catalyzed strand assimilation: stimulation by Escherichia coli single-stranded DNA-binding protein. *Proc Natl Acad Sci U S A* **77**(2)**:** 857-861

Meinke G, Bullock PA, Bohm A (2006) Crystal structure of the simian virus 40 large T-antigen origin-binding domain. *J Virol* **80**(9)**:** 4304-4312

Meinke G, Phelan P, Moine S, Bochkareva E, Bochkarev A, Bullock PA, Bohm A (2007) The crystal structure of the SV40 T-antigen origin binding domain in complex with DNA. *PLoS Biol* **5**(2)**:** e23

Melendy T, Stillman B (1993) An interaction between replication protein A and SV40 T antigen appears essential for primosome assembly during SV40 DNA replication. *J Biol Chem* **268**(5)**:** 3389-3395

Mer G, Bochkarev A, Gupta R, Bochkareva E, Frappier L, Ingles CJ, Edwards AM, Chazin WJ (2000) Structural basis for the recognition of DNA repair proteins UNG2, XPA, and RAD52 by replication factor RPA. *Cell* **103**(3)**:** 449-456

Mizuno T, Ito N, Yokoi M, Kobayashi A, Tamai K, Miyazawa H, Hanaoka F (1998) The second-largest subunit of the mouse DNA polymerase alpha-primase complex facilitates both production and nuclear translocation of the catalytic subunit of DNA polymerase alpha. *Mol Cell Biol* **18**(6)**:** 3552-3562

Mizuno T, Okamoto T, Yokoi M, Izumi M, Kobayashi A, Hachiya T, Tamai K, Inoue T, Hanaoka F (1996) Identification of the nuclear localization signal of mouse DNA primase: nuclear transport of p46 subunit is facilitated by interaction with p54 subunit. *J Cell Sci* **109**(11)**:** 2627-2636

Mizuno T, Yamagishi K, Miyazawa H, Hanaoka F (1999) Molecular architecture of the mouse DNA polymerase alpha-primase complex. *Mol Cell Biol* **19**(11)**:** 7886-7896

Moarefi IF, Small D, Gilbert I, Hopfner M, Randall SK, Schneider C, Russo AA, Ramsperger U, Arthur AK, Stahl H, Kelly TJ, Fanning E (1993) Mutation of the cyclin-dependent kinase phosphorylation site in simian virus 40 (SV40) large T antigen specifically blocks SV40 origin DNA unwinding. *J Virol* **67**(8)**:** 4992-5002

Mol CD, Izumi T, Mitra S, Tainer JA (2000) DNA-bound structures and mutants reveal abasic DNA binding by APE1 and DNA repair coordination [corrected]. *Nature* **403**(6768)**:** 451-456

Murakami Y, Hurwitz J (1993) Functional interactions between SV40 T antigen and other replication proteins at the replication fork. *J Biol Chem* **268**(15)**:** 11008-11017

Myers RM, Tjian R (1980) Construction and analysis of simian virus 40 origins defective in tumor antigen binding and DNA replication. *Proc Natl Acad Sci U S A* **77**(11)**:** 6491-6495

Nakanishi A, Clever J, Yamada M, Li PP, Kasamatsu H (1996) Association with capsid proteins promotes nuclear targeting of simian virus 40 DNA. *Proc Natl Acad Sci U S A* **93**(1)**:** 96-100

Nakanishi A, Li PP, Qu Q, Jafri QH, Kasamatsu H (2007) Molecular dissection of nuclear entry-competent SV40 during infection. *Virus Res* **124**(1-2)**:** 226-230

Nakanishi A, Nakamura A, Liddington R, Kasamatsu H (2006) Identification of amino acid residues within simian virus 40 capsid proteins Vp1, Vp2, and Vp3 that are required for their interaction and for viral infection. *J Virol* **80**(18)**:** 8891-8898

Nakanishi A, Shum D, Morioka H, Otsuka E, Kasamatsu H (2002) Interaction of the Vp3 nuclear localization signal with the importin alpha 2/beta heterodimer directs nuclear entry of infecting simian virus 40. *J Virol* **76**(18)**:** 9368-9377

Nasheuer HP, Moore A, Wahl AF, Wang TS (1991) Cell cycle-dependent phosphorylation of human DNA polymerase alpha. *J Biol Chem* **266**(12)**:** 7893-7903

Nasheuer HP, von Winkler D, Schneider C, Dornreiter I, Gilbert I, Fanning E (1992) Purification and functional charcterization of bovine RP-A in an in vitro SV40 DNA replication system. *Chromosoma* **102:** S52-S59

Norkin LC, Anderson HA, Wolfrom SA, Oppenheim A (2002) Caveolar endocytosis of simian virus 40 is followed by brefeldin A-sensitive transport to the endoplasmic reticulum, where the virus disassembles. *J Virol* **76**(10)**:** 5156-5166

Ott RD (2002) Components of the SV40 primosome and their functional interactions. Doctoral Thesis, Molecular Biology, Vanderbilt University, Nashville

Ott RD, Rehfuess C, Podust VN, Clark JE, Fanning E (2002) Role of the p68 subunit of human DNA polymerase alpha-primase in simian virus 40 DNA replication. *Mol Cell Biol* **22**(16)**:** 5669-5678

Park C-J, Lee J-H, Choi B-S (2005) Solution structure of the DNA-binding domain of RPA from *Saccharomyces cerevisiae* and its interaction with single-stranded DNA and SV40 T antigen. *Nucl Acids Res* **33**(13)**:** 4172-4181

Pipas JM (1992) Common and unique features of T antigens encoded by the polyomavirus group. *J Virol* **66**(7)**:** 3979-3985

Pizzagalli A, Valsasnini P, Plevani P, Lucchini G (1988) DNA polymerase I gene of Saccharomyces cerevisiae: nucleotide sequence, mapping of a temperature-sensitive mutation, and protein homology with other DNA polymerases. *Proc Natl Acad Sci U S A* **85**(11)**:** 3772-3776

Podust VN, Chang LS, Ott R, Dianov GL, Fanning E (2002) Reconstitution of human DNA polymerase delta using recombinant baculoviruses: the p12 subunit potentiates DNA polymerizing activity of the four-subunit enzyme. *J Biol Chem* **277**(6)**:** 3894-3901

Quartin RS, Cole CN, Pipas JM, Levine AJ (1994) The amino-terminal functions of the simian virus 40 large T antigen are required to overcome wild-type p53-mediated growth arrest of cells. *J Virol* **68**(3)**:** 1334-1341

Reddy VB, Thimmappaya B, Dhar R, Subramanian KN, Zain BS, Pan J, Ghosh PK, Celma ML, Weissman SM (1978) The genome of simian virus 40. *Science* **200**(4341)**:** 494-502

Reese DK, Meinke G, Kumar A, Moine S, Chen K, Sudmeier JL, Bachovchin W, Bohm A, Bullock PA (2006) Analyses of the interaction between the origin binding domain from simian virus 40 T antigen and single-stranded DNA provide insights into DNA unwinding and initiation of DNA replication. *J Virol* **80**(24)**:** 12248-12259

Ricke RM, Bielinsky AK (2004) Mcm10 regulates the stability and chromatin association of DNA polymerase-alpha. *Mol Cell* **16**(2)**:** 173-185

Ricke RM, Bielinsky AK (2006) A conserved Hsp10-like domain in Mcm10 is required to stabilize the catalytic subunit of DNA polymerase-alpha in budding yeast. *J Biol Chem* **281**(27)**:** 18414-18425

Robertson PD, Warren EM, Zhang H, Friedman DB, Lary JW, Cole JL, Tutter AV, Walter JC, Fanning E, Eichman BF (2008) Domain architecture and biochemical characterization of vertebrate mcm10. *J Biol Chem* **283**(6)**:** 3338-3348

Rushton JJ, Jiang D, Srinivasan A, Pipas JM, Robbins PD (1997) Simian virus 40 T antigen can regulate p53-mediated transcription independent of binding p53. *J Virol* **71**(7)**:** 5620-5623

Santocanale C, Foiani M, Lucchini G, Plevani P (1993) The isolated 48,000-dalton subunit of yeast DNA primase is sufficient for RNA primer synthesis. *J Biol Chem* **268**(2)**:** 1343-1348

Santocanale C, Neecke H, Longhese MP, Lucchini G, Plevani P (1995) Mutations in the gene encoding the 34 kDa subunit of yeast replication protein A cause defective S phase progression. *J Mol Biol* **254**(4)**:** 595-607

Sawai ET, Butel JS (1989) Association of a cellular heat shock protein with simian virus 40 large T antigen in transformed cells. *J Virol* **63**(9)**:** 3961-3973

Schelhaas M, Malmstrom J, Pelkmans L, Haugstetter J, Ellgaard L, Grunewald K, Helenius A (2007) Simian Virus 40 depends on ER protein folding and quality control factors for entry into host cells. *Cell* **131**(3)**:** 516-529

Sclafani RA, Fletcher RJ, Chen XS (2004) Two heads are better than one: regulation of DNA replication by hexameric helicases. *Genes Dev* **18**(17)**:** 2039-2045

Shen J, Gai D, Patrick A, Greenleaf WB, Chen XS (2005) The roles of the residues on the channel beta-hairpin and loop structures of simian virus 40 hexameric helicase. *Proc Natl Acad Sci U S A* **102**(32)**:** 11248-11253

Shen J-C, Lao Y, Kamath-Loeb A, Wold MS, Loeb LA (2003) The N-terminal domain of the large subunit of human replication protein A binds to Werner syndrome protein and stimulates helicase activity. *Mech Ageing Dev* **124**(8-9)**:** 921-930

Shi Y, Dodson GE, Shaikh S, Rundell K, Tibbetts RS (2005) Ataxia-telangiectasia-mutated (ATM) is a T-antigen kinase that controls SV40 viral replication in vivo. *J Biol Chem* **280**(48)**:** 40195-40200

Sibenaller ZA, Sorensen BR, Wold MS (1998) The 32- and 14-kilodalton subunits of replication protein A are responsible for species-specific interactions with single-stranded DNA. *Biochemistry* **37**(36)**:** 12496-12506

Simmons DT (2000) SV40 large T antigen functions in DNA replication and transformation. *Adv Virus Res* **55:** 75-134

Simmons DT, Loeber G, Tegtmeyer P (1990a) Four major sequence elements of simian virus 40 large T antigen coordinate its specific and nonspecific DNA binding. *J Virol* **64**(5)**:** 1973-1983

Simmons DT, Melendy T, Usher D, Stillman B (1996) Simian virus 40 large T antigen binds to topoisomerase I. *Virology* **222**(2)**:** 365

Simmons DT, Wun-Kim K, Young W (1990b) Identification of simian virus 40 T-antigen residues important for specific and nonspecific binding to DNA and for helicase activity. *J Virol* **64**(10)**:** 4858-4865

Smelkova NV, Borowiec JA (1998) Synthetic DNA replication bubbles bound and unwound with twofold symmetry by a simian virus 40 T-antigen double hexamer. *J Virol* **72**(11)**:** 8676-8681

Srinivasan A, McClellan AJ, Vartikar J, Marks I, Cantalupo P, Li Y, Whyte P, Rundell K, Brodsky JL, Pipas JM (1997) The amino-terminal transforming region of simian virus 40 large T and small t antigens functions as a J domain. *Mol Cell Biol* **17**(8)**:** 4761-4773

Stahl H, Droge P, Knippers R (1986) DNA helicase activity of SV40 large tumor antigen. *EMBO J* **5**(8)**:** 1939-1944

Stauffer ME, Chazin WJ (2004a) Physical interaction between replication protein A and Rad51 promotes exchange on single-stranded DNA. *J Biol Chem* **279**(24)**:** 25638-25645

Stauffer ME, Chazin WJ (2004b) Structural mechanisms of DNA replication, repair, and recombination. *J Biol Chem* **279**(30)**:** 30915-30918

Stenlund A (2003) Initiation of DNA replication: lessons from viral initiator proteins. *Nat Rev Mol Cell Biol* **4**(10)**:** 777-785

Stiff T, Walker SA, Cerosaletti K, Goodarzi AA, Petermann E, Concannon P, O'Driscoll M, Jeggo PA (2006) ATR-dependent phosphorylation and activation of ATM in response to UV treatment or replication fork stalling. *EMBO J* **25**(24)**:** 5775-5782

Stillman B (1989) Initiation of eukaryotic DNA replication in vitro. *Annu Rev Cell Biol* **5:** 197-245

Sugiyama T, Kowalczykowski SC (2002) Rad52 protein associates with replication protein A (RPA)-single-stranded DNA to accelerate Rad51-mediated displacement of RPA and presynaptic complex formation. *J Biol Chem* **277**(35)**:** 31663-31672

Suh WC, Burkholder WF, Lu CZ, Zhao X, Gottesman ME, Gross CA (1998) Interaction of the Hsp70 molecular chaperone, DnaK, with its cochaperone DnaJ. *Proc Natl Acad Sci U S A* **95**(26)**:** 15223-15228

Sullivan CS, Gilbert SP, Pipas JM (2001) ATP-dependent simian virus 40 T-antigen-Hsc70 complex formation. *J Virol* **75**(4)**:** 1601-1610

Sullivan CS, Grundhoff AT, Tevethia S, Pipas JM, Ganem D (2005) SV40-encoded microRNAs regulate viral gene expression and reduce susceptibility to cytotoxic T cells. *Nature* **435**(7042)**:** 682-686

Sullivan CS, Pipas JM (2002) T antigens of simian virus 40: molecular chaperones for viral replication and tumorigenesis. *Microbiol Mol Biol Rev* **66**(2)**:** 179-202

Tainer JA, Friedberg EC (2000) Dancing with the elephants: envisioning the structural biology of DNA repair pathways. *Mutat Res* **460**(3-4)**:** 139-141

Tegtmeyer P (1972) Simian virus 40 deoxyribonucleic acid synthesis: the viral replicon. *J Virol* **10**(4)**:** 591-598

Titolo S, Welchner E, White PW, Archambault J (2003) Characterization of the DNA-binding properties of the origin-binding domain of simian virus 40 large T antigen by fluorescence anisotropy. *J Virol* **77**(9)**:** 5512-5518

Tycko R, Blanco FJ, Ishii Y (2000) Alignment of biopolymers in strained gels: a new way to create detectable dipole-dipole couplings in high-resolution biomolecular NMR. *J Am Chem Soc* **122**(38)**:** 9340 -9341

Valle M, Chen XS, Donate LE, Fanning E, Carazo JM (2006) Structural basis for the cooperative assembly of large T antigen on the origin of replication. *J Mol Biol* **357**(4)**:** 1295-1305

Valle M, Gruss C, Halmer L, Carazo JM, Donate LE (2000) Large T-antigen double hexamers imaged at the simian virus 40 origin of replication. *Mol Cell Biol* **20**(1)**:** 34-41

Van Hatten RA, Tutter AV, Holway AH, Khederian AM, Walter JC, Michael WM (2002) The Xenopus Xmus101 protein is required for the recruitment of Cdc45 to origins of DNA replication. *J Cell Biol* **159**(4)**:** 541-547

Vassin VM, Wold MS, Borowiec JA (2004) Replication protein A (RPA) phosphorylation prevents RPA association with replication centers. *Mol Cell Biol* **24**(5)**:** 1930-1943

Waga S, Stillman B (1998) The DNA replication fork in eukaryotic cells. *Annu Rev Biochem* **67:** 721-751

Wang X, Haber JE (2004) Role of Saccharomyces single-stranded DNA-binding protein RPA in the strand invasion step of double-strand break repair. *PLoS Biology* **2**(1)**:** e21

Weisshart K, Bradley MK, Weiner BM, Schneider C, Moarefi I, Fanning E, Arthur AK (1996) An N-terminal deletion mutant of simian virus 40 (SV40) large T antigen oligomerizes incorrectly on SV40 DNA but retains the ability to bind to DNA polymerase alpha and replicate SV40 DNA in vitro. *J Virol* **70**(6)**:** 3509-3516

Weisshart K, Friedl S, Taneja P, Nasheuer H-P, Schlott B, Grosse F, Fanning E (2004) Partial proteolysis of simian virus 40 T antigen reveals intramolecular contacts between domains and conformation changes upon hexamer assembly. *J Biol Chem* **279**(37)**:** 38943-38951

Weisshart K, Taneja P, Fanning E (1998) The replication protein A binding site in simian virus 40 (SV40) T antigen and its role in the initial steps of SV40 DNA replication. *J Virol* **72**(12)**:** 9771-9781

Weisshart K, Taneja P, Jenne A, Herbig U, Simmons DT, Fanning E (1999) Two regions of simian virus 40 T antigen determine cooperativity of double-hexamer assembly on the viral origin of DNA replication and promote hexamer interactions during bidirectional origin DNA unwinding. *J Virol* **73**(3)**:** 2201-2211

Wessel R, Schweizer J, Stahl H (1992) Simian virus 40 T-antigen DNA helicase is a hexamer which forms a binary complex during bidirectional unwinding from the viral origin of DNA replication. *J Virol* **66**(2)**:** 804-815

Wiekowski M, Schwarz MW, Stahl H (1988) Simian virus 40 large T antigen DNA helicase. Characterization of the ATPase-dependent DNA unwinding activity and its substrate requirements. *J Biol Chem* **263**(1)**:** 436-442

Wobbe CR, Weissbach L, Borowiec JA, Dean FB, Murakami Y, Bullock P, Hurwitz J (1987) Replication of simian virus 40 origin-containing DNA in vitro with purified proteins. *Proc Natl Acad Sci U S A* **84**(7)**:** 1834-1838

Wold MS (1997) Replication protein A: a heterotrimeric, single-stranded DNA-binding protein required for eukaryotic DNA metabolism. *Annu Rev Biochem* **66:** 61-92

Wold MS, Kelly T (1988) Purification and characterization of replication protein A, a cellular protein required for in vitro replication of simian virus 40 DNA. *Proc Natl Acad Sci U S A* **85**(8)**:** 2523-2527

Wong SW, Wahl AF, Yuan PM, Arai N, Pearson BE, Arai K, Korn D, Hunkapiller MW, Wang TS (1988) Human DNA polymerase alpha gene expression is cell proliferation dependent and its primary structure is similar to both prokaryotic and eukaryotic replicative DNA polymerases. *EMBO J* **7**(1)**:** 37-47

Wu X, Avni D, Chiba T, Yan F, Zhao Q, Lin Y, Heng H, Livingston D (2004) SV40 T antigen interacts with Nbs1 to disrupt DNA replication control. *Genes Dev* **18**(11)**:** 1305-1316

Wun-Kim K, Upson R, Young W, Melendy T, Stillman B, Simmons DT (1993) The DNA-binding domain of simian virus 40 tumor antigen has multiple functions. *J Virol* **67**(12)**:** 7608-7611

Wyka IM, Dhar K, Binz SK, Wold MS (2003) Replication protein A interactions with DNA: differential binding of the core domains and analysis of the DNA interaction surface. *Biochemistry* **42**(44)**:** 12909-12918

Xu ZX, Timanova-Atanasova A, Zhao RX, Chang KS (2003) PML colocalizes with and stabilizes the DNA damage response protein TopBP1. *Mol Cell Biol* **23**(12)**:** 4247-4256

Yoo HY, Kumagai A, Shevchenko A, Shevchenko A, Dunphy WG (2007) Ataxia-telangiectasia mutated (ATM)-dependent activation of ATR occurs through phosphorylation of TopBP1 by ATM. *J Biol Chem* **282**(24)**:** 17501-17506

Yu X, Chini CC, He M, Mer G, Chen J (2003) The BRCT domain is a phospho-protein binding domain. *Science* **302**(5645)**:** 639-642

Yuzhakov A, Kelman Z, Hurwitz J, O'Donnell M (1999a) Multiple competition reactions for RPA order the assembly of the DNA polymerase delta holoenzyme. *EMBO J* **18**(21)**:** 6189-6199

Yuzhakov A, Kelman Z, O'Donnell M (1999b) Trading places on DNA--a three-point switch underlies primer handoff from primase to the replicative DNA polymerase. *Cell* **96**(1)**:** 153-163

Zalvide J, DeCaprio JA (1995) Role of pRb-related proteins in simian virus 40 large-T-antigen-mediated transformation. *Mol Cell Biol* **15**(10)**:** 5800-5810

Zhang H, Fanning E (unpublished data)

Zhao X, Fanning E (unpublished data)

Zhao X, Madden-Fuentes RJ, Lou B, Pipas JM, Gerhardt J, Rigell CJ, Fanning E (2008) ATM- and proteasome-dependent destruction of Mre11-Rad50-Nbs1 subunits in SV40-infected primate cells. *J Virol***:** accepted

Zou L, Elledge SJ (2003) Sensing DNA damage through ATRIP recognition of RPA-ssDNA complexes. *Science* **300**(5625)**:** 1542-1548

Zweckstetter M, Bax A (2000) Prediction of sterically induced alignment in a dilute liquid crystalline phase: aid to protein structure determination by NMR. *J Am Chem Soc* **122**(15)**:** 3791-3792